UNIVERSITÀ DEGLI STUDI DI MILANO

FACOLTA' DI MEDICINA
DIPARTIMENTO DI SCIENZE E TECNOLOGIE BIOMEDICHE

CORSO DI DOTTORATO IN MEDICINA MOLECOLARE
CURRICULUM GENOMICA, PROTEOMICA E TECNOLOGIE CORRELATE
XXIV CICLO

TESI DI DOTTORATO

microRNA AND GENE EXPRESSION CHANGES UNDERLYING THE PATHOLOGY OF NEMALINE MYOPATHY

settore scientifico disciplinare BIO/09

Dottoranda: Dott.ssa ALESSANDRA CASTALDI
Matricola: R08139

Tutor: Prof. MARISTELLA GUSSONI
Coordinatore del dottorato: Prof. Gianluigi Condorelli
Dott.ssa Marie-Louise Bang

ANNO ACCADEMICO 2010-2011

La miopatia nemalinica (NM) è un disordine neuromuscolare caratterizzato da debolezza muscolare e ipotonia in seguito a disorganizzazione sarcomerica e alla formazione di corpi "nemalinici"nelle fibre muscolari. La patologia colpisce 1 su 50000 nati vivi ed è causata da mutazioni delle proteine nebulina e α-actina mentre mutazioni in α-tropomiosina, β-tropomiosina, troponina T1 e cofilina-2 sono più rare. Al momento non esistono né terapie né marker della malattia. In pazienti NM è stata riportata l'alterazione di geni coinvolti in meccanismi secondari. Allo stesso tempo è stata mostrata la de-regolazione di diversi microRNAs (miRs) in muscoli di pazienti NM. Basandoci su questi dati riportati in letteratura, abbiamo ipotizzato l'esistenza di meccanismi specifici, regolati da miRs, che potrebbero sottendere alla patologia, indipendentemente dal gene malattia. Per studiare questi, abbiamo utilizzato un topo modello di NM transgenico knockin, che esprime una forma mutata della α-actina, (Acta1(H40Y)KI) (KI), che sviluppa una forma grave di NM. Mentre i maschi KI muoiono a circa 11 settimane di vita, le femmine esibiscono un fenotipo più lieve e sono fertili.

Il primo scopo del nostro studio era studiare l'espressione genica del diaframma (DIA) e del tibiale anteriore (TA) in topi KI e paragonare i risultati con quelli precedentemente pubblicati dell'analisi di espressione genica di pazienti NM e del topo Tmslow(Met9Arg) Tg (Tg), topo modello di una forma più lieve di NM. Il secondo scopo era paragonare il profilo di espressione genica tra maschi e femmine KI, per comprendere le basi molecolari per la differente severità della patologia. Il terzo scopo era studiare il profillo di espressione dei miRs in topi KI maschi, in uno stadio precoce e tardivo della patrologia, per indagare l'espressione dei miRs in relazione allo sviluppo della patologia.

Lo studio di espressione genica è stato condotto su maschi di 3 settimane e maschi e femmine di 10 settimane. I maschi giovani presentavano la più alta de-regolazione genica. Solo pochi geni de-regolati erano in comune tra DIA e TA, probabilmente a causa di un profilo di espressione genica peculiare del DIA. Tra le differenti condizioni, le femmine in stadio tardivo avevano un profilo di espressione genica più simile ai maschi in uno stadio precoce, che ai maschi in uno stadio tardivo, riflettendo uno sviluppo ritardato del fenotipo. Comunque, anche se nello specifico i geni de-regolati erano diversi, gli stessi meccanismi erano affetti nelle differenti condizioni. Alcuni di questi, ad esempio i meccanismi metabolici, sono stati trovati de-regolati anche in pazienti NM, ma non in topi Tg.

I topi KI mostravano livelli alterati dei miRs selezionati, parallelamente a quanto riportato in uomo, ma i topi Tg non mostravano la stessa de-regolazione. Il miR-381 è stato trovato espresso ad alti livelli nel KI e due dei suoi putativi targets sono stati confermati in vitro tramite saggio di luciferasi: una proteina dei canali del calcio (TRPM7) e una proteina coinvolta nel sistema dell'ubiquitina (Trim63/MURF1).

I risultati di questo studio indicano che Acta1(H40Y)KI è un buon sistema modello per lo studio della NM, sia da un punto di vista fenotipico che genetico. Questo modello è migliore del topo Tg, dal momento che presenta profili di espressione genica e di miR più simili all'uomo. Il significato biologico dei meccanismi genici alterati e la loro possibile regolazione ad opera dei miRs restano da essere studiati più a in dettaglio.

Nemaline myopathy (NM) is a clinically and genetically heterogeneous neuromuscular disorder characterized by muscle weakness and hypotonia due to sarcomeric disarray and the formation of rod-like "nemaline" bodies in the muscle fibers. The disease affects about 1 in 50.000 and is caused by mutations in nebulin and α-skeletal muscle actin, while mutations in α-tropomyosin, β-tropomyosin, troponin T1, and cofilin-2 are more rare. Currently no therapies or markers exist. Gene expression profiling has provided insights into the gene expression changes associated with NM in human patients. Furthermore, a number of microRNAs (miRs) have been shown to be specifically dysregulated in muscles from NM patients. Based on these findings, we hypothesized that unique regulatory mechanisms regulated by miRs may underlie the pathology of NM irrespective of the causative mutation. To study this, we took advantage of a transgenic knockin mouse model of NM, expressing a mutant form of α-skeletal actin (Acta1(H40Y)KI) (KI) that develops a severe form of the disease. Interestingly, while KI males exhibit a severe phenotype resulting in death from around 10 weeks of age, females are less severely affected and are fertile.

The first aim of our study was to perform gene expression profiling on diaphragm (DIA) and tibialis anterior (TA) muscle of KI mouse and compare the results with previously published gene expression analyses of NM patients and the Tmslow(Met9Arg) Tg (Tg) mouse model of a mild form of NM. The second aim was to compare the gene expression profile of male and female KI mice to provide insights into the molecular basis for the different severity of the disease in males and females. The third aim was to investigate the miR expression profile in KI males at an early and late stage of the disease to study miR expression in relation to the development of the disease.

The gene expression study was conducted on 3-week-old males and 10-week-old males and females. The highest number of dysregulated genes were found in 3-week-old males. Between muscles (DIA and TA) only few altered genes were in common, possibly due to a peculiar gene expression pattern of the DIA. Interestingly, 10-week-old females showed a gene expression pattern more similar to 3-week-old males than to 10-week-old males, reflecting a delay in the development of the phenotype. However, although the specific dysregulated genes were different, some pathways were commonly dysregulated under different conditions. The same pathways, i.e. metabolic pathways, were found to be dysregulated in KI and human NM patients, but not in Tg mice.

Expression levels of selected miRs that are altered in human NM patients were also altered in KI mice, but not in Tg mice. MiR-381 was highly upregulated and two of its predicted targets were validated in vitro by a luciferase assay: the calcium channel protein TRPM7 and the ubiquitin-related protein Trim63/MURF1.

The results of this study indicate that Acta1(H40Y)KI is a good model of NM that recapitulates NM disease from both a phenotypic and genetic point of view. It is a better model for NM than the Tg mouse, showing gene and miR expression patterns more similar to NM patients. The biological meaning of the altered gene expression patterns and their possible regulation by miRs remain to be investigated in more detail.

LISTA SIMBOLI

RNA – ribonucleic acid

miR – microRNA

NM – Nemaline Myopathy

NKO – Nebulin knock-out mouse

KI – ACTA (H40Y) knock-in mouse

Tg - alpha-Tropomyosinslow(Met9Arg) transgenic mouse

DIA – Diaphragm

TA – Tibialis Anterior

Orm – Orosomucoid

KNG – kininogen

KNG2 – kininogen2

CPB2 - carboxypeptidase B2

FG – fibrinogen

G6PC - glucose-6-phosphatase catalytic-subunit

FBP1 - fructose-1,6-bisphosphatase 1

Ncor1 - nuclear receptor corepressor 1

TPM3 - tropomyosin 3

DAG1 – dystroglycan

Mef2C - myocyte enhancer factor 2

Sepp1 - selenoprotein P1

ACAA2 - acetyl-coenzyme A acyltransferase 2

PMPCB - mitochondrial processing peptidase beta

SDHD - succinate dehydrogenase complex

AIFM1 - mitochondrion-associated 1

MRPL20 - mitochondrial ribosomal protein L20

G0S2 - G0/G1 switch gene 2

PCID2 - PCI domain containing 2

DRP1 - damaged-DNA recognition protein 1

Bmp4 - bone morphogenetic protein 4

CFD – adipsin

Foxo1 - forkhead box O1

Lep – leptin

Map3k6 - mitogen-activated protein kinase kinase kinase 6

Phlda3 - pleckstrin homology-like domain, family A, member 3

Spsb1 - splA/ryanodine receptor domain and SOCS box containing 1

Cib2 - calcium and integrin binding family member 2

Cdc34 - cell division cycle 34 homolog

Ptpre - protein tyrosine phosphatase, receptor type, E

Csnk2a2 (CK2) - casein kinase 2, alpha 1 polypeptide

Ppp3ca - protein phosphatase 3, catalytic subunit, alpha isozyme

Camk2b - calcium/calmodulin-dependent protein kinase II beta

CTD - carboxy-terminal domain, RNA polymerase II, polypeptide A

Ctdsp1 - small phosphatase 1

Cish - cytokine inducible SH2-containing protein

Dnajb2 - DnaJ (Hsp40) homolog, subfamily B, member 2

SEPP1 - selenoprotein P,plasma 1

Nat2 - N-acetyltransferase 5

C2 - component 2

Srpk3 - serine/arginine-rich protein specific kinase 3

Actg1 – Actin, gamma 1

Cd2ap - CD2 associated protein

Tln2 – Talin 2

Tpm1 – Tropomyosin 1

Trim63 - Tripartite motif containing 63

Trpm7 - Transient receptor potential cation channel, subfamily M, member.

1.INTRODUCTION

1.1 Skeletal muscle

1.1.1 Skeletal muscle structure

Skeletal muscle is a form of striated muscle composed of tissue, connective tissue, nerves and blood vessels (fig.1). The individual components of skeletal muscle are muscle fibers (approximately 50 μm in diameter and up to several centimeters in length), cylindrical multinucleated cells formed by the fusion of developmental myoblasts (muscle cell progenitors). This differentiation process occurs before birth and cells continue to grow in size thereafter. The striation seen in skeletal muscle cells is the consequence of a peculiar cytoskeletal organization: two cytoplasmic proteins, actin and myosin (also known as "thick" and "thin" filaments, respectively) are arranged in repeating units called *sarcomeres*. The sliding of filaments along each other is responsible for muscle contraction.

Skeletal muscle fibers can be classified based on the type of myosin and on their metabolism. There are two main classes of fiber types, slow twitch (Type I) and fast twitch (Type II) muscle fibers. Type I fibers are highly resistant to fatigue and show extended muscle contraction over a long time. From the biochemical point of view they present oxidative enzymes, low glycolytic markers, and ATPase activity. Type II fibers use anaerobic metabolism and contract faster, fatiguing more quickly. Biochemically they present high oxidative and glycolytic enzymes and ATPase activity. Type II fibers can be further grouped into different subtypes, depending on the myosin heavy chain isoform (MHC): type IIa, IIx, and IIb. In human, only type IIa and IIx fiber are present, while in small mammals type IIb is the major fast muscle isoform. MHCIIx (or MHCIId) was later identified in small mammals and based on DNA analysis, it is the homologue of the MHCIIb originally identified in humans. This finding has caused confusion in the literature, and sometimes human fiber type IIx is referred to as type IIb based on the original MHC nomenclature. Type IIa fibers are also known as intermediate fast-twitch fibers. They are able to use aerobic and anaerobic metabolism, and are considered intermediate because do not maintain a great amount of their force production with repeated activity. The Type IIb/IIx fibers are the “classic” fast twitch fibers, using anaerobic metabolism, and having a faster rate of fatigue. Different muscles are a mixture of different fiber types and their percentage vary depending on the action of that muscle.

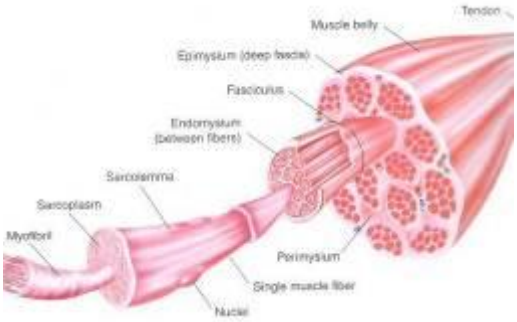

Fig.1 schematic representation of skeletal muscle

1.1.2 The sarcomere

The four major functional characteristics of muscle are excitability (it responds to stimulation by nerves and hormones), extensibility (it can be stretched), elasticity (after stretching it recoils to the original resting length), and contractility. The contractile functional unit of the skeletal muscle is the sarcomere (approximately 2.3 µm long), which gives the muscle its striated appearance visible by light microscopy as three major bands: A, I, and Z (fig.2). The A-band is composed of thick filaments (myosin) and proteins bound to myosin; the middle part of the A-band is named the “M-band” or “M-line”. The I-band is made up of thin (actin) filaments and actin-binding proteins. In the middle of the I-band between two neighboring sarcomeres is the Z-disc, or Z-line. The protein composition of the Z-line is heterogeneous: channels, cytoplasmatic, and nuclear signaling molecules, enzymes, and cytoskeletal proteins, colocalize together, conferring a multifunctional nature to the Z-band [1,2,3].

The interdigitating actin (thin) and myosin (thick) filaments slide past each other during muscle contraction. The thin filament can polymerize and depolymerize and thus presents a fast-growing end called the “barbed end”, and a slow-growing end called the “pointed end”. Since the movement of myosin motors is unidirectional, contractile force can be produced because of the orientation of thin filaments in opposite directions at each end of the sarcomere. α-actinin plays a role in stabilizing the right polarization of the thin filament, cross-linking actin filaments near their barbed ends in the Z-band, while their pointed ends are not bound to any particular structure. The cytoskeletal reorganization in which actin is involved *in vivo* is too fast to be supported only by the actin turnover rate; thus there are several actin-binding proteins that regulate actin filament turnover by promoting

polymerization, depolymerization, or filament severing [4, 5, 6]. Among these, ADF/cofilin and gelsolin are actin-severing proteins: ADF/cofilin promotes actin monomer dissociation from the pointed end [7] and gelsolin caps the barbed end in a calcium-dependent manner [8, 9] (its role in regulation of actin has to be better elucidated). Actin filament stability is maintained through the action of side-binding proteins, such as tropomyosin that is also involved in the regulation of muscle contraction [10]. It has been reported that tropomyosin spontaneously inhibits actin polymerization and depolymerization *in vitro* [11, 12, 13, 14], and protects actin filament from the severing action of ADF/cofilin and gelsolin [15, 16, 17, 18].

A third filament system is formed by the giant protein, titin, which act as a spring by keeping the thick filament centered during contraction and is thought to function in signaling pathways and dictate the assembly of other sarcomeric components. In skeletal muscle, a fourth filament system is formed by the giant modular protein, nebulin (600-800 kDa), which is associated with and spans along the thin filament in skeletal muscle with its C-terminus anchored in the Z-line and its N-terminus extending towards the thin filament pointed end [19]. In cardiac muscle, a smaller nebulin-like protein, nebulette (107 kDa), is expressed and may have overlapping functions with nebulin in the Z-line, suggesting that it covers an important role in the sarcomere [20, 21]. In the past years, *in vitro* studies on nebulin depletion have suggested a role of nebulin in regulating thin filament length ("nebulin ruler" hypothesis) [22, 23]. Recently, *Castillo et al*. observed that in rabbit skeletal muscle, nebulin does not extend to the pointed ends [24]. Furthermore, in nebulin-deficient mice, thin filaments are assembled with uniform but shorter length than in wildtype neonatal skeletal muscle, becoming more variable in length during postnatal development [25, 26]. Likewise, human patients affected by Nemaline Myopathy caused by nebulin mutations also exhibited shorter thin filament lengths [27]. Taken together, these findings show that thin filament lengths are still regulated in the absence of nebulin, suggesting that nebulin alone does not determine thin filament length. More recently, functional studies have strongly suggested that nebulin is a regulator of the dynamic exchange of actin subunits and other thin filament proteins. This is supported by the binding of nebulin to the barbed end capping protein, CapZ [28] as well as to the pointed end capping protein, tropomodulin [29]. Moreover *Pappas et al*. have shown that nebulin stabilizes sarcomeric thin filaments, not only by inhibiting actin depolymerization but also by stabilizing other thin filament proteins, such as tropomyosin and tropomodulin [30].

Several myopathies are caused by mutations in genes encoding thin filament or Z-line proteins. Nemaline Myopathy (NM), which is classified as a non-dystrophic skeletal muscle myopathy, is one of them, caused by mutations in six different thin filament proteins: α-actin, nebulin, troponin-T, cofilin-2, tropomyosin-1, and tropomyosin-3. Recently, studies have suggested alterations in adult stem cell myogenesis and the cross-bridge cycle in NM. These NM-related aspects are discussed in chapter 1.2, while the next paragraphs report the most recent findings regarding myogenesis and contractility mechanisms in normal muscle.

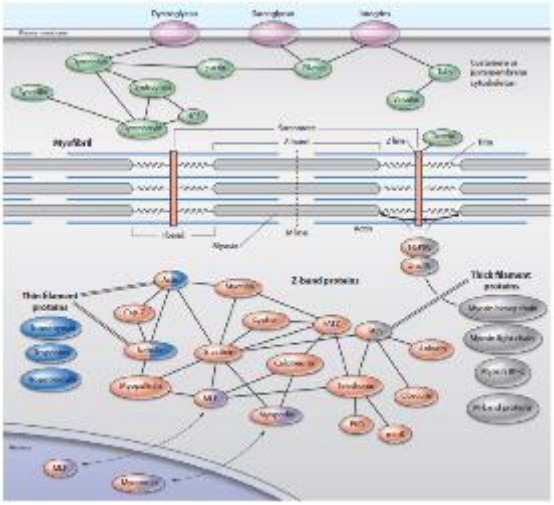

Fig.2 Schematic representation of the sarcomere and proteins associated to the Z-band (Sanger and Sanger, Science signaling, 2008)

1.1.3 Myogenesis

1.1.3.1 Genetics of the developmental myogenesis

The skeletal muscles of the trunk and the limbs originate from a subset of the paraxial mesoderm called somites. The somites are epithelial structures that result from the segmentation of the presomitic mesoderm. These structures begin to form at the anterior of the embryo and are added posteriorly as the embryo extends. During the development the somites form distinct compartments from which distinct tissues of the animal will originate. The compartments are the sclerotome (origin of vertebrae and ribs), the dermatome (origin of dorsal dermis), the syndetome (origin of axial tendons), and the myotome (origin of the muscle differentiation) [31, 32]. Before the compartmentalization in dermatome and myotome, a unique 'C'-shaped epithelial structure exists in which myogenic and dermal progenitors can first be detected, called the dermomyotome.

The myogenic precursors are labeled by the paired box transcription factors PAX3 and PAX7, that are induced by exogenous signals [36] to be highly expressed and regulate the start of the myogenic programmme in cooperation with other factors, such as DACH2, SIX1, and EYA2 proteins [37, 38, 39].

As soon as the myogenic cells are labeled by PAX3 and PAX7, they migrate around the edges of the dermomyotome, giving rise to the specific myotome compartment. At this point, the muscle specific markers are expressed while PAX3 is downregulated and PAX-7 expression is retained only in the satellite cells (adult stem muscle cells) [40, 41, 42]. This is the crucial point of myogenesis, in which there is a switch from proliferation to differentiation, from myoblast to post mitotic myocytes. The first marker of differentiation is Myf5, followed by MyoD. At later stages, cells from the central dermomyotome can either self-renew and remain in

the epithelial border of the dermomyotome or migrate to the myotome [33, 34, 35], forming the satellite cells that are the adult muscle stem cells [40, 43, 44]. However it is not yet clear how the migration of the central dermomyotome cells is regulated.
The limb muscles and the trunk muscles don't follow exactly the same myogenic programme.Here limb muscle myogenesis is illustrated, reporting the last findings in the field.
The first steps of myogenesis have recently been shown to be promoted by a short activation of NOTCH signaling [45]. NOTCH signalling displays a complex behavior on myogenesis, acting as a potent stimulator of the myogenic program for DML cells (cells of the dorsomedial lip), but only during a limited time window. In fact a sustained activation of NOTCH reverses the myogenic program, resulting in downregulation of MRF (myogenic regulatory factor) expression and a return to a PAX7-positive state. Transient activation of the NOTCH signaling pathway has been shown to be fundamental for the initiation of myogenesis [45] and to be induced by the interaction of muscle progenitor cells with a ligand (DLL1) exposed on neural crest cells. A model of a 'kiss and run' mode of signaling transduction has been suggested, in which there is a rapid interaction between muscle progenitor cells and neural crest cells. Moreover this links the timing of myotome formation to that of neural crest migration, providing a mechanistic link for the concurrence of these two events [45].
Subsequent to NOTCH signaling the MRFs, including Myf5, MyoD, Mrf4 (sometimes referred to as Myf6), and myogenin, are activated. These proteins have distinct functions and cooperate in inducing the expression between each other. It has been reported that they are partially redundant so that the loss of one MRF member can be compensated for by the upregulation of another [46]. Myf5 acts at the top of the myogenic cascade and its expression is regulated by a multiple enhancer controlled pathway. The other MRFs are often induced by the expression activation of another MRF. It is possible that this self-reinforcing mechanism is required to lock down the myogenic programme and inactivate other differentiation programmes [47, 48, 49].
Although the interactions between MRFs are complex, mouse mutants have given some indication of specific functions of individual MRFs. *Myogenin*-null mice die at birth due to a severe deficiency in myoblast differentiation [50], while mice carrying mutations in Myf5, MyoD, or Mrf4 are viable and produce morphologically normal muscle. On the other hand, simultaneous lack of all three genes causes muscle defects at embryonic stage [51 , 52]. Taken together, these findings indicate a high degree of plasticity and the presence of compensatory mechanisms that are able to induce myogenesis even when normal mechanisms are severely compromised. Recent studies have suggested that non-MRF-dependent mechanisms exist that can lead to muscle differentiation [53, 54]. For example it has been shown that MRFs can be bypassed altogether in some muscle stem cells and that Pax3 alone can drive differentiation in these cells [53].

1.1.3.2 Genetics of the regenerative myogenesis

During muscle injury and under pathological conditions (i.e. muscular dystrophy) occurs the degeneration of myofibers. Consequently, the satellite cells, the adult stem cell of the skeletal muscle, present at the basal lamina of the myofibers, are

activated to, differentiate and fuse with each other or preexisting myofibers to regenerate the muscle [55, 56]. Satellite cells are classified as stem cells since following injury some fraction of them self-renew, contributing to the maintenance of the quiescent satellite cell pool. It has recently been shown that only one single satellite cell is able to self-renew and differentiate when transplanted in an injured muscle [57].

It is thought that the cellular mechanisms at the basis of developmental, postnatal, and adult regenerative myogenesis are similar. However, in the last years some differences in the genetics for embryonic, fetal, postnatal, and adult regenerative myogenesis have been reported. For example, while myogenin-null mice have defects in developmental myogenesis, myogenin deficient satellite cells form myotubes normally *in vitro*, and an altered pattern of gene expression is present in myogenin-conditionally-deleted muscle *in vivo* [50, 58]. However the ability of adult myogenin-null mice to repair muscle injury has not yet been assessed.

Pax7 is expressed in all adult satellite cells and is required for their maintenance in the postnatal period [59]; Pax7-null mice show severe defects in regenerative myogenesis [60, 61]. Surprisingly, when Pax7 is removed after three weeks of age, no defects are reported in limb muscle regeneration [62], suggested also in this case a difference in developmental and regenerative myogenesis programmes.

1.1.4 Muscle contraction

One of the major characteristics of striated muscle is the ability to contract, owing to the presence of the functional contractile unit, the sarcomere. Contraction occurs by the “sliding mechanism” when thick (myosin) and the thin (actin) filaments are mutually sliding over each other [63, 64]. The length of the thick and thin filaments is unchanged before and after shortening of the muscle. In the thick-thin filament overlapping region, bridge-like structures (actin-myosin interaction) called “cross-bridges” can be identified, as responsible for the movement and force developed during contraction [65, 66]. It is known that ATP is involved in muscle contraction, serving at least two functions: first, ATP disconnects actin from myosin, and second, ATP is hydrolyzed by the myosin molecule to produce the energy required for muscle contraction [67]. The structure of the globular head of the myosin (myosin S1 region) has been revealed by X-ray diffraction [68] and appears like a “back door” enzyme, in which the ATP (substrate) and actin (catalyst) bind on opposite sites of the molecule. These observations have provided the basis for a molecular mechanism by which ATP binding leads to actin dissociation and force generation. In the steady-state, myosin and actin are tightly bound to each other and the long cleft connecting ATP to the actin binding site is “closed”. This cleft is opened after the binding of ATP to myosin, causing changes in the shape of S-1. Cleft opening disrupts the interaction between actin and myosin so that myosin “lets go” of the actin filament. ATP is hydrolyzed and ADP and Pi are released, chemical energy from ATP is transferred to the myosin molecule, and the cross-bridge shows the “cocking” conformation. In the last step, actin rebinds to myosin and the terminal phosphate group of ATP is released. It is believed that this allows the myosin molecule to reverse the conformational changes while bound to actin, thus providing the power stroke of muscle contraction.

The mechanism described above is referred to as the activity of the contractile system of muscle under full activation (ON state). During relaxation the muscle is in OFF state. A calcium-dependent mechanism regulates the ON (contraction) - OFF (relaxation) states of the contractile system of muscle as an important part of the excitation-contraction (E–C) coupling pathway. The protein that binds to Ca^{2+} is troponin C, which is located in the thin filament. In the presence of ATP, the formation of force-generating cross-bridges is inhibited when troponin does not bind Ca^{2+}[69, 70, 71]. However in the E–C coupling pathway there are several hierarchical feedback loops. Among the feedback regulations, mechano-electric feedback has been extensively investigated [72]. It is also well-known that the Ca^{2+} binding to troponin induces cross-bridge formation, and conversely that the cross-bridge formation enhances the Ca^{2+} binding affinity of troponin [73]. This is one of the reported feedback loops and it is supposed that also other feedback loops exist, such as in the regulation of Ca^{2+}-release/uptake by the sarcoplasmic reticulum (SR) due to deformation of the SR by the force generated by the cross-bridges.
It has been reported that in the steady state conditions intermediate between full contraction and relaxation conditions, auto-oscillation of sarcomere length occurs. This phenomenon is called SPOC (*SP*ontaneous *O*scillatory *C*ontraction of myofibrils) [74, 75]. Recently it has been suggested that even a molecular system composed of a small number of myosin molecules and a single actin filament is an auto-oscillator [76]. It is possible that the contractile system constituting a hierarchic structure from a molecular level, up to myofibrils and fibers having auto-oscillatory properties characteristic for each level of hierarchy [77].

1.2 Nemaline Myopathy

1.2.1 Clinical features of Nemaline Myopathy

Nemaline myopathy (NM), first described in the 1963 by Conen *et al* [78] and Shy *et al.*[79], is a slowly- or non-progressive neuromuscular disorder characterized by muscle weakness and the presence of rod-shaped structures called *nemaline rods* in affected muscle fibers, that give the name to the disease (nema being the Greek word for thread). Even if it is a rare disease, affecting 1 per 50000 live births, it is the most common of the non-dystrophic congenital myopathies. Many cases are sporadic, but the majority of NM cases exhibit either autosomal recessive or dominant patterns of inheritance.

Patients affected by nemaline myopathy suffer from hypotonia and general muscle weakness, predominantly in facial muscles and finger extensor muscles. Moreover dysphagia, respiratory insufficiency, foot deformities, arched palate, scoliosis, chest deformities, and superior and inferior limbs contractures has been reported in NM patients.

Currently, the NM forms are grouped into six classes [80]. In all the clinical forms, the central nervous system is unaffected, and intelligence and cardiac contractility are usually normal.

- The **typical** (i.e. most common) form of NM is usually autosomal recessive and present with congenital or infantile hypotonia, weakness, and often, feeding difficulties. Neonates that present profound weakness and hypotonia often improve their strength with age, delaying attainment of gross motor skills and starting later to walk. The gross motor activity is usually impaired in adult, while fine motor activity is normal. Patients are usually thin with a narrow face and a high arched palate; atrophy also occurs sometimes. Proximal muscles are generally more affected than distal ones, although distal weakness, especially later in life, is not uncommon. The most common problem in these patients, even in those less affected, is in breathing, since respiratory muscles are always involved, leading to nocturnal hypoxia and hypercarbia. Problems with the joints like hypermobility, deformities, or contracture are also common, occurring congenitally or occasionally in the later stages of NM. However many patients are able to conduct an active life and only in some cases a wheelchair is required. The eventual death is often due to respiratory insufficiency.
- **Mild NM:** The difference from patients affected by the typical form is the childhood onset. Otherwise these patients show the same phenotype as the typical form, being indistinguishable from typical cases at later stages. From a genotypic point of view, mild NM is heterogeneous, counting sporadic case, autosomal recessive, and also autosomal dominant cases.
- **Severe NM:** Usually this form of the disease is sporadic, although in few cases autosomal recessive inheritance is reported. The major problem of the patients is respiratory insufficiency, resulting from a profound diaphragm and intercostals muscle weakness and hypotonia present in all the skeletal muscles. Death from respiratory insufficiency or pneumonia often occurs in the first months of life, and in general patients with severe NM never survive to reproduce.

Difficulties in swallowing and sucking are often reported. Sometimes patients initially classified as “severe” survive with minimal residual disabilities and become classified as “intermediate” or “typical”.

- **Intermediate NM:** Some patients cannot be classified as “typical”, even if they show typical presentations due to the progressive course of the disease. In the same way some patients presenting profound muscle weakness survive infancy and cannot be classified as “severe”. The characteristics of these “intermediate” cases are the survival past one year, the inability to sit and/or walk, or the loss of ambulation and progressive worsening by age of 11 years.
- **Adult onset NM:** Some patients don’t present any symptom before the third decade of life; it is possible that the onset of the disease occurs even later, until the sixth decade. Inflammatory changes are found in muscle biopsies of muscles affected by progressive weakness, suggesting that these cases might represent a distinctly different pathophysiological

mechanism. Others with only minimal muscle weakness present cardiomyopathy.

- **Amish NM:** This is a clinically distinct autosomal recessive form described in only a single genetic isolate of related Old Order Amish families with neonatal onset. The symptoms are hypothonia, contractures, and tremors during the first 2-3 months of life. The severe pectus carinatum associated with muscle atrophy, progressive weakness, and contractures often leads to death at around 2 years of age owing to respiratory insufficiency.
- **Other forms of NM:** Patients with nemaline rods, presenting atypical symptoms such as ophthalmoplegia, are included in this heterogeneous category. In relation to the pathophysiology, it is unclear whether it is right to categorize these cases as variants of NM or as other rods-associated diseases.

Nemaline rods are the hallmarks of the disease and are revealed by the Gomori trichrome method on frozen sections. Some fibers exhibit size variation and predominance of type 1 fibers is a common feature of NM with some patients showing exclusively type 1 fibers or poor fiber type differentiation [81]. However, cases of patients with increased proportions of fast (type 2) fibers have also been reported. Fiber degereration/regeneration is not reported as a characteristic of NM, even though recently studies have shown signs of degeneration/regeneration in some patients as well as in a mouse model carrying a mutation in TPM3 gene.

Recent studies based on the analysis of biopsies from NM patients and mouse models of NM have revealed that the weakness associated with NM may at least partly be due to a reduced number of actomyosin cross-bridges and in some cases also reduced thin filament length, suggesting the potential for developing future therapies targeted towards restoring the altered cross-bridge cycling kinetics

1.2.2 The hallmarks of the NM: nemaline bodies

Nemaline bodies (fig.3) are electron dense rods, measuring 1-7μm in length and 0.3-2μm in width. They are in structural continuity with Z-disks and often associated with sarcomeric disarray and loss of registration [82, 83]. The presence of areas of complete sarcomeric disorganization close to relatively normal sarcomeres is quite frequent; this phenomenon is poorly understood. Nuclear nemaline bodies could be present as well.
In human myopathies, there is no firm association between the number and location of the rods and the severity of muscle weakness or age at the onset [92]; a big variability in rod frequency in different skeletal muscles of different patients or within the same patient has been reported. These findings suggest that the disease phenotype is more influenced by variations in the underlying pathological processes that result in rods, rather than by the presence of rods themselves.
The analysis of rod composition has revealed the presence of aggregates of thin filament proteins in nemaline bodies, mainly derived from the Z-line, including actin, α-actinin 2, telethonin, γ-filamin, myozenin, myopalladin, and myotilin, but not

desmin. Rods are not only present in NM patients but are also observed in polymyositis, human immunodeficiency virus infection, and myofibrillar myopathy as well as in normal aging muscle, and not all of them show the same protein composition. They are generally formed in skeletal muscle under inflammation and degeneration as a pathophysiological response. Moreover, rods association with abnormal mitochondria have been described, and this pathology has been classified as nemaline-mitochondrial myopathy.

It has been shown that is possible to induce *in vitro* rod formation in non-muscle and muscle cells [84] by using different cell stressors such as adenosine triphosphate (ATP) depletion, dimethyl sulfoxide, and heat shock. Furthermore, it has been suggested that metabolic alterations during formation and turnover of the sarcomere can lead to rod formation [84]. However the mechanisms underlying rod formation in skeletal muscle is still unclear, in particular in disorders characterized by both structural and metabolic defects. Moreover, even if the rod localization is often cytoplasmic, intranuclear rods have been found in some patients.

Recently, Vanderbrouck *et al.*[85] investigated rod formation associated with structural disorganization of the thin filament transfecting cells with several constructs carrying ACTA1 mutations reported in NM patients, and compared that with the rod formation induced by ATP depletion. In this study it was demonstrated that not all rods are formed in the same way and have different protein composition and conformation. However, these differences are not dependent on the different origin from structural or metabolic defects.

Skeletal actin was observed in all the rods, but actin dynamics, binding partners, and conformation were different under different pathological conditions and in relation to rod localization. In intranuclear rods, actin was monomeric and not bound to α-actinin while α-actinin is one of the major constituents of cytoplasmic rods in human NM [86, 87, 88, 89 90]. It is possible that α-actinin-actin cross-linking occurs later in rod formation when rods are localized to the cytoplasm. This *in vitro* observation is well supported by a report regarding a patient with an ACTA1 mutation that was biopsied at 7 weeks and then again at 15 months of age [91]. In this case the rods were reported to be "vague cytoplasmic bodies" at the earlier time point, while at the later time point the rods demonstrated a typical "cross-hatched" or "grid-like" structure. Differences in rod appearance in biopsies from the same patient at different time points have been shown to be caused by α-actinin-actin cross-linking that doesn't occur in the beginning of rod formation. Moreover, Vanderbrouck *et al.* showed a different expression of cofilin in nuclear and cytoplasmic rods. As discussed above, cofilin is involved in actin depolymerization and enhances the dissociation of ADP-actin monomers from the growing-end of F-actin. Mutations in the cofilin gene result in a form of NM and independent from the underlying structural or metabolic abnormalities, cofilin has been observed in cytoplasmic, but not intranuclear rods.

Actin turnover is influenced by the site of the mutation, the anatomical localization of rods, and the cellular ATP levels [85]. These different actin dynamics influence the time course of rod formation as well as actin turnover in the sarcomere. This leads to structural and functional deficits in muscles associated with muscle weakness, such as myofibrillar disruption observed in nemaline myopathy and

alterations in the interaction between actin and tropomyosin seen in congenital fiber-type disproportion.
In conclusion, rods derived from the presence of actin mutations and ATP depletion show similar features, suggesting that both, structural and metabolic defects contribute to rod formation and composition. However, the mechanisms of rod formation in these conditions need to be investigated in order to shed light on their function in NM.

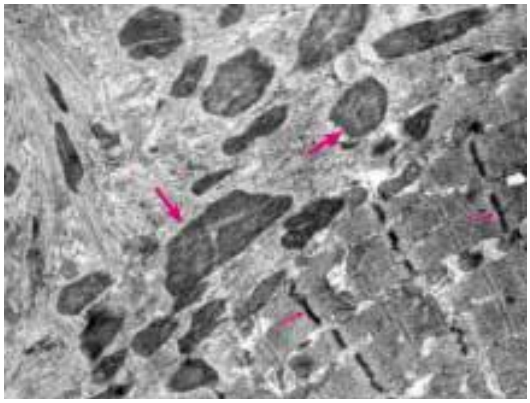

Fig.3 Nemaline rods in NM patient - Electron micrograph. An area of relatively normal muscle structure (small arrows, bottom right) is seen next to a structurally disorganized region with multiple nemaline rods (large arrows) and disorganized thin filaments (top left). (Sanoudou and Beggs, trends in Molecular Medicine, 2001)

1.2.3 Genetics of Nemaline Myopathy

1.2.3.1 Causative genes

NM is heterogeneous also from a genetic point of view. Causative mutations leading to NM disease can occur in *Acta1* (skeletal muscle α-actin), *Neb* (nebulin), *Tpm3* (slow alpha-tropomyosin; alpha-3 chain), *Tpm2* (beta tropomyosin), *Tnnt1* (slow troponin T), and *Cfl2* (cofilin 2). All these genes encode thin filament proteins. This huge heterogeneity in terms of inheritance and causative genes makes the genetic test for NM complex. Based on the literature, about half of NM cases result from Neb mutations. Neb genetic testing is available but is expensive because of the large size of the gene. Acta1 mutations are responsible for 20-25% of all NM, while mutations in the other causative genes are responsible for the remaining 30% of NM cases. This distribution among NM patients reflects the important role of nebulin in the sarcomere due to its giant size (isoforms from 600 to 800 kDa). In fact, when a mutation occurs in *Neb,* it seriously affects thin filament stability. Since over 20 years ago nebulin was considered a “molecular ruler”, specifying actin

filament length. However, due to its large size and susceptibility to proteolysis, it has been always hard to work with nebulin and directly demonstrate its role in specification of thin filament length. In a nebulin knockout developed by Bang *et al*, shorter, but uniform thin filaments were observed [25], in contrast to the expected lack of the thin filament regulation. This suggested that a nebulin-independent mechanism controls immature actin filament length, while nebulin is responsible for specifying filament mature length. Apparently in contrast to Bang *et al*., a study on another nebulin knockout mouse reported the presence of shorter non-uniform thin filaments. However, while in the first study the mice were analyzed at 1 day after birth, the second study was carried on 10-15 days old mice. This could provide the basis for the discrepancy, suggesting that the actin filament length non-uniformity arise from muscle use over time.
More recently, studies have definitely shown that nebulin is not a molecular ruler of thin filaments: i.e. when nebulin was replaced with a constructed "mini-nebulin" in skeletal muscle cells, actin filament assembly was not restricted to the size of mini-nebulin. Taken together these findings reveal that nebulin regulates thin filament length by stabilizing the filament and preventing depolymerization, but not by a traditional ruler mechanism.
In addition, it has been reported that while nebulin's C-terminus bind and colocalize with the barbed-end actin binding protein, CapZ, its N-terminus does not colocalize with the pointed end capping protein tropomodulin (Tmod) as previously thought. How nebulin interacts with CapZ is not clear, since the precise layout that nebulin adopts in the Z-disc is unknown. One of the most recent hypothesis is that a significant amount of nebulin is placed in the Z-disc where it crosses from one thin filament to the next, connecting adjacent sarcomeres. It has been also supposed that nebulin stabilizes actin filaments, either directly by providing actin monomers with additional molecular contacts and preventing their dissociation from the filament, and/or indirectly by stabilizing tropomyosin, which prevents actin depolymerization (see paragraph 1.1.2). Finally, a last hypothesis is that nebulin stabilizes the thin filament by exerting a compressive force as suggested by the evidence that nebulin is quite compliant, and when fully extended may apply a significant restorative force to the thin filament. This force could prevent actin depolymeriazation by protecting the thin filament.
In the last years nebulin has shown to exhibit additional other functions, such as specifation of Z-disc structure and width as well as proper contractile function of skeletal muscle.

1.2.3.2 Genetic pathways underlying NM

Owing to the genetic heterogeneity of NM, Sanaoudou *et al*. investigated the gene expression profile of NM patients with the intent to shed light onto the genetic defects at the basis of the disease. In this study, muscle specimens from patients of all ages, disease states, and genders, were used to minimize the bias introduced by each of these factors. Deregulated genes were found in different pathways, such as glucose/glycogen metabolism-related, fatty acid metabolism, cell cycle control, transcription/translation-related, ubiquitin-related, muscle and nerve, Ca^{2+} homeostasis, and signal transduction.
The most interesting changes are reported in the paragraphs below.

- *1.2.3.2.1 Changes in satellite cells: indication of regenerative response in NM muscles?*

  An increase in satellite cell number was found in myofibers from NM patients and was confirmed by the overexpression of NCAM1 and CDK4, two genes expressed in myoblasts. However the expression level of Pax7, *MyoD1*, *Myf5*, desmin, *GLUT1*, *GLUT4*, *BCL2*, *MET*, α-7 integrin, and M-cadherin was unchanged. This was unexpected since the immunofluorescence study showed an increased number of NCAM1 and CDK4 mononucleate cells in NM muscles. Sanoudou *et al.* hypothesized that the relatively unchanged expression of satellite muscle cell markers could be due to a dilution effect as satellite cells make up only a few percent of total myonuclei [95]. Moreover CDK4 overexpression went together with downregulation of *CUL1*, *RBL2*, and *BCL6*, three inhibitors of the cyclin D2/CDK4 pathway, the pathway promoting the progression from G1 to S-phase. At the same time, FIBP, a mitogenesis-promoter gene was overexpressed too. The possibility that other cells, such as fibroblasts, could account for this alteration does not seem reasonable. In fact, fibroblast proliferation and increased fibrosis are not detected in NM skeletal muscle patients and Duchenne muscular dystrophy muscles, for which fibrosis is a prominent feature [97], do not present these genetic alterations.
  However, *TGFB2*, a potent inhibitor of skeletal muscle differentiation [98], was upregulated, while some inhibitors of the myogenin/MyoD pathways (*CARM1*, *MADH3,* and *NFATC3)* were downregulated [99, 100, 101]. In other words, while proliferation seems to be promoted, differentiation is inhibited. Thus the increased number of satellite cells, in the context of several other changes in expression of cell cycle and transcription factors, suggests the possible existence of an abort of the regenerative response in NM muscles.

- *1.2.3.2.2 Altered metabolism in NM muscle*

  The altered expression of several genes directly or indirectly involved in the glycolytic pathway was revealed in NM muscles. Genes usually expressed at high levels in skeletal muscle were under-expressed in NM muscles, such as 6-Phosphofructo-2-kinase/fructose-2,6-biphosphatase1 (*PFKFB1*), fructose-1,6-bisphosphatase (*FBP2*), phosphoglucomutase (*PGM1*), and phosphofructokinase (*PFKM*).
  Other metabolic changes were reported in the gene expression analysis, which seemed related to the switch from fast to slow fiber type. In fact, the cardiac/slow (type 1 fiber) isoform of lactate dehydrogenase (*LDHB*) was upregulated, even though *LDHA*, the predominant skeletal muscle fast isoform, was unchanged.
  At the same time key enzymes for glycogen metabolism and pathway regulators were found to be downregulated. It is well known that NM muscles are enriched in glycogen stores [83], but the molecular origin of this phenomenon has remained unknown. Based on the gene expression studies by Sanoudou *et al*., the gene changes show a reduced reliance on glycolytic energy production above and beyond that expected from a shift from fast to slow fiber types in many NM patients. This could be the reason for the increased number of glycogen deposits in NM muscles. Moreover, several glycolytic enzymes (i.e. phosphofructokinase (*PFK*) and lactate dehydrogenase) bind actin.
  It is known that fatty acid oxidation is increased in NM (because of an increase in type I fibers), and as expected the related genes were found altered in the gene

expression study, such as PPARD, PPARalpha, PPARgamma, and RXRA, promoting fatty acid oxidation.
The most downregulated gene in NM was the uncoupling protein 3 (*UCP3*) (range 5.1- to 12.6-fold for three probe sets), while UCP3 protein was found to be increased by immunoblotting. This observation suggests the existence of a negative feedback loop where increased protein levels downregulate *UCP3* gene expression. An inverse relation between mRNA and protein levels for UCP3 has been reported, i.e. in normal muscle this protein is the most abundant in human fast type 2B fibers [106], whereas mRNA expression is directly correlated with percentage of slow type 1 fibers [107]. In NM muscles, UCP3 regulation appears reversed, with mRNA levels indicating an increase in slow type I fibers, while there is no clear correlation between fiber type proportions and UCP3 protein levels. UCP3 has been reported to be involved in the regulation of mitochondrial fatty acid transport and glucose metabolism in skeletal muscle, protection against excessive production of reactive oxygen species, and regulation of whole-body energy metabolism [108]. Thus, the increase in UCP3 protein levels and the subsequent enhancement of fatty acid oxidation is consistent with the shift from the glycolytic to oxidative pathway of energy production, from fast fibers to slow fibers.

- *1.2.3.2.3 Alterations in Ca^{2+} pathways*

The gene expression study revealed an aberrant expression pattern of genes involved in calcium (Ca^{2+}) homeostasis, such as *ATP2A1*, *ANX7*, *CASQ2*, *DMPK*, and *HSBP2* that are responsible for the translocation of Ca^{2+} from the cytoplasm to the sarcomplasmic reticulum (SR) [109, 110, 111], suggesting an overall increase in cytosolic Ca^{2+}. The increase in cytosolic Ca^{2+} could be also explained by the reported changes (*FADS1*, *PAFAH1B1*, and *CYP2J2* genes*)* in the arachidonic acid metabolism [112]. The increase in cytosolic Ca^{2+} has been correlated to insulin resistance [113] and the presence of altered genes related to a mild form of insulin resistance in NM patients has been identified in the gene expression study. For example, hexokinase and insulin receptor substrate (IRS1), two proteins with potentially significant roles in insulin resistance, are downregulated [118].
The gene expression study also revealed a downregulation of calcium-regulated signaling molecules that might be caused by a negative-feedback loop where the chronic increased cytoplasmic Ca^{2+} level leads to a compensatory reduction in transcription of corresponding genes, similar to observations in muscular dystrophies [119, 120]. Moreover, changes in Ca^{2+} homeostasis could affect sarcomere structure and muscle contraction.

1.2.4 Mouse models of NM

- Several mouse models of NM exist with varying degree of disease severity. In this study we took advantages of three mouse models: a nebulin knock-out mouse, an ACTA (H40Y) knock-in mouse, and an alpha-Tropomyosin$_{slow}$(Met9Arg) transgenic mouse.
-

1.2.4.1 Nebulin knock-out mouse

The nebulin knockout mouse (NKO) is the one generated by Bang *et al.* [25]. It develops progressive sarcomeric disorganization, misalignment, and Z-line

widening reminiscent of NM, resulting in death within 11 days after birth due to decreased milk intake and muscle weakness.
However, although this mouse line develops some features of NM, it is not an optimal model for NM since no patients with complete absence of nebulin have been described.

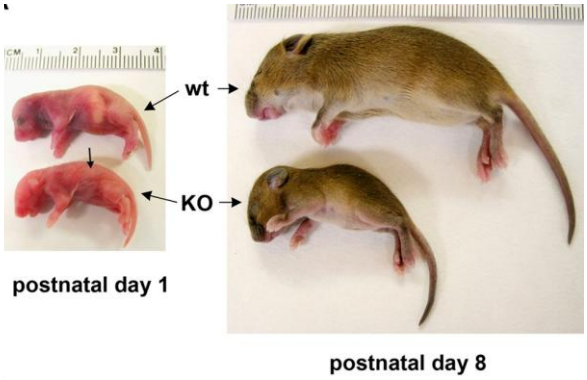

Fig.4 NKO mice 1-day and 8-days old compared with the wt littermates. The NKO mice are small and die at 8-11 days after birth (Bang et al, JBC, 2007)

1.2.4.2 alpha-Tropomyosin$_{slow}$(Met9Arg) transgenic mouse

This model is a mouse line with transgenic expression of the dominant negative alpha-Tropomyosin$_{slow}$(Met9Arg) mutant (human TPM3 gene) in skeletal muscle (Tm$_{slow}$(Met9Arg) Tg; 13), a mutation identified in a childhood form of NM [221]. This mouse line develops a mild form of NM but exhibits all features of the human disease, including the presence of nemaline rods in skeletal muscle as well as an increase in the number of slow/oxidative fibers and late onset muscle weakness starting from around 7 months of age.
Similar to observations in human patients, gene expression profiling on this mouse model revealed activation of satellite cells and focal repair processes in multiple muscles, a feature that was previously not considered characteristic for NM. On the other hand, no signs of metabolic changes were found except for in the most affected diaphragm where a number of mitochondrial genes involved in energy production were downregulated. This suggests that reduced energy production is a secondary effect observed in more severe stages of NM, such as in the diaphragm of Tm$_{slow}$(Met9Arg) Tg mice and the majority of human patients included in the gene expression study [217].

1.2.4.2 ACTA (H40Y) knock in mouse

This is a knock-in mouse model expressing a mutant form of α-skeletal actin, containing a single AA change (H40Y) that causes an early onset dominant form of NM [18]. This mouse line exhibits an early onset severe form of the disease and displays all the clinical and pathological features of patients with the ACTA1(H40Y) mutation, including the presence of both cytoplasmic and nuclear nemaline rods. Similar to patients harboring the ACTA(H40Y) mutation, Acta1(H40Y) KI mice contained nemaline rods both in the cytoplasm and the nucleus and died early, i.e. 61% of male and 3% of female Acta1(H40Y) KI mice died by 13 weeks of age. Forelimb strength was significantly reduced in KI mice and Acta1(H40Y) KI mice had watery eyes and kyptosis (drooping eyelids). Furthermore, Acta1(H40Y) KI mice exhibited muscle atrophy and an increased number of slow oxidative fibers. In addition, Acta1(H40Y) KI muscle contained areas of myofiber degeneration, infiltrating mononucleated cells, and fibers with internal nuclei, indicating ongoing chronic repair and regeneration as recently recognized as characteristic features of NM [12, 15].
Besides fiber atrophy, other changes are likely to contribute to the muscle dysfunction in Acta1(H40Y) KI mice, such as a reduced twitch force of isolated whole muscles, that suggests changes in the quality of contraction. Interestingly, ACTA (H40Y)KI mouse muscle has been shown to have a reduced proportion of strongly bound myosin cross-bridges during contraction that well correlate with the recent findings in NM patients (Hardeman lab, data not published).

The ACTA (H40Y)KI characteristics are reported in fig.5.

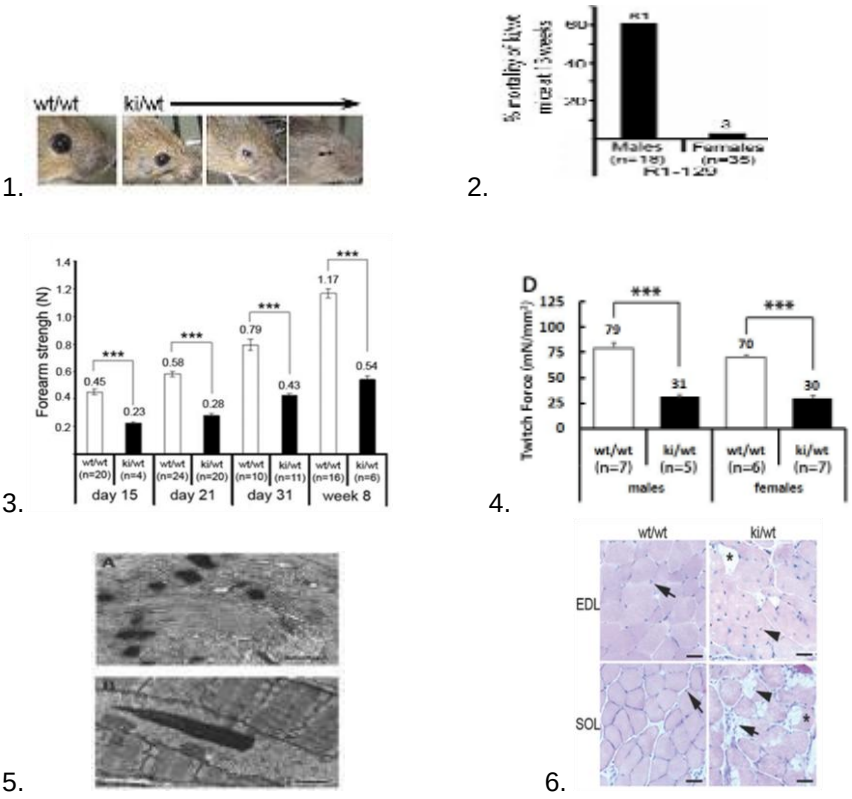

Fig.5 Major characteristics of ACTA (H40Y)KI mouse phenotype: 1.Atrophy of facial muscles evident in some knock-in mice 2. Increased mortality 3. Marked decrease in forearm grip strength 4. Decrease in force 5. Cytoplasmic (5A) and nuclear (5B) rods 6. Evidence of myofiber repair/regeneration (Hardeman lab, data not published)

1.3 microRNAs

1.3.1 miR biogenesis

MiRs (miRs) are a class of small RNAs, usually 20-24 nucleotides long, that function as post-transcriptional regulators of gene expression [122]. The pathways in which miRNAs are involved are numerous, including cell proliferation, differentiation, apoptosis, and development [123, 124, 125]. As they regulate the expression of fundamental physiological processes, their deregulation leads to many disorders, such as cancer [126, 127, 128] and neuromuscular disorders [129, 130]. Most miRs are located in introns of protein-coding genes and in intergenic regions and their transcription is operated by RNA polymerase II (Pol II) [131, 132], except for some that are transcribed by RNA polymerase III (Pol III) [133]. However, miR biogenesis is a long process, where the transcribed sequence is subsequently modified by endonucleolytic proteins.

The primary miR (pri-miRNA) is capped and polyadenylated and is a long hairpin structure with unique features that distinguish it from the various RNA stem-loop-like structures present in the nucleus. In particular, a long imperfect stem of approximately 30 bp is flanked by single-stranded RNA segments at its base [134, 135]. This peculiar structure is recognized by the Microprocessor complex, that contains Drosha (RNase III enzyme), the RNA binding protein DGCR8 [136, 137, 138] and other proteins [139, 140]. The region of the pri-miRNA, containing the junction single-stranded RNA–dsRNA, is identified by DGCR8 [135], and Drosha operates the first cut at a distance of approximately 11 bp from the junction. This process occurs co-transcriptionally, before the splicing of the host RNA [141, 142].

As all RNAse III products, the resulted structure, called precursor miR (pre-miR) has 2 nucleotides protruding at the 3' end [143]. It is a long truncated harpin formed by 60 nt with a minimal double-stranded stem length of 16 bp [144]. These structural elements are essential for the recognition by Exportin-5 (Exp-5) [145, 146]. This is the protein that in cooperation with the guanine triphosphatase (GTPase) Ran transports the pre-miRNA from the nucleus to the cytoplasm, allowing it to be recruited by Dicer (another RNase III enzyme), maybe passing it directly to Dicer or via additional components [147]. The 3'-ends generated by Drosha are recognized by Dicer that cleaves the pre-miRNA near the terminal loop, generating a miRNA–miRNA* duplex having 2-nt 3' overhangs at both ends [148, 149].

Human Dicer is a multidomain protein of approximately 200 kD. The N-terminal DEAD-box helicase domain, a domain of unknown function (DUF283), a PAZ domain, two conserved catalytic RNase III domains (RIIIA and RIIIB) and a C-terminal dsRNAbinding domain (dsRBD) are contained in this protein [150]. RIIIB and RIIIA cut the 5' and 3' arms of the pre-miR, respectively [151, 152]. Different members of the RISC loading complex (RLC) cooperate with Dicer during its function [153, 154]. Among them there are members of the argonaute (AGO) family [155, 156], HIV-1 transactivation response (TAR), RNA-binding protein (TRBP) [157, 158], and possibly other proteins. The miRNA strand (guide strand) of the duplex resulting from Dicer cleavage of the pre-miRNA is loaded onto AGO to form the RNA-induced silencing complex (RISC or mi-RISC) and the released other strand (passenger strand or miRNA*) is degreaded [157, 159, 160]. The strand selection is a crucial step of the miR biogenesis; it has suggested that thermodynamic stability of the ends of the miRNA duplexes [161, 162], structural features of the miRNA/miRNA* duplex (e.g. positions of base mismatches) [163, 164, 165], and sequence composition [166, 167] are the factors contributing to strand selection. However cases where both miRNA and miRNA* strands may be involved in RISC-mediated gene silencing have been reported [165, 168].

The miR biogenesis illustrated until now is the canonical pathway, but ''non-canonical'' pathways of miRNA biogenesis exist too [169]. One of the most common is involving sequences spliced out of mRNA transcripts that are pre-miRNA-like introns called mirtrons [170, 171, 172]. As they are already pre-miR-like sequences, they bypass the Drosha requirements, following the canonical pathway [173]. In fig.6 are shown all the known canonical and non-canonical miR biogenesis pathways [174, 175, 176].

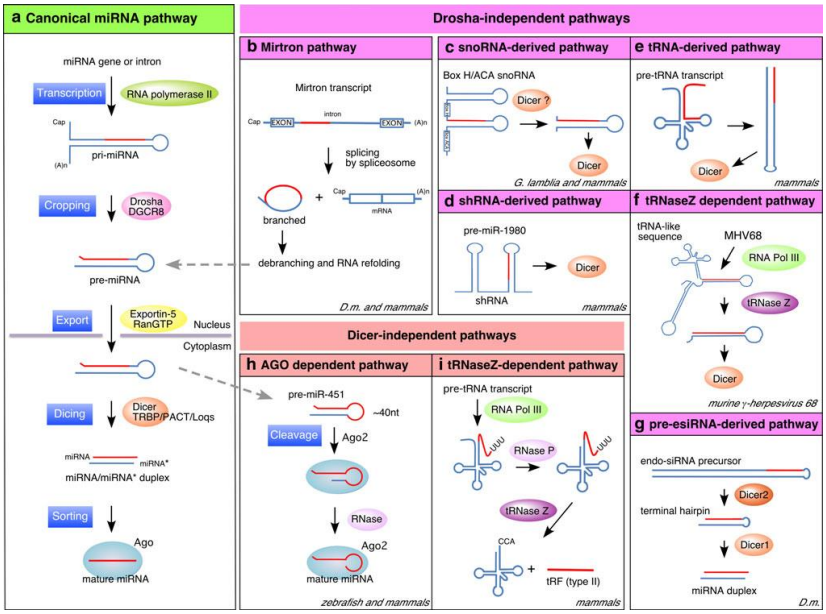

Fig.6 Canonical and non canonical pathways of microRNA biogenesis (Miyoshi et al, Molecular Genetics Geomics, 2010)

1.3.2 miRNA-mRNA interaction

A central goal for understanding miR functions has been to understand how they recognize their target message. The 5' region of the miR called the SEED sequence is important for target recognition with nucleotides from 2 to 7 that pairs with the 3'UTR of the mRNA target [177, 178, 179]. The region of mRNA pairing with the SEED sequence has been conserved in one-third of human genes [180].

There are four different types of sites associated with messages downregulated by miRNAs. This includes one 6mer, two 7mers, and one 8mer (fig.7).

The 6mer is the perfect 6 nt match to the miRNA seed (miRNA nucleotides 2–7) [180]. The best association is the 7mer site, in which the seed match is augmented by a match to miRNA nucleotide 8 [177, 178, 179]. The seed match augmented by an A at target position 1 is typical of the 7mer-A1 site, while in the 8mer site the seed match is flanked by both the match at position 8 and the A at position 1 [180].

Not perfect matches in the SEED sequence have also been observed in functional miRs.

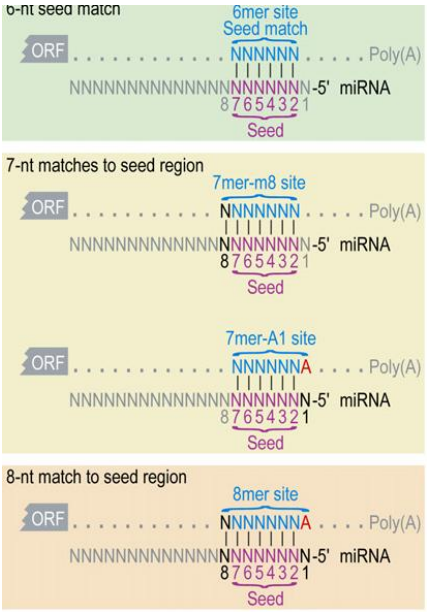

Fig.7 Canonical miRNA complementary sites (Grimson et al, Molecular Cell, 2007)

However, seed sites do not always confer repression, and when repression occurs, the degree of repression is highly variable in different UTR contexts. Interestingly, in a tissue in which a miR is highly expressed, messenger RNAs of genes encoding proteins with an important role in the tissue have 3'UTRs that are depleted in 7mer sites, presumably to avoid acquiring sites for the co-expressed miRNAs that would compromise their function [[181]].

The mechanism of specificity can be explained at least partly in terms of site accessibility and site affinity, which influence the association and dissociation of the silencing complex. It has been shown that the context features that help specificity miRNA targeting is important [[182]], i.e. there are supplemental pairing outside of the seed region, particularly to nucleotides 13–16 of the miRNA, that could decrease the dissociation rate of the bound RISC. Moreover the accessibility of the seed site on the mRNA could be increased by the presence of weak mRNA secondary structure, conferred by the presence of AU enrichment in the region immediately flanking the SEED region.

It is well known that miRs can have multiple targets, and multiple sites on the same mRNA target. This allows one miR to regulate the gene expression of hundreds of targets. In the same way, one target can be regulated by more than one miR. The possibility that two or more sites for one or more miRs on a mRNA target lead to a cooperative regulation of gene expression has been investigated. It has been observed that multiple sites for the same miR cooperate in increasing repression, while the overlapping or near-overlapping sites for two different miRNAs cause less

downregulation than more distantly spaced sites, possibly due to cooperative contacts with the repressive machinery [182].
Recently, a new class of miR targets containing simultaneous 5'UTR and 3'UTR interaction sites has been identified [183]. Of these, many miRNAs with their 3'-end interaction sites in the 5'-UTRs turn out to simultaneously contain 5'-end interaction sites in the 3'-UTRs, leading to a combinatory interactions between a single miRNA and both end regions of an mRNA.

1.3.3 microRNAs-mediated gene expression regulation

It is known that miRs can inhibit gene expression by affecting protein synthesis or by destabilizing mRNA structure, leading to its degradation. The regulation at the translational level is the most common. However, whether it occurs at the initiation or post-initiation step (or both) is not yet well understood. In the next paragraphs the most recent models of gene expression regulation by miRs are discussed (fig.9).

1.3.4. Models of translational repression

1.3.4.1 Repression at the initiation step

During initiation of transcription the presence of several initiation factors (eIF) and in particular the ability of one of them (eIF4G) to interact simultaneously with eIF4E (bound to the mRNA 5'UTR) and PABP1 (bound to the mRNA 3'UTR), brings the two ends of the mRNA in close proximity [184, 185].
The presence of a limited sequence homology between AGO proteins and the cap-binding region of eIF4E [186] has recently been reported. Even if limited, the similarity includes two aromatic residues crucial for the cap binding of eIF4E [186], suggesting the possibility of competition between AGO2 protein and eIF4E for cap binding, thus preventing translation initiation. The RISC complex is directed to the 3'UTR thanks to the miR interaction with the seed site of the target, and the circularization of the mRNA allows AGO2 protein interaction with the cap-binding site protein. Moreover, the requirement for multiple miRNPs or tethered AGO molecules for robust repression could be necessary to increase the likelihood of AGO association with the cap [187, 188, 189, 190].

1.3.4.2 Repression by preventing 60S subunit joining

One model of translational initiation repression by miRs comes from the observation that eiF6 and 60S ribosomal subunits co-immunoprecipitate with the RISC complex [191]. eiF6 is involved in the biogenesis of the 60S subunit in the nucleolus and is associated to the this subunit in the cytoplasm [192, 193, 194]. It is supposed that the RISC complex interacts with the eiF6 factor, promoting the repression of the transcription by the impediment of the 60S joining to the translational machinery. This is supported by the evidence that partial depletion of eIF6 rescues mRNA targets from miRNA inhibition [191]

1.3.4.3 Repression at post-initiation steps

In the last years several studies have shown that mRNA repression through miRs is not occurring only at the translation inititation step. The mRNA targets, together

with miRNAs and AGO proteins, have been found associated with polysomes, suggesting that gene expression repression is possible after the initiation of translation [195, 196, 197]. It has to be considered that not only one miR-directed RISC complex bound to the mRNA is able to repress gene expression alone. Thus, it is possible that the miRISC-mRNA found to be associated with polysomes reflect the failed translation repression, and thus a productive translation [189, 190].
However, a model of post-initiation repression has been suggested by Peterson et al [198], that proposed a drop-off model, in which miRs induce the drop off of the ribosome and the consequent premature termination of translation. The post-initiation repression has been reported in IRES-containing targets, where the translation is not started in the conventional way, but with the entry of the ribosome directly on the IRES (Internal Ribosome Entry Sites) [199].
The mechanism for the modulation of elongation or termination processes through miRs has not yet been elucidated. However, it has been hypothesized that initiation and post-initiation repression can occur together; it is possible that initiation is always inhibited and that the simultaneous repression of the elongation step causes the presence of more ribosomes stopped on the mRNA [122].

1.3.4.4 mRNA deadenylation and decay

Recently studies have shown that gene expression repression of miRNAs targets is sometimes associated with their destabilization, revealed by low levels of mRNA [200, 201, 202]. mRNA degradation can be achieved through two different pathways, both of them starting with mRNA poly(A) tail shortening. After that or degradation of mRNA by 3′→5′ decay, catalysed by the exosome, or by 5′→3′ degradation after removing of the cap, catalysed by the exonuclease XRN1, can occur [203]. The mRNA under degradation are moved to the P-bodies, cellular structures that are enriched in mRNA-catabolizing enzymes and translational repressors [204, 205]. It is evident that the association with AGO instead of eIF4E leads to a disruption of mRNA structure, making it more vulnerable to degradation, but it is not clear whether the degradation is always secondary to translational repression.
Recently it has been demonstrated that under certain conditions, or in specific cells, the miRNA-mediated repression can be reversed or prevented [206, 207, 208, 209]. The possibility and the ability of mi-RISC complexes to be removed from the target mRNA confer a much more dynamic regulation function to the miRs.

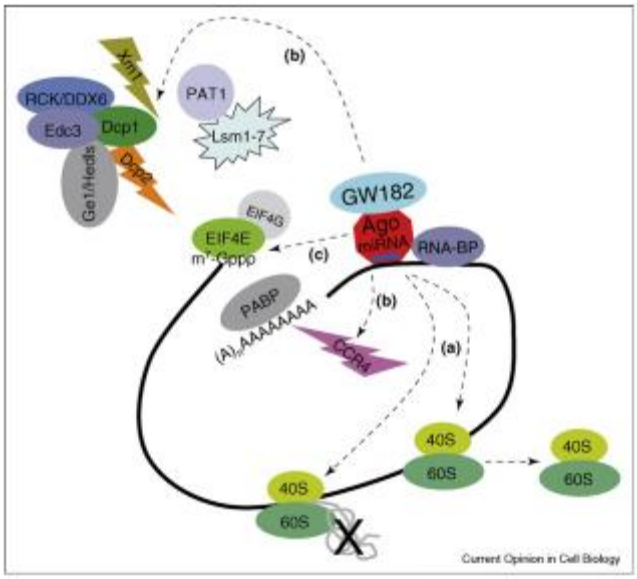

Fig.8 microRNAs mediate gene expression through multiple mechanisms: (a) microRNAs could repress translationally competent ribosomes after initiation, either promoting ribosome drop off during elongation or cotranslational degradation of the nascent polypeptide, (b) microRNAs promote deadenylation and degradation of their targets.(c) microRNAs block translation initiation through competition for the cap structure between microRNP and EIF4E
(Maroney et al, Nature Structural and Molecular Biology, 2006)

1.3.5 miRs in serum

One of the most recently discoveries regarding miRs is their ability to circulate in serum, remaining stable. In a recent study circulating miRs have been subjected to severe conditios, such as boiling, very low or high pH, extended storage, and 10 freeze-thaw cycles, in which they have been shown to be stable [[210]]. As well as their stability under these hard conditions, they are protected in the serum from RNAse activity [[211], [212]], and the mechanism at the basis of this protection has been object of several recent studies.
It is thought that inclusion in lipid or lipoprotein complexes protects the circulating miRs from RNAse digestion [[213]]. Moreover it has been reported that miRs are exchanged between cells, going out from one donor cell, circulating in the intracellular space, and being included in the recipient cell. During this exchange miRs are protected either in microvescicles (up to 1 μm) or in small membrane vesicles of endocytic origin called exosomes (50 – 90 nm) [[214], [215]]. The miRs are included in the multivesicular bodies (MVB) in their precursor form (pre-miRNA) and then associated with exosomes. The MVBs fuse with the plasma membrane, releasing the exosomes in the circulating compartments and bloodstream. When the exosomes contact the recipient cell, the miRs are donated to that cell by

endocytosis. At this point the pre-miR is processed by DICER and loaded into the RISC complex as an endogenous miR. However it remains to be elucidated if pre-miRNAs or mature miRNAs are involved in this process [216].
It has been reported in the literature that altered levels of miRs in the serum can be related to pathologies such as cancer and hypertrophy, and can be used as biomarkers [217, 218].

1.3.6 Target prediction algortihms

In the past years several bioinformatic tools for miR target prediction have been developed, based on the rules for miRNA-mRNA interaction reported in the literature. Here the most commonly used target prediction tools available in the web are described.
The miRanda target prediction algorithm [219, 220] predicts targets adopting a three steps procedure: first miR recognition elements (MREs) for the miR of interest are searched among the mRNA sequence; then the free energy of the putative pairing is calculated, and in the end the predicted targets are filtered by evolutionary conservation. The definition of cutoff parameters for the algorithm is subjected to heuristics, which follow the incremental knowledge about the experimentally verified MREs.
The TargetScan algorithm [221] is mainly based on the hypothesis that highly conserved miRNAs are more involved in regulation and that membership in large miRNA families lead to more targets. As a consequence it includes in input sequences the miRNA mature sequences as well as a set of orthologous 3'-UTR sequences conserved in multiple organisms. This algorithm is based on a different three steps procedure than miRanda. First perfect Watson-Crick complementarity along the SEED sequence is required; then it extends the seed matches in both directions, allowing wobble pairs and stopping at the first mismatch encountered. In the end the algorithm explores the remaining 3' region of miRNA and spreads sequence matching for the 35 nucleotide away from the seed. A thermodynamical evaluation is performed on the miRNA-mRNA duplex. The entire process is for performed for each of the organisms, belonging to the UTR dataset. In this way the conserved miRNA target pairs are taken into account.
RNAhybrid [222] is based on the prediction of RNA secondary structure, exploring the conformational space of all possible secondary structures established between the miRNA and target sequences. A statistical analysis of thermodynamical evaluation is carried on the predicted interactions. The most favorable structures are referred to as minimum free energies (MFEs) and are scored by the p-value.
PITA [223] stands for Probability of Interaction by Target Accessibility. This target prediction method is based on the evaluation of MRE site accessibility based on thermodynamics. Moreover the interaction score is weighted by also taking into account the steric hindrance of the entire ribonucleoprotein complex.

1.3.7 microRNAs in Nemaline Myopathy

In a recent study, a large number of miRs were shown to be dysregulated in 10 major congenital muscle disorders, including NM, suggesting that miRs may play important roles in the regulation of pathological pathways leading to muscle dysfunction [224]. Interestingly, while some miRs were dysregulated in all the

studied muscle disorders, suggesting their involvement in common regulatory or compensatory mechanisms, others were dysregulated only in a specific disease. In particular NM patients were characterized by a miR expression profile distinct from that of any of the other muscle disorders, possibly reflecting the fundamental difference between NM and other neuromuscular diseases. Thus, more than 150 miRs were dysregulated in NM, more than in any of the other studied disorders, and 36 miRs were specific to NM, suggesting the existence of unique regulatory mechanisms modulated by miRs underlying the pathology of NM. In NM, as in all the studied muscle disorders, the vast majority of dysregulated miRs (140 of the 153) were upregulated; 7 of the upregulated miRs (hsa-miR-125a, hsa-miR-128a, hsa-miR-128b, ambi-miR-4983, hsa-miR-28, hsa-miR-362, hsa-miR-542-5p) were identified as class predictor of the NM compared to normal muscle, with 100% of accurancy.

Target prediction analysis was carried out in the study and to analyze the role that the differentially expressed miRNAs play in the regulatory networks in muscular disorders, Eisenberg et al. used the KEGG database and the DAVID bioinformatics resources [225]. In this way they identified significantly overrepresented biological pathways among the miR predicted targets.

In NM, the pathways more enriched by predicted targets of dysregulated miRs were the focal adhesion pathway (involved in cell communication), the calcium signaling and TGF beta signaling pathways, as well as the regulation of actin cytoskeleton. Enrichment in the MAPK signaling pathway, the T cell receptor signaling pathway, tight junction, ECM receptor interactions, and inositol phosphate metabolism was also shown, but with a lower significance.

2.RESULTS

2.1 Difficulties in the beginning of the project

The aim of the project was to study the role of microRNA (miR)-regulated pathways underlying Nemaline Myopathy (NM) based on the use of mouse models with mutations directly mimicking human NM-causing mutations. The first step was to investigate the miR expression profile.

Initially, the idea was to have a complete overview on dysregulated miRs in the mouse models to further compare them with the miRs already found to be dysregulated in NM patients [212]. An alternative approach could be to select the most changed miRs from the human patient study and investigate their expression in our mouse models. However, we hypothesized that also other miRs may be dysregulated that may have been missed in the human study because of the heterogeneity of the human samples. For this reason we found it useful to study the miR expression profile in a cleaner system such as a mouse model.

The first mouse model that we had the possibility to work on was the nebulin knockout (NKO) mouse, developed by Bang *at al.* [25]. Although no patients with complete absence of nebulin have been described, these mice develop progressive sarcomeric disorganization, misalignment, and Z-line widening reminiscent of NM, resulting in death within 1-2 weeks after birth due to decreased milk intake and muscle weakness. For a pilot study, we selected three miRs (miR128, miR-181, and miR-196a), which were highly and uniquely expressed in human NM patients. By quantitative realtime PCR (qRT-PCR) (QuantimiR kit – SBI) we confirmed their overexpression also in the diaphragm and tibialis anterior of NKO mice compared to wildtype (WT) (data not shown). Based on this result we went on to investigate the whole miR expression profile in diaphragm and tibialis anterior from NKO mice compared to WT using the Illumina miR microarray platform, which was supposed to be robust and cost effective. However, unfortunately the scanned chips showed errors not related to sample quality but to the chips themselves and although we repeated the miR microarray experiment twice, we got no useful results. For that reason we decided to move to another system for analysis of the miR expression profile and the Illumina chips have subsequently gone out of production

At that time we had the opportunity to start a collaboration with Prof. Hardeman, who provided us with two mouse models: the Tm_{slow}(Met9Arg) Tg and the ACTA1(H40Y)KI mice that better recapitulate the NM patient characteristics than the NKO mouse line. In particular, the Tm_{slow}(Met9Arg) Tg mouse shows the mildest phenotype, with onset of the disease at 8 months of age, while the ACTA1(H40Y)KI mice have a severe form of the disease, resulting in death of males around 10 weeks of age. Intriguingly, ACTA1(H40Y)KI females are less severely affected than the males and are able to breed.

Using the quantimiR profiling System (System Bioscience) we investigated the miR expression profile in diaphragm and tibialis anterior muscle from 3- and 10-week-old ACTA1(H40Y)KI mice compared to WT (biological triplicates). This system is based on qRT-PCR technology and provides two 384-well plates containing probes for all miRs reported in miRBase (database of published miR sequences and annotation). This approach turned out to be much more cumbersome than expected since for each sample the operator is required to move each probe from the stock plate to the sample plate and subsequently add the PCR mix. This is not only time consuming but also causes inaccuracies due to pipetting errors given the high number of samples as well as the high sensitivity of the real-time PCR instrument. Also, no technical replicates were provided so it was difficult to evaluate if the results were reliable and the biological replicates often showed conflicting results. For that reason we concluded that this was not the optimal approach to adopt for our studies.

Finally, owing to these technical problems we decided to carry on the analysis of miR expression levels only on miRs pre-selected from the most upregulated miRs in NM patients [212].

2.2 Gene expression microarray study on the ACTA(H40Y)KI mouse

As discussed above (paragraph 1.2.4.2), the ACTA (H40Y)KI (KI) mouse model shows gender-related differences in the development of the phenotype, with males developing an early onset of the disease, resulting in death at around ten weeks, while females show a milder phenotype and survive up till at least a year of age. To determine the molecular basis for the development of the disease and the difference between males and females, we performed the gene expression study on diaphragm (DIA) and tibialis anterior (TA) muscle of WT and KI mice from 3-week-old males and 10-week-old males and females. The study was performed in triplicates and the correlation (expressed in r^2 value, the closer it is to 1, the better the samples correlate) between biological triplicates was analyzed and reported for each condition in the following paragraphs. GeneSifter was the software used for the analysis. The complete lists of altered genes in each condition with fold ≥ 1.4 and pvalues <0.05 are reported in Appendix A.

2.2.1 Gene expression analysis of 3-week-old males

Biological triplicates of 3-week-old males correlated well with an r^2 value over 0.9 for both DIA and TA. The DIA of 3-week-old males showed the highest level of gene dysregulation, presenting 493 genes with altered expression with fold changes ≥ 1.4 and p-values < 0.05; in particular 421 genes were downregulated and 72 were upregulated. In terms of fold change, downregulated genes were most changed, with fold changes between 1.5 and 8.1, while upregulated genes showed differences ranging from 1.5 to 2.3 fold change. When the fold change cut-off was set to 3, 187 genes were found to be downregulated, of which the major part (110) were involved in metabolic processes, in particular metabolism, such as protein, lipid, and nucleic acid metabolic processes.

The most downregulated gene was orosomucoid (Orm) (8.1 fold), also called alpha-1 acid glycoprotein, which is an abundant plasma protein that works as immune-modulator induced by stress conditions such as infections. The role of Orm has been investigated in adipose tissue of obese mice [214] and was shown to suppress excess inflammation that otherwise disturbs energy homeostasis.
Other genes involved in the acute phase response were highly downregulated; in particular four members of the serpin family: serpind1 (5.4 fold), serpina10 (6.1 fold), serpinf2 (6.5 fold), and serpina6 (6.5 fold). Serpins are a group of proteins with similar structure, first identified as a set of proteins able to inhibit proteases. Serpind1, serpina10, and serpinf2 inhibit thrombin, coagulation factors Xa and Xia, and plasmin, respectively. Serpina6 is a non-inhibitory member of the serpin-family and is the high-affinity transport protein for glucocorticoids in vertebrate blood, playing a crucial role in efficient glucocorticoid action in physiology. As illustrated in fig.9 the downregulated serpins are involved in pathways that activate the complement system, a proteolytic cascade in blood plasma, and a mediator of innate immunity.

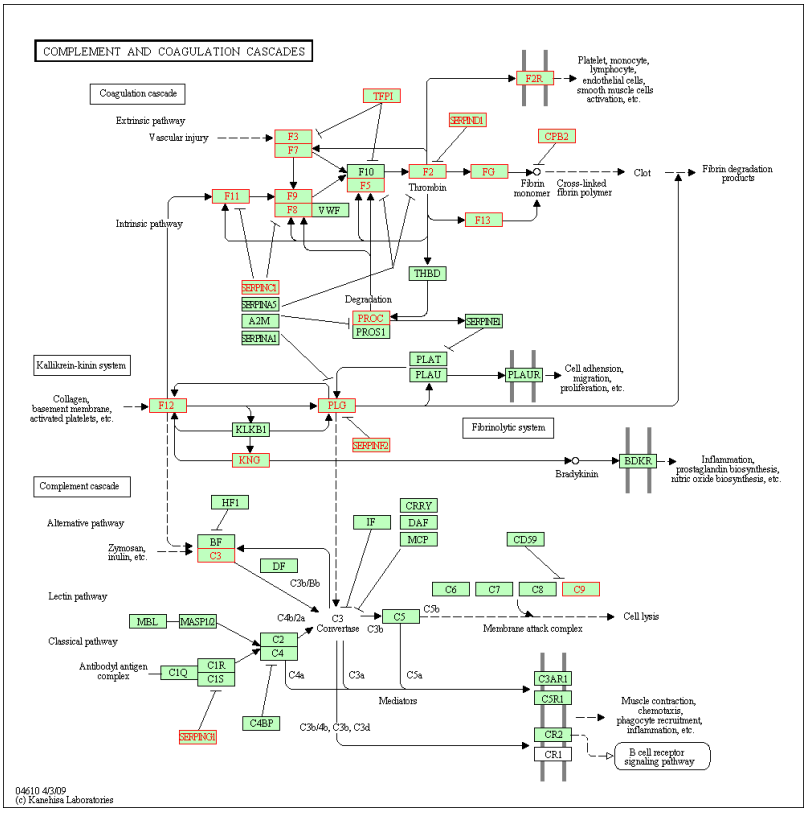

Fig.9 Complement and coagulation cascade KEGG pathways. In red are highlighted genes found dysregulated in DIA of 3-week-old males KI

Serpins are also involved in the coagulation cascade in which plasminogen (PLG), kininogen1 (KNG), kininogen2 (KNG2), carboxypeptidase B2 (CPB2), and fibrinogen (FG) are involved as well. These genes are also downregulated 5.1, 5.6, 4.3, 5.8 and 4.6 fold, respectively.

Glycolysis was also impaired in the DIA of 3-week-old males, where the glucose-6-phosphatase catalytic-subunit (G6PC), and fructose-1,6-bisphosphatase 1 (FBP1), a gluconeogenesis regulatory enzyme, that catalyzes the hydrolysis of fructose 1,6-bisphosphate to fructose 6-phosphate and inorganic phosphate, were downregulated (2.4 and 5.3 fold, respectively).
Among the upregulated genes, the most altered gene was RIP13, also known as nuclear receptor corepressor 1 (Ncor1), a transcriptional repressor (2.3 fold).

Muscle specific genes such as tropomyosin 3 (TPM3), dystroglycan (DAG1), and myocyte enhancer factor 2 (Mef2C) were also upregulated (1.6, 1.7, and 2.1 fold, respectively).

In the TA of 3-week-old males the expression of 122 genes were shown to be changed with fold changes ≥ 1.4 and p-values < 0.05: 115 upregulated and 7 downregulated.

The most downregulated genes were selenoprotein P1 (Sepp1), an extracellular antioxidant involved in the transport of selenium (1.5 fold), and acetyl-coenzyme A acyltransferase 2 (ACAA2), involved in mitochondrial fatty acid metabolism (1.6 fold). Other mitochondrial genes were upregulated, including methyltransferase C20orf7 homolog (2310003L22Rik) (2.0 fold), mitochondrial processing peptidase beta (PMPCB) (1.8 fold), NADH dehydrogenase (ubiquinone) (1.7 fold), subunit D of the succinate dehydrogenase complex (SDHD) (1.7 fold), apoptosis-inducing factor, mitochondrion-associated 1 (AIFM1) (1.7 fold), and mitochondrial ribosomal protein L20 (MRPL20) (1.6 fold).

2.2.2 Gene expression analysis of 10-week-old males

Biological triplicates of 10-week-old males showed a correlation value over 0.9 in TA, while in DIA two samples showed a lower correlation value and were therefore removed from the analysis.

In the DIA, 41 genes were dysregulated with fold changes ≥ 1.4 and p-values < 0.05: 20 were upregulated and 21 downregulated. The most dysregulated genes encoded proteins involved in the cell cycle, where G0/G1 switch gene 2 (G0S2) and PCI domain containing 2 (PCID2) were downregulated (2.3 and 1.4 fold, respectively) and damaged-DNA recognition protein 1 (DRP1) was upregulated (1.5 fold). 15.4% of altered genes were involved in cellular process, 10.9% in biological regulation, 9.9% in metabolic process, and 9.4% in regulation of biological process, as showed in fig.10.

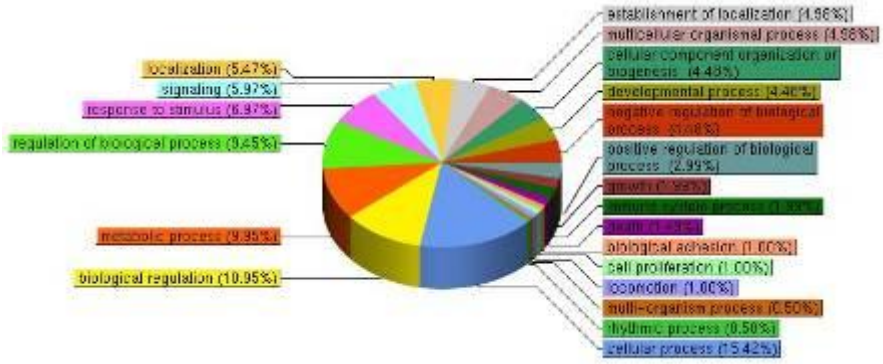

Fig.10 Genes dysregulated in DIA of 10-week-old males grouped in functional categories

When we looked more in details which were functional categories affected in cellular processes, we found that regulation of cellular processes and cellular metabolic processes were the most affected, as illustrated in fig.11.

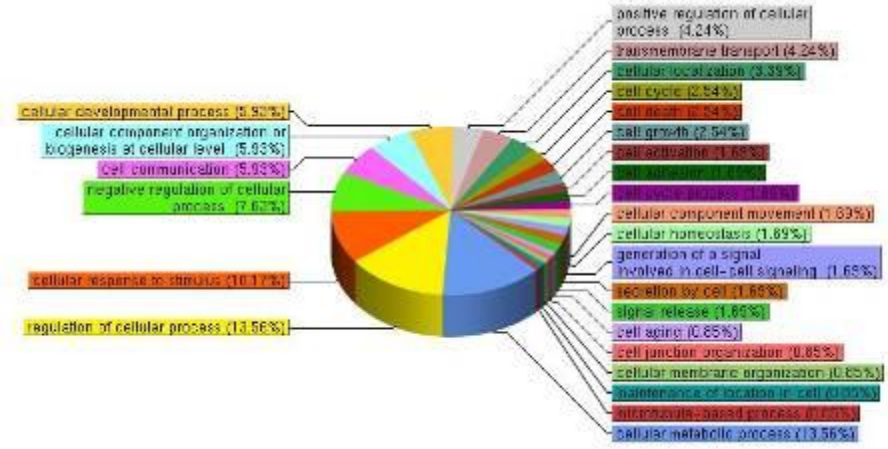

Fig.11 Functional categories affected in cellular processes by genes dysregulated in DIA of 10-week-old males

In the TA of 10-week-old males, 46 genes were dysregulated with fold changes ≥ 1.4 and p-values < 0.05: 10 were upregulated and 36 downregulated.
10.5% of altered genes were involved in cellular processes, 9.7% in biological regulation, 9.7% in regulation of biological processes, and 8.5% in metabolic processes, as illustrated in fig 12

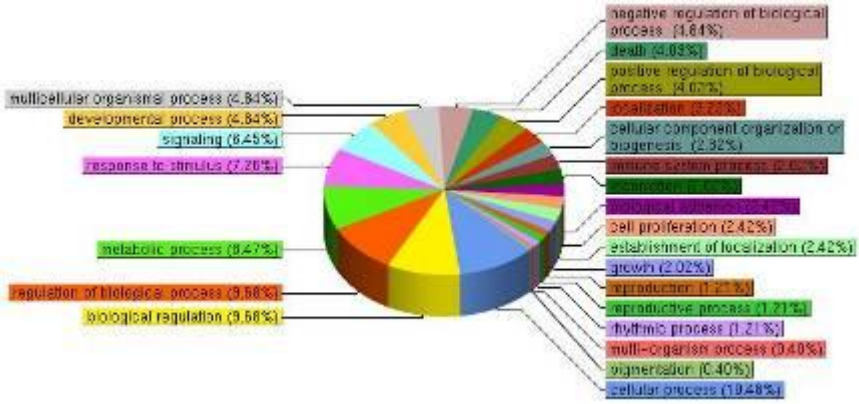

Fig.12 Genes dysregulated in TA of 10-week-old males grouped in functional categories

Of the 10.5% altered genes involved in cellular processes, 13.7% were involved in regulation of cellular processes, and when we looked more in details which were functional categories included in cellular processes, we found that 12.73% of that genes were involved in signaling transduction (fig.13).

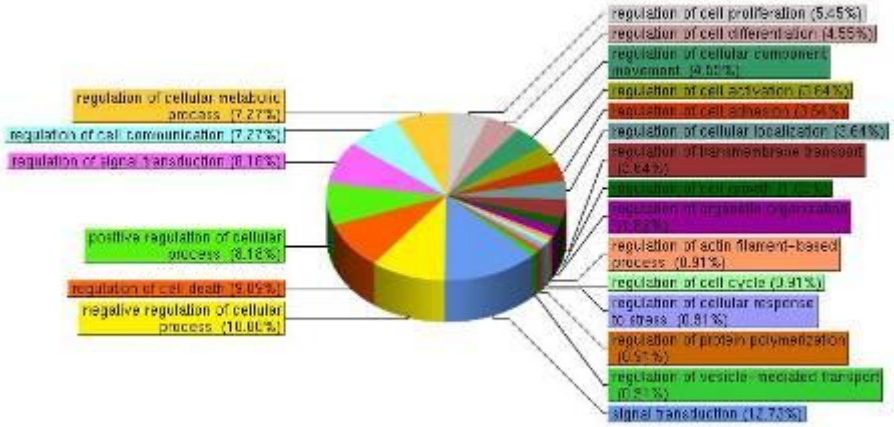

Fig.13 Functional categories affected in cellular processes by genes dysregulated in TA of 10-week-old males

In particular, 11 genes involved in signaling transduction were downregulated: adiponectin (2.0 fold), AXL receptor tyrosine kinase (1.6 fold), bone morphogenetic protein 4 (Bmp4) (1.4 fold), adipsin (CFD) (2.1 fold), forkhead box O1 (Foxo1) (1.4 fold), leptin (Lep) (2.3 fold), Map3k6 (1.5 fold), NF1GRP (1.4 fold), plasminogen

activator (1.4 fold), pleckstrin homology-like domain, family A, member 3 (Phlda3) (1.6 fold), splA/ryanodine receptor domain and SOCS box containing 1 (Spsb1) (1.4 fold). Three genes involved in signaling were upregulated: calcium and integrin binding family member 2 (Cib2) (1.5 fold), cell division cycle 34 homolog (Cdc34) (1.4 fold) and protein tyrosine phosphatase, receptor type, E (Ptpre) (1.4 fold).

2.2.3 Gene expression analysis of 10-week-old females

Biological triplicates of 10-week-old females showed a correlation value over 0.9 in DIA, while in TA two samples showed a lower correlation value and were therefore removed from the analysis.

In the DIA, 83 genes were dysregulated with fold changes ≥ 1.4 and p-values < 0.05: 61 were upregulated and 22 downregulated. Several genes involved in the cell cycle had altered expression levels and in particular Csnk2a2 (CK2), Ppp3ca (CaN), and Camk2b, which were 1.6, 1.4, and 1.4 fold upregulated, respectively. These genes code for proteins involved in the WNT pathway, as illustrated in fig 14.

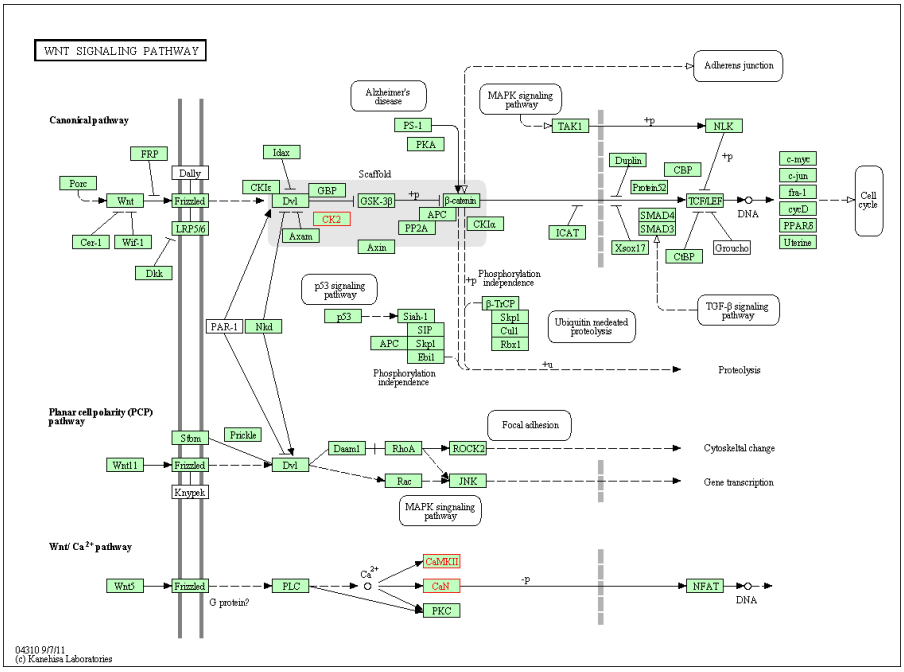

Fig.14 WNT signaling pathway. In red are highlighted genes altered in DIA of 10-week-old females KI

Many genes involved in cellular metabolic processes showed altered expression, in particular genes involved in protein metabolic process (fig 14); of these, 41.3%

were involved in protein modification, i.e CTD (carboxy-terminal domain, RNA polymerase II, polypeptide A) small phosphatase 1 (Ctdsp1) and cytokine inducible SH2-containing protein (Cish) were 1.9 and 1.8 fold downregulated, respectively, while DnaJ (Hsp40) homolog, subfamily B, member 2 (Dnajb2) and dual specificity phosphatase 1 (Dusp1) were both upregulated 1.69 and 1.52 fold respectively.

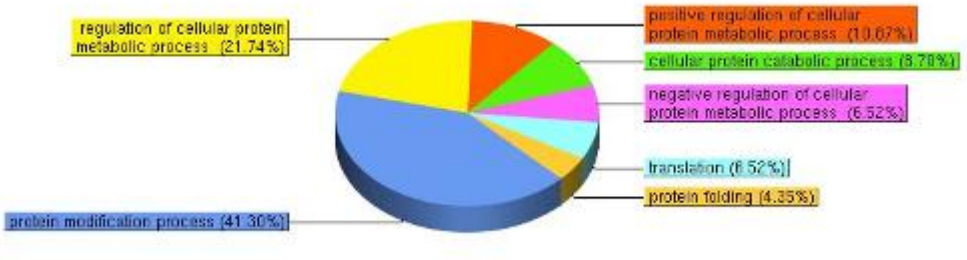

Fig.15 Functional categories affected in protein metabolic processes by genes dysregulated in TA of 10-week-old females

In the TA of 10-week-old females, 102 genes were dysregulated with fold changes ≥1.4 and p-values < 0.05: 51 were upregulated and 51 downregulated.
Hbb-b1, the beta adult minor chain hemoglobin gene, was the most downregulated gene (5.1 fold), and Hba-a1, the alpha adult chain 1 hemoglobin gene was also downregulated (2.0 fold). Moreover, Hspd1, which is involved in inflammation, was downregulated (2.0 fold).

2.2.4 Comparison between different conditions and human patients

As illustrated in fig16-17. there were not so many genes commonly dysregulated in DIA and TA in different conditions. Only in 3-week-old males there were two genes commonly dysregulated in DIA and TA (fig.16): selenoprotein P,plasma 1 (SEPP1) was downregulated 1.54 fold down in TA and 2.97 down in DIA, while N-acetyltransferase 5 (Nat2) was upregulated 1.59 fold in TA 1.47 fold in DIA.

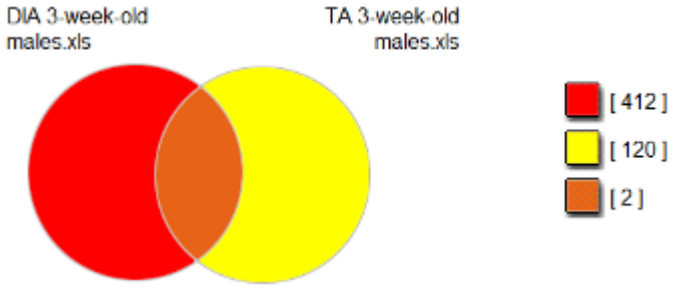

Fig.16 Intersection of dysregulated genes in DIA and TA of 3-week-old males

In 10-week-old males and females there were not genes commonly dysregulated between DIA and TA.

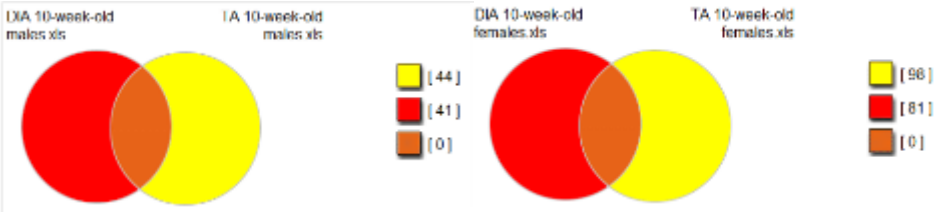

Fig.17 Intersection of dysregulated genes in DIA and TA of 10-week-old males and females

When we looked for genes commonly dysregulated in DIA and in TA between 3-week-old males and 10-week-old males and females, there were no genes that were common to all the three different conditions (fig18-19).

In fig18 is illustrated the Venn diagram for genes dysregulated in DIA in 3-week-old males and 10-week-old males and females

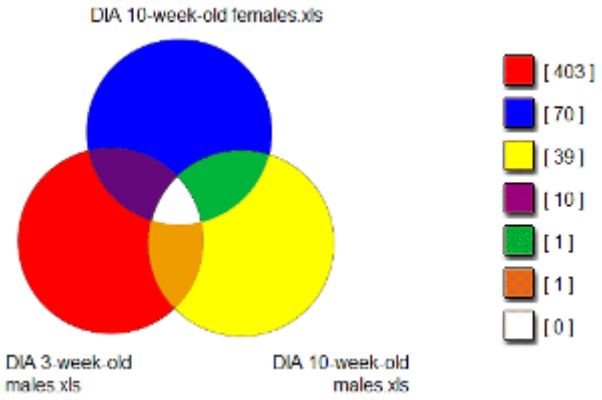

Fig.18 Intersection of dysregulated genes in DIA of 3-week-old males and 10-week-old males and females

In DIA the only commonly downregulated gene between 3- (1.4 fold) and 10-week-old (1.7 fold) males was complement component 2 (within H-2S) (C2). Also, only one dysregulated gene was common between 10-week-old males and females; serine/arginine-rich protein specific kinase 3 (Srpk3), that was upregulated 1.6 fold in males and 1.5 fold in females. On the other hand, 10 genes were commonly dysregulated in 3-week-old males and 10-week-old females, which are shown in table 1.

Table 1 - Genes commonly dysregulated in DIA of 3-week-old males and 10-week-old females

		Diaphragm	
Gene name	Gene ID	10-week-old females	3-week-old males
MAP/microtubule affinity-regulating kinase 2	Mark2	1.45up	1.45up
Mitochondrial ribosomal protein S9	Mrps9	1.43up	1.43up
N-acetyltransferase 2 (arylamine N-acetyltransferase)	Nat	1.40down	1.53down
Monoamine oxidase B	Maob	1.40down	1.69down
Sorbitol dehydrogenase	Sord	1.45 down	1.89down
Multiple coagulation factor deficiency 2	Mcfd2	1.48 down	1.63down
Sterol carrier protein 2, liver	Scp2	1.55down	1.77down
CD1d1 antigen	Cd1d1	1.82down	2.22down
Thiopurine methyltransferase	Tpmt	2.01down	2.57down
Cysteine dioxygenase 1, cytosolic	Cdo1	3.41down	2.46down

In fig.19 is illustrated the Venn diagram for genes dysregulated in TA in 3-week-old males and 10-week-old males and females

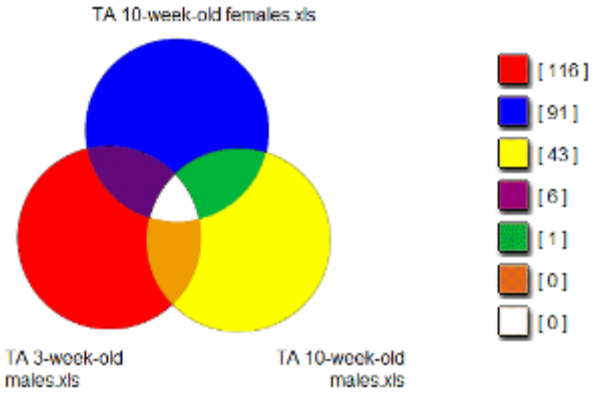

Fig.19 Intersection of dysregulated genes in TA of 3-week-old males and 10-week-old males and females

In the TA, no genes were commonly dysregulated between 3- and 10-week-old males, while one gene, leucine-rich repeats and transmembrane domains 1 (Lrtm1) was commonly downregulated in 10-week-old females (2.30 fold) and 10-week-old males (1.60 fold). Again the most commonly dysregulated genes were found in 3-week-old males and 10-week-old females (6 genes) as shown in table.

Table 2 - Genes commonly dysregulated in TA of 3-week-old males and 10-week-old females

		Tibialis anterior	
Gene name	Gene ID	10-week-old females	3-week-old males
Glucuronidase, beta	Gusb	2.27up	1.50up
Ubiquitin specific protease UBP43	Usp18	1.40up	1.44down
Transmembrane 9 superfamily member 2	Tm9sf2	1.46down	1.68up
Brain protein 44	Brp44	1.49down	1.76up
EPM2A (laforin) interacting protein 1	Epm2aip1	1.53down	1.50up
Hemoglobin, beta adult minor chain	Hbb-b1	5.11down	1.89up

In order to understand if the ACTA KI mouse is a good mouse model for NM, we grouped the dysregulated genes for each condition in the same functional groups as were found to be altered in the human patient study [217]: glucose metabolism, glycogen metabolism, fatty acid metabolism, cell cycle, transcription, ubiquitin related and muscle related genes. In almost all the conditions, we found altered genes belonging to the different functional groups.
Subsequenty, we checked if proteins codified by altered genes were conserved in human as shown in the following tables (tables 3-8).

Table 3 – Dysregulated genes in DIA of 3-week-old males

Illumina no.	Gene name	Symbol	RefSeq Prot in human	% identity in human	Fold change
Glucose metabolism					
ILMN_2599997	RIP13	Ncor1	NP_006302.2	100	+2.25
ILMN_3041839	Pyruvate dehydrogenase (lipoamide) beta	Pdhb	NP_000916.2	100	+1.57
ILMN_2805945	Stress-associated endoplasmic reticulum protein 1	Serp1	NP_055260.1	100	-1.5
ILMN_2782964	Ectonucleotide pyrophosphatase/phosphodiesterase 1 allotype b	Enpp1	NP_001543.2	92.1	-1.5
ILMN_2759108	DCXR mRNA for Dicarbonyl/L-Xylulose Reductase	Dcxr	NP_057370.1	100	-1.75
ILMN_2694955	Insulin-like growth factor binding protein 4	Igfbp4	NP_001543.2	100	-2.37
ILMN_1245103	Glucose-6-phosphatase, catalytic	G6pc	NP_000142.1	100	-2.44
ILMN_2710811	Glucokinase regulatory protein	Gckr	NP_001477.2	100	-2.64
ILMN_2840533	Aldolase 2, B isoform	Aldob	NP_000026.2	100	-2.64
ILMN_1237767	Hepatic nuclear factor 4, alpha	Hnf4a	NP_000448.3	100	-2.70
ILMN_1252185	Retinol binding protein 4, plasma	Rbp4	NP_006735.2	100	-3.34
ILMN_2774160	Hydroxysteroid 11-beta dehydrogenase 1	Hsd11b1	NP_861420.1	100	-3.74
ILMN_1255497	Serine dehydratase	Sds	NP_006834.2	100	-3.76
ILMN_1221105	Glycine N-methyltransferase	Gnmt	NP_061833.1	100	-4.25
ILMN_1224012	Aldolase 2, B isoform	Aldob	NP_000026.2	100	-4.33
ILMN_2785586	Fructose bisphosphatase 1	Fbp1	NP_000498.2	84.9	-5.25
Glycogen metabolism					
ILMN_2782964	Ectonucleotide pyrophosphatase/phosphodiesterase 1 allotype b	Enpp1	NP_001543.2	92.1	-1.5
ILMN_1245103	Glucose-6-phosphatase, catalytic	G6pc	NP_000142.1	100	-2.44
ILMN_1221105	Glycine N-methyltransferase	Gnmt	NP_061833.1	100	-4.25
ILMN_2913078	Carbamoyl-phosphate synthetase 1	Cps1	NP_001116105.1	100	-4.75
Fatty acid metabolism					
ILMN_2739364	2-hydroxyacyl-CoA lyase 1	Hacl1	NP_036392.2	100	-1.55
ILMN_2611874	Protein tyrosine phosphatase-like A domain containing 1	Ptplad1	NP_057479.2	90.9	-1.72
ILMN_2966632	Cytochrome b-5	Cyb5	NP_683725.1	100	-1.78
ILMN_3136542	Glutaryl-Coenzyme A dehydrogenase	Gcdh	NP_000150.1	100	-1.78
ILMN_1216822	INSIG-2 membrane protein	Insig2	NP_057217.2	100	-2.12
ILMN_1247156	Apolipoprotein A-II	Apoa2	NP_001634.1	61.2	-2.19
ILMN_2649199	Hydroxyprostaglandin dehydrogenase 15	Hpgd	NP_000851.2	89.8	-2.24
ILMN_1227398	Angiotensinogen (serpin peptidase inhibitor, clade A, member 8)	Agt	NP_000020.1	100	-2.52
ILMN_2641301	Apolipoprotein A-V	Apoa5	NP_001160070.1	100	-2.56
ILMN_1237767	Hepatic nuclear factor 4, alpha	Hnf4a	NP_000448.3	100	-2.70
ILMN_1259009	Bile acid-Coenzyme A: amino acid N-acyltransferase	Baat	NP_001121082.1	69.4	-2.74
ILMN_2657980	Fatty acid amide hydrolase	Faah	NP_001432.2	84.1	-3.33
ILMN_1228469	Apolipoprotein C-I	Apoc1	NP_001636.1	100	-3.75
ILMN_2648445	Solute carrier family 27 (fatty acid transporter), member 2	Slc27a2	NP_003636.2	100	-4.07
ILMN_2651539	Apolipoprotein C-III	Apoc3	NP_000031.1	62.9	-4.20
ILMN_1252618	Acyl-Coenzyme A oxidase 2, branched chain	Acox2	NP_003491.1	100	-4.39
ILMN_2875475	Glycolate oxidase	Hao1	NP_060015.1	100	-4.48
ILMN_1214498	Cytochrome P450, family 2, subfamily d, polypeptide 22	Cyp2d22	NP_000097.2	75.8	-5.01
ILMN_2847061	Solute carrier family 27 (fatty acid transporter), member 5	Slc27a5	NP_036386.1	71.6	-5.22
ILMN_3009225	Apolipoprotein C-IV	Apoc2	NP_000474.2	61.9	-5.53
Cell cycle					
ILMN_2599997	RIP13	Ncor1	NP_006302.2	100	+2.25
ILMN_1218761	Leucine zipper, putative tumor suppressor 2	Lzts2	NP_115805.1	100	+1.49
ILMN_2611821	Protein phosphatase 2 (formerly 2A), catalytic subunit, alpha isoform	Ppp2ca	NP_002706.1	99.7	+1.48
ILMN_2649199	Hydroxyprostaglandin dehydrogenase 15	Hpgd	NP_000851.2	89.8	-2.24
ILMN_1237767	Hepatic nuclear factor 4, alpha	Hnf4a	NP_000448.3	100	-2.70
Transcription					
ILMN_2599997	RIP13	Ncor1	NP_006302.2	100	+2.25
ILMN_1214950	Myocyte enhancer factor 2C	Mef2c	NP_001124477.1	98.8	+2.06
ILMN_1253387	Kruppel-like factor 5	Klf5	NP_001721.2	100	+1.59
ILMN_2723108	TSC22-related inducible leucine zipper 1b	Tsc22d1	NP_904358.2	100	+1.48
ILMN_2893993	LAG1 homolog, ceramide synthase 2	Lass2	NP_071358.1	92.4	-1.55
ILMN_2514689	Tumor necrosis factor receptor superfamily, member 8	Tnfrsf8	NP_001234.2	100	-1.70
ILMN_2926661	Nuclear receptor subfamily 1, group I, member 3	Nr1i3	NP_001070950.1	100	-2.04
ILMN_2826110	Mutant catalase	Cat	NP_001743.1	100	-2.06
ILMN_2693913	One cut domain, family member 2	Onecut2	NP_004843.2	99	-2.18
ILMN_1237767	Hepatic nuclear factor 4, alpha	Hnf4a	NP_000448.3	100	-2.70
ILMN_1224637	Forkhead box Q1	Foxq1	NP_150285.3	81.1	-3.35
ILMN_2727013	Nuclear receptor subfamily 1, group H, member 4	Nr1h4	NP_005114.1	100	-3.57
Ubiquitin related					
ILMN_1246758	Amplified in osteosarcoma	Os9	NP_006803.1	100	-1.61
Muscle					
ILMN_1227398	Angiotensinogen (serpin peptidase inhibitor, clade A, member 8)	Agt	NP_000020.1	100	-2.52
ILMN_1243128	Apolipoprotein H	Apoh	NP_000033.2	100	-4.54
ILMN_1214950	Myocyte enhancer factor 2C	Mef2c	NP_001124477.1	98.8	+2.06
ILMN_1228718	Syndecan 1	Sdc1	NP_002988.3	100	-1.80
ILMN_2933463	Plasminogen	Plg	NP_000292.1	100	-5.07
ILMN_1234111	Vitronectin	Vtn	NP_000629.3	100	-4.32
ILMN_1252185	Retinol binding protein 4, plasma	Rbp4	NP_006735.2	100	-3.34
ILMN_2426966	Tropomyosin 3, gamma	Tpm3	NP_689476.2	87	+1.56
ILMN_2724585	Dystroglycan 1	Dag1	NP_004384.4	100	+1.65

Table 4 - Dysregulated genes in DIA of 10-week-old males

Illumina no.	Gene name	Symbol	RefSeq Prot in human	% identity in homo sapiens	fold change
Glucose metabolism					
ILMN_1259322	Pyruvate dehydrogenase kinase, isoenzyme 4	Pdk4	NP_002603.1	100	+1.87
Cell cycle					
ILMN_2620930	Damaged-DNA recognition protein 1	Ddb1	NP_001914.3	100	+1.41
ILMN_2776271	PCI domain containing 2	Pcid2	NP_060856.2	100	-1.44
ILMN_1257299	G0/G1 switch gene 2	G0s2	NP_056529.1	77.7	-2.27
Transcription					
ILMN_2749669	Nuclear receptor subfamily 1, group D, member 1	Nr1d1	NP_068370.1	95.8	+1.82
ILMN_2603178	Transcription factor A, mitochondrial	Tfam	NP_003192.1	63.6	+1.43
ILMN_2677921	Vasorin (Vasn)	Dnaja3	NP_612449.2	100	-1.41
ILMN_2776271	PCI domain containing 2	Pcid2	NP_060856.2	100	-1.44
ILMN_2727472	ISL1 transcription factor, LIM/homeodomain	Isl1	NP_002193.2	100	-1.48
ILMN_2450096	Zinc finger protein 30	Zfp30	NP_055713.1	85.3	-1.56
Ubiquitin related					
ILMN_2453620	Ubiquitin-conjugating enzyme E2G 1 (UBC7 homolog, C. elegans)	Ube2g1	NP_003333.1	100	+1.47
Muscle					
ILMN_2677921	Vasorin (Vasn)	Dnaja3	NP_612449.2	100	-1.41
ILMN_3018017	Coxsackie virus and adenovirus receptor	Cxadr	NP_001329.1	89.9	-1.44
ILMN_2684515	Serine/arginine-rich protein specific kinase 3	Srpk3	NP_055185.2	100	+1.64
ILMN_2657543	Gamma sarcoglycan	Sgcg	NP_000222.1	100	+1.44

Table 5 - Dysregulated genes in DIA of 10-week-old females

Illumina no.	Gene name	Symbol	RefSeq Prot in human	% identity in homo sapiens	fold change
Glycogen metabolism					
ILMN_2859847	Liver glycogen phosphorylase	Pygl	NP_002854.3	100	-2.06
Fatty acid metabolism					
ILMN_1250882	MLIP1 mRNA for lipoic acid synthase	Lias	NP_006850.2	100	+1.41
ILMN_2985282	enoyl-CoA delta isomerase	Peci	NP_996667.2	100	-1.40
ILMN_2846194	Enoyl Coenzyme A hydratase domain containing 2	Echdc2	NP_001185890.1	100	-1.45
Cell cycle					
ILMN_1228485	Casein kinase 2, alpha prime polypeptide	Csnk2a2	NP_001887.1	98.9	+1.77
ILMN_2630438	Proteasome (prosome, macropain) 26S subunit, non-ATPase, 7	Psmd7	NP_002802.2	100	+1.65
ILMN_3048503	Nipped-B homolog (Drosophila)	Nipbl	NP_597677.2	100	+1.55
ILMN_2622983	Dual specificity phosphatase 1	Dusp1	NP_004408.1	100	+1.52
ILMN_3139514	T-box 3, mRNA	Tbx3	NP_057653.3	100	+1.49
ILMN_1225196	Transforming growth factor, beta 2	Tgfb2	NP_001129071.1	100	+1.45
ILMN_1236009	Calcium/calmodulin-dependent protein kinase II, beta	Camk2b	NP_742077.1	98.6	+1.44
ILMN_2971286	protein phosphatase 3, catalytic subunit, alpha isozyme	Ppp3ca	NP_000935.1	100	+1.41
ILMN_2794796	E2F transcription factor 4	E2f4	NP_001941.2	100	-1.40
ILMN_2640401	Platelet-activating factor acetylhydrolase, isoform 1b, beta1 subunit	Pafah1b1	NP_000421.1	100	-1.53
Transcription					
ILMN_3048503	Nipped-B homolog (Drosophila)	Nipbl	NP_597677.2	100	+1.55
ILMN_1216416	Ring finger protein (C3H2C3 type) 6	Rnf6	NP_898864.1	100	+1.50
ILMN_3139514	T-box 3, mRNA	Tbx3	NP_057653.3	100	+1.49
ILMN_1258406	Kelch-like ECH-associated protein 1	Keap1	NP_036421.2	100	+1.49
ILMN_2625451	Ankyrin repeat domain 1 (cardiac muscle)	Ankrd1	NP_055206.2	100	+1.47
ILMN_1220834	Calmodulin binding transcription activator 2	Camta2	NP_055914.2	92.6	+1.45
ILMN_2691192	Retinoblastoma binding protein 7	Rbbp7	NP_001185648.1	100	+1.45
ILMN_2736347	Protein arginine N-methyltransferase 7	Prmt7	NP_061896.1	85.4	+1.44
ILMN_3023230	Jumonji domain containing 3	Kdm6b	NP_001073893.1	92.7	+1.42
ILMN_2762514	Mesoderm induction early response 1, family member 2	Mier2	NP_060020.1	100	+1.42
ILMN_2741538	MAF1 homolog (S. cerevisiae)	Maf1	NP_115648.2	100	+1.42
ILMN_2971286	Calcineurin catalytic subunit	Ppp3ca	NP_000935.1	100	+1.41
ILMN_1213307	CTD (carboxy-terminal domain, RNA polymerase II, polypeptide A) small phosphatase 1	Ctdsp1	NP_067021.1	100	-1.86
Ubiquitin related					
ILMN_2725428	DnaJ (Hsp40) homolog, subfamily B, member 2	Dnajb2	NP_006727.2	100	+1.69
ILMN_2630438	Proteasome (prosome, macropain) 26S subunit, non-ATPase, 7	Psmd7	NP_002802.2	100	+1.65
ILMN_1216416	Ring finger protein (C3H2C3 type) 6	Rnf6	NP_898864.1	100	+1.50
ILMN_1255736	Valosin containing protein (Vcp)	Vcp	NP_004290.2	100	+1.42
Muscle					
ILMN_1220834	Calmodulin binding transcription activator 2	Camta2	NP_055914.2	92.6	+1.45
ILMN_3139514	T-box 3, mRNA	Tbx3	NP_057653.3	100	+1.49
ILMN_2971286	Calcineurin catalytic subunit	Ppp3ca	NP_000935.1	100	+1.41
ILMN_1225196	Transforming growth factor, beta 2	Tgfb2	NP_001129071.1	100	+1.45
ILMN_2853658	Pelota homolog (Drosophila) (Pelo)	Itga1	NP_057030.3	96.4	+1.41
ILMN_2684515	Serine/arginine-rich protein specific kinase 3	Srpk3	NP_055185.2	100	+1.45
ILMN_1235230	PDZ and LIM domain 3	Pdlim3	no		+1.42
ILMN_2625451	Ankyrin repeat domain 1 (cardiac muscle)	Ankrd1	NP_055206.2	100	+1.47

Table 6 - Dysregulated genes in TA of 3-week-old males

Illumina no.	Gene name	Symbol	RefSeq Prot in human	% identity in homo sapiens	fold change
Glycogen metabolism					
ILMN_2674720	Prostaglandin E synthase 3 (cytosolic)	Ptges3	NP_006592.3	98.8	+1.70
Fatty acid metabolism					
ILMN_2703657	Dihydrolipoamide dehydrogenase	Dld	NP_000099.2	100	+1.74
ILMN_2674720	Prostaglandin E synthase 3 (cytosolic)	Ptges3	NP_006592.3	98.8	+1.70
ILMN_2704826	Acetyl-Coenzyme A acyltransferase 2 (mitochondrial 3-oxoacyl-Coenzyme A thiolase)	Acaa2	NP_006102.2	100	-1.60
Cell cycle					
ILMN_1216211	Proteasome (prosome, macropain) 26S subunit, non-ATPase, 12	Psmd12	NP_078968.3	96.2	+1.69
Transcription					
ILMN_1239860	SRA stem-loop interacting RNA binding protein	Slirp	NP_112487.1	70.8	+1.92
ILMN_2728830	TAF13 RNA polymerase II, TATA box binding protein (TBP)-associated factor	Taf13	NP_005636.1	100	+1.64
ILMN_2903440	Heterogeneous nuclear ribonucleoprotein D-like	Hnrpdl	NP_112740.1	99.7	+1.63
ILMN_3007959	GDNF-inducible zinc finger protein	Gzf1	NP_071927.1	82.6	+1.62
ILMN_1252757	Myeloid/lymphoid or mixed-lineage leukemia	Mllt3	NP_004520.2	98.6	+1.55
ILMN_1252121	SAFB-like, transcription modulator	Sltm	NP_079031.2	91.2	+1.53
ILMN_2680262	Polymerase (RNA) II (DNA directed) polypeptide G	Polr2g	NP_002687.1	100	+1.52
ILMN_2650040	MKIAA1041 protein	Foxj3	NP_055762.3	94.7	+1.48
ILMN_2637365	Mediator of RNA polymerase II transcription, subunit 28 homolog	Med28	NP_079481.2	100	+1.46
ILMN_3009572	Thioredoxin 1	Txn1	NP_003320.2	100	+1.45
ILMN_1254256	Actin-like 6A	Actl6a	NP_004292.1	100	+1.45
ILMN_1238852	TAF12 RNA polymerase II, TATA box binding protein (TBP)-associated factor	Taf12	NP_001128690.1	100	+1.44
ILMN_1240149	Vacuolar protein sorting 36	Vps36	NP_057159.2	100	+1.43
ILMN_2845208	Leucine-rich PPR-motif containing	Lrpprc	NP_573566.2	100	+1.42
ILMN_2765015	Embryonic ectoderm development	Eed	NP_003788.2	100	+1.42
ILMN_2953700	MAD homolog 1	Smad1	NP_001003688.1	99.1	+1.40
ILMN_3148662	Splicing factor, arginine/serine-rich 5	Sfrs5	NP_008856.2	97.4	-1.42
ILMN_2870320	Protein kinase D2	Prkd2	NP_001073349.1	100	-1.44
ILMN_1256775	Thyroid hormone responsive SPOT14 homolog	Thrsp	NP_003242.1	85.5	-1.46
Ubiquitin related					
ILMN_1216211	Proteasome (prosome, macropain) 26S subunit, non-ATPase, 12	Psmd12	NP_078968.3	96.2	+1.69
ILMN_2933914	Proteasome (prosome, macropain) 26S subunit, non-ATPase, 14	Psmd14	NP_005796.1	100	+1.60
ILMN_2465770	Ubiquitin specific peptidase 14	Usp14	NP_005142.1	100	+1.44
ILMN_2793503	Ubiquitin carboxyl-terminal esterase L5	Uchl5	NP_057068.1	100	+1.41
ILMN_3131679	Ubiquitin specific protease UBP43	Usp18	NP_059110.2	100	-1.44
ILMN_1241976	Ubiquitin associated domain containing 1	Ubac1	NP_057256.2	100	+1.73
Muscle					
ILMN_2623859	ATP-binding cassette, sub-family C (CFTR/MRP), member 9	Abcc9	NP_005682.2	100	+1.50
ILMN_2660766	CD59b antigen	Cd59b	NP_000602.1	100	+1.48

Table 7 - Dysregulated genes in TA of 10-week-old males

Illumina no.	Gene name	Symbol	RefSeq Prot in human	% identity in homo sapiens	fold change
Glucose metabolism					
ILMN_2785586	Fructose bisphosphatase 1	Fbp1	NP_000498.2	84.9	+1.43
ILMN_2738082	Adiponectin, C1Q and collagen domain containing	Adipoq	NP_001171271.1	100	-2.03
ILMN_2695964	Leptin	Lep	NP_000221.1	100	-2.29
Fatty acid metabolism					
ILMN_2738082	Adiponectin, C1Q and collagen domain containing	Adipoq	NP_001171271.1	100	-2.03
ILMN_2695964	Leptin	Lep	NP_000221.1	100	-2.29
Cell cycle					
ILMN_2763115	Cell division cycle 34 homolog	Cdc34	NP_004350.1	100	+1.40
ILMN_1215252	Bone morphogenetic protein 4	Bmp4	NP_001193.2	100	-1.42
Transcription					
ILMN_3150811	TSC22 domain family, member 3	Tsc22d3	NP_932174.1	100	-1.41
ILMN_1215252	Bone morphogenetic protein 4	Bmp4	NP_001193.2	100	-1.42
ILMN_2656498	Forkhead box O1	Foxo1	NP_002006.2	100	-1.44
ILMN_2695964	Leptin	Lep	NP_000221.1	100	-2.29
Ubiquitin related					
ILMN_2763115	Cell division cycle 34 homolog (S. cerevisiae)	Cdc34	NP_004350.1	100	+1.40
Muscle					
ILMN_2629582	Plasminogen activator, urokinase	Plau	NP_002649.1	100	-1.40
ILMN_2738082	Adiponectin, C1Q and collagen domain containing	Adipoq	NP_001171271.1	100	-2.03
ILMN_2697304	Elastin	Eln	NP_000492.2	75.5	+1.40
ILMN_1231104	NF1GRP mRNA for neurofibromatosis type-1-GTPase activating-protein type IV	Nf1	NP_001035957.1	98.5	-1.40
ILMN_3150811	TSC22 domain family, member 3	Tsc22d3	NP_932174.1	100	-1.41
ILMN_1215252	Bone morphogenetic protein 4	Bmp4	NP_001193.2	100	-1.42
ILMN_2440823	Tenascin XB (Tnxb)	Clcn1	NP_061978.6	100	-2.05

Table 8 - Dysregulated genes in TA of 10-week-old females

Illumina no.	Gene name	Symbol	RefSeq Prot in human	% identity in homo sapiens	fold change
Glucose metabolism					
ILMN_2647627	Protein phosphatase 1 (dis2m2)	Ppp1cb	NP_996759.1	99.7	-2.09
Glycogen metabolism					
ILMN_2647627	Protein phosphatase 1 (dis2m2)	Ppp1cb	NP_996759.1	99.7	-2.09
Fatty acid metabolism					
ILMN_2613908	Arachidonate 12-lipoxygenase	Alox12	NP_000688.2	85.5	+1.72
ILMN_2741117	Ankyrin repeat domain 23	Ankrd23	NP_659431.5	82.6	+1.40
ILMN_2592925	Monoglyceride lipase	Mgll	NP_009214.1	100	-1.40
ILMN_2622671	Acyl-CoA synthetase long-chain family member 1	Acsl1	NP_001986.2	100	-1.65
ILMN_2678547	Lysophospholipase 1	Lypla1	NP_006321.1	91.7	-1.71
Cell cycle					
ILMN_1239724	Proteasome (prosome, macropain) subunit, beta type 1	Psmb1	NP_002784.1	100	+1.82
ILMN_2676181	Sirtuin 2	Sirt2	NP_036369.2	100	+1.60
ILMN_1249224	Tumor protein D52-like 1	Tpd52l1	NP_003278.1	90.7	+1.50
ILMN_2725429	U7 snRNP-specific Sm-like protein LSM10	Lsm10	NP_116270.1	90.8	+1.43
ILMN_2763602	Macrophage erythroblast attacher	Maea	NP_001017405.1	98.7	-1.44
ILMN_2647627	Protein phosphatase 1 (dis2m2)	Ppp1cb	NP_996759.1	99.7	-2.09
Transcription					
ILMN_2676181	Sirtuin 2	Sirt2	NP_036369.2	100	+1.60
ILMN_1246841	Avian reticuloendotheliosis viral (v-rel) oncogene related B	Relb	NP_006500.2	89.9	+1.51
ILMN_1253650	SWI/SNF related, matrix associated, actin dependent regulator of chromatin, subfamily a, member 1	Smarca1	NP_003060.2	100	+1.50
ILMN_2778111	Ets variant gene 4 (E1A enhancer binding protein, E1AF)	Etv4	NP_001073143.1	100	+1.49
ILMN_2938047	Ets variant gene 5	Etv5	NP_004445.1	100	+1.49
ILMN_2909248	Vestigial like 2 homolog (Drosophila)	Vgll2	NP_872586.1	100	+1.47
ILMN_2825803	Poly (ADP-ribose) polymerase family, member 14	Parp14	NP_060024.2	64.3	+1.44
ILMN_3086192	Y box protein 2	Ybx2	NP_057066.2	100	-1.63
ILMN_2647605	SET and MYND domain containing 1	Smyd1	NP_938015.1	100	-1.92
Ubiquitin related					
ILMN_1239724	Proteasome (prosome, macropain) subunit, beta type 1	Psmb1	NP_002784.1	100	+1.82
ILMN_2433990	Ubiquitin specific protease UBP43	Usp18	NP_059110.2	100	+1.40
ILMN_2593356	Cereblon (Crbn), transcript variant 1	Crbn	NP_057386.2	100	-1.48
Muscle					
ILMN_3005873	Sortilin 1	Sort1	NP_002950.3	100	+1.57
ILMN_2599748	MAP Kinase	Map2k6	NP_002749.2	100	-1.46
ILMN_2613908	Arachidonate 12-lipoxygenase	Alox12	NP_000688.2	85.5	+1.72
ILMN_2674213	L-type calcium channel beta 1C subunit	Cacnb1	NP_000714.3	100	+1.56
ILMN_1223437	GNAS (guanine nucleotide binding protein, alpha stimulating) complex locus	Gnas	NP_536350.2	100	-1.47
ILMN_2678218	Matrix metallopeptidase 2	Mmp2	NP_004521.1	100	+1.82
ILMN_2741117	Ankyrin repeat domain 23	Ankrd23	NP_659431.5	82.6	+1.40

2.3 microRNA expression profiling

2.3.1 Selection of microRNAs

Expression levels of 20 selected miRs out of the 153 miRs that were found to be dysregulated in NM patients were investigated in our mouse models. The criteria for selection of miRs was that they had to be uniquely and more than 2.5 fold upregulated in NM patients, or, if upregulated also in other neuromuscular diseases, show a significantly higher fold change in NM patients. Although let-7a, let-7f, let-7d, and miR-188 were less than 2.5 times upregulated in NM patients, they were included because they were found to be upregulated in our initial studies using the quantimiR profiling System. The selected miRs are shown in table.

Table 9. miRs selected from the Eisenberg et al paper (PNAS,2007)

hsa-name	SIGNATURE	BMD	DMD	FSHD	LGMD2A	LGMD2B	Miyoshi	NM	DM	PM	IBM
hsa_miR_368	shared		8.56	4.85	6.33	7.77	4.39	30.09	4.53		
hsa_miR_381	shared		7.63		3.41	6.20	2.28	23.24	3.37		3.30
hsa_miR_410	shared					2.96		11.24			
hsa_miR_127	shared		2.66					9.36		2.38	
hsa_miR_493_5p	unique							7.44			
hsa_miR_409_5p	unique							7.10			
hsa_miR_128b	unique							4.82			
hsa_miR_337	unique							3.85			
hsa_miR_181c	unique							3.73			
hsa_miR_483	unique							2.30			
hsa_let_7f	unique							1.89			
hsa_let_7d	unique							1.83			
hsa_miR_188	unique							1.82			
hsa_let_7a	unique							1.60			
hsa_miR_376a	shared		5.77		3.48	5.72	2.44	14.78			
hsa_miR_542_5p	shared				1.93			14.75		2.27	
hsa_miR_98	unique							2.52			
hsa_miR_199a	shared		3.90	4.35	4.30	5.09	2.66	5.14	3.64	5.47	
hsa_miR_196a	unique							10.29			
hsa_miR_181a	shared				1.52		1.65	5.35			

2.3.2 miR expression in TA and DIA muscles from Acta1(H40Y)KI mice

The expression levels of selected miRs were determined in Acta1(H40Y)KI mice and Tm_{slow}(Met9Arg)Tg (Tg) mice using the QuantiMiR RT Kit (Systems Biosciences) in combination with the Power SYBR Green PCR Master mix (Applied Biosystems). To allow us to study the miR expression profile at early and late stages of NM, we chose to perform our studies on TA and DIA from 3- and 10-week-old KI male mice as well as 8-month-old TPM3Tg (Tg) mice compared to littermate controls. As shown in paragraph 1.2.4.2 KI males die around 10 weeks of age, while females show a mild phenotype around that age. For this reason we considered the males a better model for studying miR expression levels during the progression of NM. As presented above, the same time points were chosen for our gene expression studies, and we used the same samples for the miR and gene expression studies, allowing us to compare miR and gene expression profiles. For the less affected Tg mice we chose a time point of 8 months, which is around the time where they start showing signs of the disease. A gene expression study on 8-month-old Tg mice has previously been published [215].

RNA was extracted using Trizol reagent (Invitrogen) and the integrity of the RNA was checked on a bioanalyzer (Agilent). Only samples with a RIN value ≥ 8 were included in the study. qRT-PCR was performed in triplicates on three biological replicates for each miR and U6 and U1 (small RNAs) were used as endogenous controls for normalization. Fold changes were calculated based on average miR expression levels in WT littermate controls. The miR expression levels in mutant mice were not pooled because of too much difference between mice.
miR expression levels in the different groups are shown in table 10.

-

Table 10 -. Upregulated miRs are shown in red, while downregulated miRs are shown in green.

	KI DIA 3weeks			KI DIA 10weeks			KI TA 3weeks			KI TA 10weeks			Tg DIA 8months			Tg TA 8months		
	1	2	3	1	2	3	1	2	3	1	2	3	1	2	3	1	2	3
miR-376c	10.42	14.16	59.63	0.31	0.71	0.11	26.70	12.42	3.79	0.01	0.01	0.00	3.44	-	1.03	2.00	-	5.00
miR-381	2.02	1.97	0.71	4.42	14.32	2.36	2.64	2.13	1.30	0.35	0.53	0.02	-	1.00	1.41	-	1.52	0.85
miR-410	0.50	0.88	0.06	1.01	4.47	0.34	1.63	0.63	0.91	-	-	-	-	-	-	-	-	-
miR-127	0.62	1.05	0.07	2.47	12.90	0.58	4.05	1.70	1.28	0.47	0.68	0.13	0.68	-	0.80	0.76	-	1.06
miR-493	1.32	1.53	2.52	2.40	4.31	0.43	4.31	2.25	0.93	0.29	0.81	0.05	0.98	0.44	-	3.16	1.14	-
miR-409-5p	1.07	1.52	0.48	1.99	6.97	0.96	2.54	1.49	1.35	-	-	-	-	0.55	-	-	1.43	-
miR-128	0.48	0.68	0.19	0.32	1.53	0.58	0.67	0.37	0.31	0.28	0.84	0.08	1.72	3.63	1.55	2.49	2.00	2.17
miR-337-3p	0.82	2.02	-	3.82	14.52	1.48	1.92	0.85	1.49	0.63	2.34	0.21	-	7.29	0.69	-	-	3.32
miR-181c	1.83	1.20	0.64	0.45	1.84	0.13	0.84	0.92	0.41	0.07	0.52	0.00	1.36	1.70	0.75	1.71	1.11	1.05
miR-483	0.73	2.38	4.38	0.63	2.53	0.80	1.47	2.54	1.64	0.02	0.09	0.02	1.60	0.33	0.15	-	0.09	1.42
let-7f	0.30	-	1.26	1.94	0.49	0.47	1.08	0.58	0.38	0.42	0.32	0.05	1.57	3.13	0.53	0.91	0.04	1.71
let-7d	2.43	0.55	22.98	5.96	0.55	11.46	5.35	0.45	2.75	2.22	0.12	0.41	1.49	0.46	0.17	1.51	0.11	0.76
miR-188-5p	0.75	0.70	2.38	0.96	1.35	3.24	2.85	1.08	4.23	0.10	0.15	0.98	-	1.24	0.08			1.24
let-7a	1.78	0.86	10.40	1.35	1.56	0.54	1.82	1.89	0.25	0.05	0.25	0.06	1.49	0.48	0.13	1.51	0.07	0.90
miR-376a	-	-	-	-	-	-	-	-	-	-	-	-	-	-	-	-	-	-
miR-542-5p	-	-	-	-	-	-	-	-	-	-	-	-	-	-	-	-	-	-
miR-98	0.45	0.61	0.31	0.62	2.10	0.38	0.81	2.41	0.22	0.20	1.52	0.14	1.49	0.40	0.13	1.42	0.22	1.89
miR-199a5p	0.63	1.84		1.13	4.21	2.09	1.33	0.85	2.37	0.39	1.51	4.74	-	1.89	0.12	-	10.68	1.55
miR-196a	-	-	-	-	-	-	2.87	1.25	1.28	0.67	1.38	0.48	-	0.10	-	2.14	0.41	2.69
miR-181a	1.29	1.00	0.54	0.97	1.88	0.85	1.23	0.47	0.55	0.30	0.41	0.28	1.17	143.37	0.12	2.21	7.60	1.12

2.4 Target prediction

In order to predict putative targets of the 20 studied miRs we applied prediction algorithms based on complementary base-pair extension and thermodynamic evaluation of the complex (miRanda, TargetScan and RNAhybrid packages). Subsequently, the obtained target list was further refined by adopting the PITA target prediction method to search for accessible sites (for more details about target prediction tools see paragraph 1.3.6 in introduction). Since the majority of miRs were predicted to target a very large number of transcripts, we conducted an enrichment analysis over Gene Ontology terms to narrow down the list of targets and focus on biological functions that were most significantly affected by multiple miRs and were related to NM disease. Target prediction was performed against 17,231 mouse genes (genome assembly mm9 -NCBI37) and putative target genes were filtered for functional annotation in Gene Ontology (UCSC) that describe genes involved in the Nemaline Myopathy (Acta1;Cfl2;Neb;Tnnt1;Tpm1;Tpm2). Predicted targets of dysregulated miRs and the functional categories that they belong to are shown in table 5. In particular, predicted targets involved in muscle contraction and actin binding could be particularly interesting since the muscle weakness associated with NM has been shown to be due to altered cross-bridge cycling kinetics [216].

Table 11.Functional categories of predicted targets of dysregulated miRs

GO terms	number predicted targets	number predicted and conserved targets
Actin binding	*200*	*49*
Actin cytoskeleton	*53*	*15*
Actin filament	*11*	*2*
Actin filament binding	*2*	*0*
Cardiac muscle contraction	*12*	*2*
Filamentous actin	*8*	*4*
Muscle contraction	*8*	*2*
Myofibril	*2*	*0*
Regulation of muscle contraction	*11*	*1*
Sarcomere	*6*	*0*
Sarcomere organization	*1*	*0*
Skeletal muscle fiber development	*4*	*0*
Stress fiber	*17*	*7*
Tropomyosin binding	*4*	*0*
Ventricular cardiac muscle morphogenesis	*4*	*1*
Z disc	*10*	*2*

The number of predicted targets was restricted when we considered only targets conserved in human.

In particular, miR-381, which is highly upregulated in human NM muscle, appeared to be the most interesting miR as it has many potential targets in skeletal muscle that are conserved between mouse and human (table 12).

Table 12 - miR381 targets

Target gene	Description	Target gene	Description
Actg1	actin, gamma, cytoplasmic 1	Mbnl1	muscleblind-like 1
Actr3	ARP3 actin-related protein 3 homolog	Met	met proto-oncogene
Adrb2	adrenergic receptor, beta 2	Mtap1b	microtubule-associated protein 1 B
Arf6	ADP-ribosylation factor 6	Mtpn	myotrophin
Cd2ap	CD2-associated protein	Myh10	myosin heavy chain 10, non-muscle
Coro1c	coronin, actin binding protein 1C	Nf1	neurofibromin
Ctnnb1	catenin (cadherin associated protein), beta 1,	Nr2f2	nuclear receptor subfamily 2, group F, member 2
Cxcr4	chemokine (C-X-C motif) receptor 4	Rhoa	ras homolog gene family, member A
Fgfr2	fibroblast growth factor receptor 2 isoform	Rock1	Rho-associated coiled-coil forming kinase 1
Foxp2	forkhead box P2	Rock2	Rho-associated coiled-coil forming kinase 2
Gja1	gap junction membrane channel protein alpha 1	Tln2	talin 2
Grlf1	glucocorticoid receptor DNA binding factor 1	Tpm1	tropomyosin 1, alpha
Jup	junction plakoglobin	Trim63	tripartite motif-containing 63
Klhl2	kelch-like 2, Mayven	Trpm7	transient receptor potential cation channel
Kras	c-K-ras2 protein	Twist1	twist gene homolog 1
Map2k3	mitogen activated protein kinase kinase 3	Utrn	utrophin
Marcks	myristoylated alanine rich protein kinase C	Zfpm2	zinc finger protein, multitype 2

2.5 In vitro target validation: luciferase assay

To determine whether predicted targets were real targets, selected miR-381 targets of interest (Actg1, Cd2ap, Tln2, Tpm1, Trim63, Trpm7) were tested by experimental validation *in vitro*. The 3'UTR of predicted targets were cloned downstream of the luciferase gene in the pGL3-promoter vector (Promega) and co-transfected with an expression plasmid containing miR-381 fused to Green Fluorescent Protein into 293 myoblasts. Significant changes in TRPM7 and TRIM63 luciferase expression levels were observed (fig 20), while no changes in expression levels of the other tested potential targets were found.

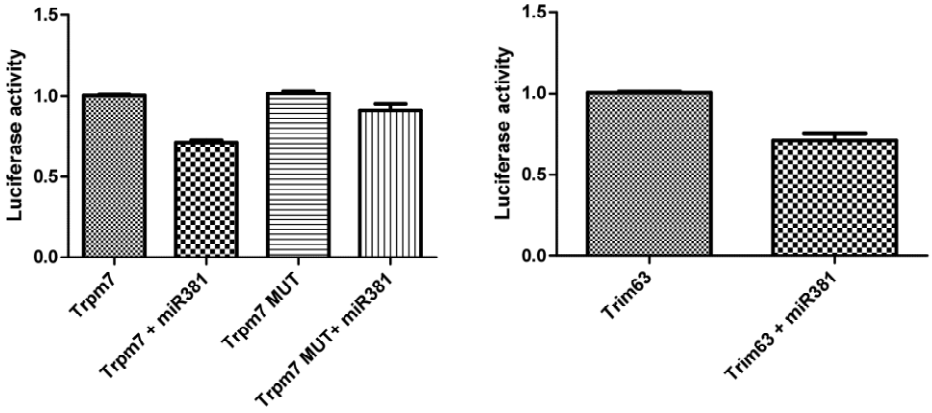

Fig.20 miR-381 regulation of Trpm7 and TRIM63 gene expression, shown by the luciferase assay

3. DISCUSSION

Nemaline Myopathy (NM) is a heterogeneous neuromuscular disease both from a clinical and a genetic point of view. Causative mutations have been identified in six different genes encoding thin filament proteins, including *Acta1*, skeletal muscle alpha-actin, *Neb*, nebulin, *Tpm3*, slow alpha-tropomyosin (alpha-3 chain), *Tpm2*, beta tropomyosin, *Tnnt1*, slow troponin T, and *Cfl2*, cofilin2. The disease is characterized by muscle weakness and the presence of protein aggregates called nemaline bodies. Furthermore, dependent on the causative mutation and the severity of the disease, NM has been associated with respiratory problems, muscle atrophy, and an increase in type I fibers. .The heterogeneity of the disease makes the diagnosis difficult and reduces the possibility for developing a therapy. Thus, more insights into molecular pathways underlying the pathology that are commonly affected in NM patients may open up for new treatment options targeted towards commonly affected pathways.

During the last years, gene expression studies on patients [217] and a mouse model, Tm_{slow}(Met9Arg)Tg (Tg) [215] of NM have been carried out, providing information about the gene expression changes associated with NM. However, the Tg mouse presents a mild form of the disease, and alterations present in the more severe cases of NM may therefore have been missed in that study. In our study we performed a gene expression analysis on the ACTA (H40Y)KI (KI) mouse model, which shows a more severe phenotype compared to the Tg mouse. In order to analyze changes in gene expression at an early and late stage of the disease, we performed our analyses on both 3- and 10-week-old mice. Due to a milder phenotype in KI females compared to KI males, the analysis of 10-week-old mice was performed both on males and females. The gene expression analysis was conducted on diaphragm (DIA) and tibialis anterior (TA) of wildtype (WT) and knockin (KI) mice.

3.1 Gene expression study

The results discussed here are still preliminary since the gene expression experiment has just recently been performed. One approach for analyzing the gene expression study would be to focus on genes that are commonly dysregulated at all the different conditions. However, this kind of analysis would be too restricted and we could miss genes that are altered in one condition and not in others, which could be still of interest. To get a general overview over which genes are altered and in which pathways they are involved, we independently analyzed the results from the three different conditions (3-week-old males, 10-week-old males, and 10-week-old females) in the two different muscles (DIA and TA).

Interestingly, the DIA of 3-week-old males showed the highest level of altered gene expression in our analysis, presenting 493 dysregulated genes with a significant fold change over 1.4, while 41 and 83 genes were dysregulated in DIA of 10-week-old males and females, respectively. TA of 3-week-old males was the most affected as well with 122 dysregulated genes with a significant fold change over

1.4 versus 46 and 102 genes dysregulated in 10-week-old males and females, respectively. The high number of dysregulated genes in 3-week-old males genes suggests the impairment of several processes with the early onset of the disease, while maybe only specific pathways remain altered later on in the late stage of the disease. The fact that the DIA shows the most altered gene expression pattern is consistent with the fact that the DIA is generally the most affected muscle in neuromuscular diseases, most likely because the DIA as opposed to other muscles is continuously used from the time of birth.

In our analyses we particularly focused on the DIA of 3-week-old males in order to reveal altered pathways that may be relevant for the early onset of NM. Interestingly, 22 genes, which were among the most changed genes, were involved in the same pathway: the coagulation cascade. Normally coagulation is activated immediately after an injury to the blood vessels that damages the endothelium lining the vessels and causes the exposure of the tissue factor protein. Two different processes (intrinsic and extrinsic) culminate in fibrin clot formation. In KI mice the coagulation cascade is impaired in both its pathways, with a general downregulation of several key genes for the formation of clots of fibrin. In particular, serpin proteins, which are proteases activated in the cascade to cut the serine-rich domains of the inactive form of coagulation proteins, are downregulated. One such protein is an anti-thrombin; thrombin plays a crucial role in the conversion of fibrinogen to fibrin during the coagulation process. Based on the downregulation of anti-thrombin serpin proteins, we would expect thrombin to be upregulated. However, thrombin levels are unchanged in KI DIA compared to WT, suggesting that other factors regulate its expression. Also fibrinogen is downregulated. During infection, activation of coagulation and subsequent fibrin deposition are essential parts of the host's defense in order to contain the invading microorganisms and the subsequent inflammatory response, and to avoid sepsis. Impairment of the coagulation cascade could affect the pathway of the complement system, possibly causing increased inflammation. However, further analyses need to be done to better elucidate these pathways and to reveal if this pathway is impaired also in the late stage of the disease.
Comparison of the gene expression analyses in the two different muscles, DIA and TA at the same stage, revealed only few commonly dysregulated genes. This finding confirms the results of the gene expression study conducted on the Tg mouse [215] in which different muscles, TA, gastrocnemius (GAS), plantaris (PLT), DIA, and extensor digitorum longus (EDL), were analyzed and DIA showed a peculiar alteration of the gene expression, distinct from all the other muscles.
Comparison of dysregulated genes between different conditions (3-week-old males, 10-week-old males and females) revealed that 3-week-old males shared the highest number of genes with 10-week-old females in both DIA and TA. This reflects the difference between males and females in developing the disease, with the genetic expression pattern of old females closer to young than to old males, in agreement with the delayed development of the disease in females.
Interestingly, the only gene that was commonly downregulated in 3- and 10-week-old males was complement component 2 (C2), which is involved in the pathway of

the complement system during inflammation, suggesting that this pathway is impaired also in 10-week-old males.
The presence of such a low number of altered genes shared between different conditions in terms of muscle type, age, and gender was unexpected. However, we observed that, even if the specific dysregulated genes are different, some pathways, such as metabolic pathways, are commonly dysregulated under different conditions, suggesting that the altered genes can be different, while their biological function may be similar.
In particular, alterations in seven specific functional categories (glucose metabolism, glycogen metabolism, fatty acid metabolism, cell cycle, transcription, ubiquitin, and muscle related genes) were investigated, to look for similarities with the human gene expression analysis in which these categories showed impaired gene expression patterns [217]. As reported in table in tables 3-8, genes belonging to all the seven categories were dysregulated in the DIA of 3-week-old males, while glycogen and fatty acid metabolism were unaltered in the DIA of 10-week-old males; the DIA of 10-week-old females did not show altered expression of genes involved in glucose metabolism. In the TA, glucose metabolism was not impaired in 3-week-old males and in 10-week-old females, while in 10-week-old males glycogen metabolism was not impaired, suggesting once again a closer gene expression pattern between young males and old females than with old males. Among the altered genes almost all encode proteins that are highly conserved in human.
When compared to the human study [217], some genes that were altered in KI mice were the murine homologues (sometimes other isoforms) of human dysregulated genes; in DIA, Fbp1, Cyp2d22, Ppp2ca, Nr1i3, Nr1h4 (3-week-old males); Nr1d1, Zfp30, and Ube2g1 (10-week-old males); Dusp1, Ppp3ca and Tgfb2 (10-week-old females). In TA, Usp18, and Ubac1 (3-week-old males); Fbp1 (10-week-old males) Ppp1cb, Sirt2, and Usp18 (10-week-old females).
Based on our preliminary analysis of gene expression in the KI mouse model, this is a better model for NM than the Tg mouse, since like in the human study, an impairment in metabolic pathways was found in KI mice which was not found in Tg mice.

3.2. MicroRNA expression study

In a study published in 2007 in PNAS [212], a peculiar miR expression pattern was found in NM patients compared to other neuromuscular diseases (Duchenne muscular dystrophy, Becker muscular dystrophy, facioscapulohumeral muscular dystrophy, limb-girdle muscular dystrophies types 2A and 2B, Miyoshi myopathy, polymyositis, dermatomyositis, and inclusion body myositis). The presence of 150 dysregulated miRs of which 36 were uniquely dysregulated in NM patients, suggests an important role of miRs in the disease, leading us too hypothesize their involvement in the regulation of pathological pathways underlying NM.
In our study expression levels of 20 selected miRs were investigated in 3- and 10-week-old KI males to study their expression in relation to the development of the disease. As evident from Tables 3-8, many of the miRs that have been found to be dysregulated in human NM patients were also found to be dysregulated in our

mouse models. However, we observed a high number of individual differences in miR expression levels that sometimes followed the same trend (upregulation/downregulation) in biological replicates with a variability in fold change, but also often went in opposite directions, i.e. downregulated in one replicate and upregulated in another. It appears that one of the KI replicates in 3-week-old mice is an outlier, showing a different miR expression pattern compared to the other replicates. However, it is strange that the dysregulation of miRs in that sample is not random, as it shows downregulation of most of the miRs compared to the average expression levels in the controls. One explanation for the big variability in miR expression levels, could be that the development of the disease is different between individuals; during the collection of muscles of WT and KI mice we noticed that while some KI mice showed a clear phenotype, no visible phenotype was observed in others.

In the TA of 10-week-old KI males, the expression levels of most of the studied miRs were consistently downregulated. This could indicate a complete change in gene expression regulation by miRs, but further analysis are required to address the biological meaning of this observation.

Moreover, we observed that the expression of many of the miRs that are dysregulated in NM patients are likewise altered in KI mice, while they are less affected in Tg mice, showing once again that the KI mouse model better recapitulate the NM patient phenotype than the Tg mouse model

Of particular interest was miR-381, which was overexpressed in the different conditions and was predicted to target muscle specific genes involved in the pathology of NM. In particular, many of the predicted targets of miR-381 are involved in muscle contraction and actin binding, which could be of particular interest since the muscle weakness associated with NM has been shown to be due to altered cross-bridge cycling kinetics [216]. The human miR-381 has been reported to be an oncomiR that by regulating LRRC4 (a glioma tumor suppressor) increases the *in vitro* and *in vivo* proliferation of glioma cells [218]. No data are reported in the literature about its expression in skeletal muscle, except its high upregulation in NM patients.

Two of the predicted miR-381 targets, TRIM63 and TRPM7, were validated *in vitro* by an luciferase assay.

Trim63, also known as MURF1 (Muscle specific RING Finger E3 ligase), is a member of the ubiquitin system. Muscle degeneration, due to inactivity, denervation, or severe catabolic states, activates the ubiquitin–proteasome protein degradation pathway and the induction of many of its component enzymes [15, 25–28]; in NM an impairment in ubiquitin related genes has been reported in human patients [217], which was also found in KI mice at all the different conditions. Moreover, it has been reported that Trim63 is differentially expressed under conditions of muscle atrophy [29], and that skeletal muscle atrophy occurs in Nemaline Myopathy [219]. In the luciferase assay, the expression level of the Renilla luciferase fused to the 3'UTR of Trim63 was downregulated by 25% when cotransfected with miR-381. However in our gene expression analysis on KI mice we did not observe any differences in Trim63 expression levels. Since depending on complementarity, miRs often affect their targets at the translational level, it is possible that miR-381 affects Trim63 at the protein level but not at the mRNA level.

Trmp7 (transient receptor potential cation channel, subfamily M, member 7) belongs to the TRP superfamily of ion channels that is a structurally defined group of cation channels showing an enormous functional diversity. TRPM7 is the most frequent non-voltage gated cation channel in skeletal muscle [220]. Though TRPM7 preferentially conducts Mg^{2+} it provides a significant Ca^{2+}entry pathway [47]. Although the possibility of altered Ca^{2+} regulation has not been studied in NM, it has previously been suggested that muscle weakness can be caused by a reduced Ca^{2+} sensitivity of the contractile apparatus in this disease [221; 222] and the idea is reinforced by the fact that NM can also be caused by mutations in tropomyosin and troponin [223]. In the luciferase assay the expression level of the Renilla luciferase fused to the 3'UTR of TRPM7 was downregulated by 30% when cotransfected with miR-381. The TRPM7 mRNA level was unchanged in the gene expression study on KI mice and also in this case further analyses at the protein level need to be performed.

We hypothesized that alterations in miR expression levels influence gene expression levels by miR-mediated regulation. On the other hand, it is possible that upregulation of miR-381 and the dysregulated miR expression pattern in general is a consequence of secondary gene pathways that underlie the disease. In this respect, it is possible that a dysregulation of a large number of genes occurs at the initial stage the disease, causing the overexpression of miRs to modulate the gene.

4. CONCLUSION

In the present study gene and miR expression levels have been investigated in a mouse model of Nemaline Myopathy (NM). The mouse model used in the analysis was the ACTA(H40Y)KI (KI) mouse, that well recapitulates the NM phenotype. Interestingly, the KI mouse shows differences in disease development between males and females, with males exhibiting early onset of the disease resulting in death from around 10 weeks of age and females still showing a mild phenotype around 10 weeks of age. The molecular basis for this difference was investigated in the gene expression study.

The gene expression analysis was performed in triplicates on 3-week-old males and 10-week-old males and females. However, in two cases, the diaphragm (DIA) of 10-week-old males and the tibialis anterior (TA) of 10-week-old females, there was a bad correlation between a WT and a KI sample and the other samples and we therefore performed the analysis at these conditions on duplicates instead of triplicates. Although we performed student's t-test and only considered gene expression changes with a p-value < 0.05, we will perform gene expression analysis on additional samples in order to perform all analyses on triplicates. Moreover, the results will be confirmed by real-time PCR for dysregulated genes on the same samples.

The preliminary analysis of the gene expression results showed impairment in the coagulation cascade in the DIA of 3-week-old males with 22 genes dowregulated in the pathway. It would be interesting to determine the levels of the proteins encoded by the dysregulated genes and to investigate if the same pathway or related pathways are impaired in older males.

The main feature of KI mice compared to Tg mice, a mouse model of a mild form of NM, is the dysregulation of genes involved in metabolic pathways that were also found to be dysregulated in human patients [217]. This suggests that the KI mouse model better recapitulates NM than the Tg mouse model. However, these results need to be investigated in more detail.

The miR expression analysis of KI mice revealed the dysregulation of a group of miRs that has been reported dysregulated in human patients [217]. Of the dysregulated miRs, miR-381 was of particular interest based on its high upregulation in human and in mouse as well as its predicted targets.

Two targets of miR-381 were validated *in vitro* by luciferase assay: a gene involved in calcium homeostasis (TRPM7) and a gene involved in the ubiquitin system (Trim63/MURF1). The specific interaction of miR-381 with the 3'UTR of TRPM7 was confirmed after mutagenesis of its miR interaction site in the 3'UTR. Mutagenesis will likewise be performed for Trim63. In order to confirm that TRPM7 and Trim63 are targets of miR-381, Western blot analysis will be performed to determine the protein level in KI mice in which miR-381 is upregulated

In conclusion, the results of the presented project suggest that the KI mouse model is a better NM mouse model than the previously described Tg mouse model, both from a phenotipic and a genetic point of view. It is evident that specific miRs are dysregulated (mainly upregulated) in NM and that they may influence the abnormal expression of genes that we highlighted in our analysis. However, in order to better understand this possible correlation, a deeper analysis needs to be performed.

BIBLIOGRAPHY

1. A.S., Beckerle, M.C. & Gregorio, C.C. Striated muscle cytoarchitecture: an intricate web of form and function. *Annu. Rev. Cell Dev. Biol.* **18**, 637-706 (2002).
2. Lange, S., Ehler, E. & Gautel, M. From A to Z and back? Multicompartment proteins in the sarcomere. *Trends Cell Biol.* **16**, 11-18 (2006).
3. Faul, C., Dhume, A., Schecter, A.D. & Mundel, P. Protein kinase A, Ca2+/calmodulin-dependent kinase II, and calcineurin regulate the intracellular trafficking of myopodin between the Z-disc and the nucleus of cardiac myocytes. *Mol. Cell. Biol.* **27**, 8215-8227 (2007).
4. Paavilainen, V.O., Bertling, E., Falck, S. & Lappalainen, P. Regulation of cytoskeletal dynamics by actin-monomer-binding proteins. *Trends Cell Biol.* **14**, 386-394 (2004).
5. Nicholson-Dykstra, S., Higgs, H.N. & Harris, E.S. Actin dynamics: growth from dendritic branches. *Curr. Biol.* **15**, R346-357 (2005).
6. Ono, S. Mechanism of depolymerization and severing of actin filaments and its significance in cytoskeletal dynamics. *Int. Rev. Cytol.* **258**, 1-82 (2007).
7. Van Troys, M. *et al.* Ins and outs of ADF/cofilin activity and regulation. *Eur. J. Cell Biol.* **87**, 649-667 (2008).
8. Sun, H.Q., Yamamoto, M., Mejillano, M. & Yin, H.L. Gelsolin, a multifunctional actin regulatory protein. *J. Biol. Chem.* **274**, 33179-33182 (1999).
9. Silacci, P. *et al.* Gelsolin superfamily proteins: key regulators of cellular functions. *Cell. Mol. Life Sci.* **61**, 2614-2623 (2004).
10. Gunning, P. Emerging issues for tropomyosin structure, regulation, function and pathology. *Adv. Exp. Med. Biol.* **644**, 293-298 (2008).
11. Lal, A.A. & Korn, E.D. Effect of muscle tropomyosin on the kinetics of polymerization of muscle actin. *Biochemistry* **25**, 1154-1158 (1986).
12. Hitchcock-DeGregori, S.E., Sampath, P. & Pollard, T.D. Tropomyosin inhibits the rate of actin polymerization by stabilizing actin filaments. *Biochemistry* **27**, 9182-9185 (1988).
13. Broschat, K.O., Weber, A. & Burgess, D.R. Tropomyosin stabilizes the pointed end of actin filaments by slowing depolymerization. *Biochemistry* **28**, 8501-8506 (1989).
14. Broschat, K.O. Tropomyosin prevents depolymerization of actin filaments from the pointed end. *J. Biol. Chem.* **265**, 21323-21329 (1990).
15. Bernstein, B.W. & Bamburg, J.R. Tropomyosin binding to F-actin protects the F-actin from disassembly by brain actin-depolymerizing factor (ADF). *Cell Motil.* **2**, 1-8 (1982).
16. Ono, S. & Ono, K. Tropomyosin inhibits ADF/cofilin-dependent actin filament dynamics. *J. Cell Biol.* **156**, 1065-1076 (2002).
17. Fattoum, A., Hartwig, J.H. & Stossel, T.P. Isolation and some structural and functional properties of macrophage tropomyosin. *Biochemistry* **22**, 1187-1193 (1983).
18. Ishikawa, R., Yamashiro, S. & Matsumura, F. Differential modulation of actin-severing activity of gelsolin by multiple isoforms of cultured rat cell tropomyosin. Potentiation of protective ability of tropomyosins by 83-kDa nonmuscle caldesmon. *J. Biol. Chem.* **264**, 7490-7497 (1989).

19. Kazmierski, S.T. *et al.* The complete mouse nebulin gene sequence and the identification of cardiac nebulin. *J. Mol. Biol.* **328**, 835-846 (2003).
20. Moncman, C.L. & Wang, K. Nebulette: a 107 kD nebulin-like protein in cardiac muscle. *Cell Motil. Cytoskeleton* **32**, 205-225 (1995).
21. Wright, J., Huang, Q.Q. & Wang, K. Nebulin is a full-length template of actin filaments in the skeletal muscle sarcomere: an immunoelectron microscopic study of its orientation and span with site-specific monoclonal antibodies. *J. Muscle Res. Cell. Motil.* **14**, 476-483 (1993).
22. Nwe, T.M. & Shimada, Y. Inhibition of nebulin and connectin (titin) for assembly of actin filaments during myofibrillogenesis. *Tissue Cell* **32**, 223-227 (2000).
23. McElhinny, A.S., Schwach, C., Valichnac, M., Mount-Patrick, S. & Gregorio, C.C. Nebulin regulates the assembly and lengths of the thin filaments in striated muscle. *J. Cell Biol.* **170**, 947-957 (2005).
24. Castillo, A., Nowak, R., Littlefield, K.P., Fowler, V.M. & Littlefield, R.S. A nebulin ruler does not dictate thin filament lengths. *Biophys. J.* **96**, 1856-1865 (2009).
25. Bang, M.-L. *et al.* Nebulin-deficient mice exhibit shorter thin filament lengths and reduced contractile function in skeletal muscle. *J. Cell Biol.* **173**, 905-916 (2006).
26. Witt, C.C. *et al.* Nebulin regulates thin filament length, contractility, and Z-disk structure in vivo. *EMBO J.* **25**, 3843-3855 (2006).
27. Ottenheijm, C.A.C. *et al.* Thin filament length dysregulation contributes to muscle weakness in nemaline myopathy patients with nebulin deficiency. *Hum. Mol. Genet.* **18**, 2359-2369 (2009).
28. Pappas, C.T., Bhattacharya, N., Cooper, J.A. & Gregorio, C.C. Nebulin interacts with CapZ and regulates thin filament architecture within the Z-disc. *Mol. Biol. Cell* **19**, 1837-1847 (2008).
29. McElhinny, A.S., Kolmerer, B., Fowler, V.M., Labeit, S. & Gregorio, C.C. The N-terminal end of nebulin interacts with tropomodulin at the pointed ends of the thin filaments. *J. Biol. Chem.* **276**, 583-592 (2001).
30. Pappas, C.T., Krieg, P.A. & Gregorio, C.C. Nebulin regulates actin filament lengths by a stabilization mechanism. *J. Cell Biol.* **189**, 859-870 (2010).
31. Brent, A.E., Schweitzer, R. & Tabin, C.J. A Somitic Compartment of Tendon Progenitors. *Cell* **113**, 235-248 (2003).
32. Christ, B., Huang, R. & Scaal, M. Amniote somite derivatives. *Developmental Dynamics* **236**, 2382-2396 (2007).
33. Otto, A., Schmidt, C. & Patel, K. Pax3 and Pax7 expression and regulation in the avian embryo. *Anatomy and Embryology* **211**, 293-310 (2006).
34. Heanue, T.A. *et al.* Synergistic regulation of vertebrate muscle development by Dach2, Eya2, and Six1, homologs of genes required for Drosophila eye formation. *Genes & Development* **13**, 3231 -3243 (1999).
35. Kardon, G., Heanue, T.A. & Tabin, C.J. Pax3 and Dach2 positive regulation in the developing somite. *Developmental Dynamics* **224**, 350-355 (2002).
36. Grifone, R. *et al.* Eya1 and Eya2 proteins are required for hypaxial somitic myogenesis in the mouse embryo. *Developmental Biology* **302**, 602-616 (2007).

37. Gros, J., Manceau, M., Thome, V. & Marcelle, C. A common somitic origin for embryonic muscle progenitors and satellite cells. *Nature* **435**, 954-958 (2005).
38. Kassar-Duchossoy, L. *et al.* Pax3/Pax7 mark a novel population of primitive myogenic cells during development. *Genes Dev.* **19**, 1426-1431 (2005).
39. Relaix, F., Rocancourt, D., Mansouri, A. & Buckingham, M. A Pax3/Pax7-dependent population of skeletal muscle progenitor cells. *Nature* **435**, 948-953 (2005).
40. Denetclaw, W.F., Jr, Berdougo, E., Venters, S.J. & Ordahl, C.P. Morphogenetic cell movements in the middle region of the dermomyotome dorsomedial lip associated with patterning and growth of the primary epaxial myotome. *Development* **128**, 1745-1755 (2001).
41. Venters, S.J. & Ordahl, C.P. Persistent myogenic capacity of the dermomyotome dorsomedial lip and restriction of myogenic competence. *Development* **129**, 3873-3885 (2002).
42. Gros, J., Scaal, M. & Marcelle, C. A two-step mechanism for myotome formation in chick. *Dev. Cell* **6**, 875-882 (2004).
43. Relaix, F., Rocancourt, D., Mansouri, A. & Buckingham, M. A Pax3/Pax7-dependent population of skeletal muscle progenitor cells. *Nature* **435**, 948-953 (2005).
44. Lepper, C. & Fan, C. Inducible lineage tracing of Pax7-descendant cells reveals embryonic origin of adult satellite cells. *genesis* **48**, 424-436 (2010).
45. Rios, A.C., Serralbo, O., Salgado, D. & Marcelle, C. Neural crest regulates myogenesis through the transient activation of NOTCH. *Nature* **473**, 532-535 (2011).
46. Rudnicki, M.A., Braun, T., Hinuma, S. & Jaenisch, R. Inactivation of MyoD in mice leads to up-regulation of the myogenic HLH gene Myf-5 and results in apparently normal muscle development. *Cell* **71**, 383-390 (1992).
47. Delfini, M.-C. & Duprez, D. Ectopic Myf5 or MyoD prevents the neuronal differentiation program in addition to inducing skeletal muscle differentiation, in the chick neural tube. *Development* **131**, 713 -723 (2004).
48. de la Serna, I.L. *et al.* MyoD Targets Chromatin Remodeling Complexes to the Myogenin Locus Prior to Forming a Stable DNA-Bound Complex. *Mol. Cell. Biol.* **25**, 3997-4009 (2005).
49. Sweetman, D. *et al.* Specific requirements of MRFs for the expression of muscle specific microRNAs, miR-1, miR-206 and miR-133. *Developmental Biology* **321**, 491-499 (2008).
50. Hasty, P. *et al.* Muscle deficiency and neonatal death in mice with a targeted mutation in the myogenin gene. *Nature* **364**, 501-506 (1993).
51. Rudnicki, M.A. *et al.* MyoD or Myf-5 is required for the formation of skeletal muscle. *Cell* **75**, 1351-1359 (1993).
52. Kassar-Duchossoy, L. *et al.* Mrf4 determines skeletal muscle identity in Myf5:Myod double-mutant mice. *Nature* **431**, 466-471 (2004).
53. Young, A.P. & Wagers, A.J. Pax3 induces differentiation of juvenile skeletal muscle stem cells without transcriptional upregulation of canonical myogenic regulatory factors. *Journal of Cell Science* **123**, 2632 -2639 (2010).
54. Mok, G.F. & Sweetman, D. Many routes to the same destination: lessons from skeletal muscle development. *Reproduction* **141**, 301 -312 (2011).

55. Kuang, S., Gillespie, M.A. & Rudnicki, M.A. Niche regulation of muscle satellite cell self-renewal and differentiation. *Cell Stem Cell* **2**, 22-31 (2008).
56. Zammit, P.S. All muscle satellite cells are equal, but are some more equal than others? *J. Cell. Sci.* **121**, 2975-2982 (2008).
57. Sacco, A., Doyonnas, R., Kraft, P., Vitorovic, S. & Blau, H.M. Self-renewal and expansion of single transplanted muscle stem cells. *Nature* **456**, 502-506 (2008).
58. Meadows, E., Cho, J.-H., Flynn, J.M. & Klein, W.H. Myogenin regulates a distinct genetic program in adult muscle stem cells. *Dev. Biol.* **322**, 406-414 (2008).
59. Kang, J.-S. & Krauss, R.S. Muscle stem cells in developmental and regenerative myogenesis. *Curr Opin Clin Nutr Metab Care* **13**, 243-248 (2010).
60. Oustanina, S., Hause, G. & Braun, T. Pax7 directs postnatal renewal and propagation of myogenic satellite cells but not their specification. *EMBO J.* **23**, 3430-3439 (2004).
61. Seale, P. *et al.* Pax7 is required for the specification of myogenic satellite cells. *Cell* **102**, 777-786 (2000).
62. Lepper, C., Conway, S.J. & Fan, C.-M. Adult satellite cells and embryonic muscle progenitors have distinct genetic requirements. *Nature* **460**, 627-631 (2009).
63. HUXLEY, H. & HANSON, J. Changes in the cross-striations of muscle during contraction and stretch and their structural interpretation. *Nature* **173**, 973-976 (1954).
64. HUXLEY, A.F. & NIEDERGERKE, R. Structural changes in muscle during contraction; interference microscopy of living muscle fibres. *Nature* **173**, 971-973 (1954).
65. Gordon, A.M., Huxley, A.F. & Julian, F.J. Tension development in highly stretched vertebrate muscle fibres. *J. Physiol. (Lond.)* **184**, 143-169 (1966).
66. Gordon, A.M., Huxley, A.F. & Julian, F.J. The variation in isometric tension with sarcomere length in vertebrate muscle fibres. *J. Physiol. (Lond.)* **184**, 170-192 (1966).
67. Webb, M.R. & Trentham, D.R. The stereochemical course of phosphoric residue transfer catalyzed by sarcoplasmic reticulum ATPase. *J. Biol. Chem.* **256**, 4884-4887 (1981).
68. Rayment, I. *et al.* Structure of the actin-myosin complex and its implications for muscle contraction. *Science* **261**, 58-65 (1993).
69. Ebashi, S. & Endo, M. Calcium ion and muscle contraction. *Prog. Biophys. Mol. Biol.* **18**, 123-183 (1968).
70. Ebashi, S., Endo, M. & Otsuki, I. Control of muscle contraction. *Q. Rev. Biophys.* **2**, 351-384 (1969).
71. Ebashi, S. Excitation-contraction coupling and the mechanism of muscle contraction. *Annu. Rev. Physiol.* **53**, 1-16 (1991).
72. Kohl, P. & Ravens, U. Cardiac mechano-electric feedback: past, present, and prospect. *Prog. Biophys. Mol. Biol.* **82**, 3-9 (2003).
73. Bremel, R.D. & Weber, A. Cooperation within actin filament in vertebrate skeletal muscle. *Nature New Biol.* **238**, 97-101 (1972).
74. Okamura, N. & Ishiwata, S. Spontaneous oscillatory contraction of sarcomeres in skeletal myofibrils. *J. Muscle Res. Cell. Motil.* **9**, 111-119 (1988).

75. Ishiwata, S. *et al.* Spontaneous tension oscillation (SPOC) of muscle fibers and myofibrils minimum requirements for SPOC. *Adv. Exp. Med. Biol.* **332**, 545-554; discussion 555-556 (1993).
76. Plaçais, P.-Y., Balland, M., Guérin, T., Joanny, J.-F. & Martin, P. Spontaneous oscillations of a minimal actomyosin system under elastic loading. *Phys. Rev. Lett.* **103**, 158102 (2009).
77. Ishiwata, S., Shimamoto, Y. & Suzuki, M. Molecular motors as an auto-oscillator. *HFSP J* **4**, 100-104 (2010).
78. Conen, P.E., Murphy, E.G. & Donohue, W.L. Light and Electron Microscopic Studies of "Myogranules" in a Child with Hypotonia and Muscle Weakness. *Can Med Assoc J* **89**, 983-986 (1963).
79. SHY, G.M., ENGEL, W.K., SOMERS, J.E. & WANKO, T. NEMALINE MYOPATHY. A NEW CONGENITAL MYOPATHY. *Brain* **86**, 793-810 (1963).
80. Sanoudou, D. & Beggs, A.H. Clinical and genetic heterogeneity in nemaline myopathy – a disease of skeletal muscle thin filaments. *Trends in Molecular Medicine* **7**, 362-368 (2001).
81. Ryan, M.M. *et al.* Clinical course correlates poorly with muscle pathology in nemaline myopathy. *Neurology* **60**, 665-673 (2003).
82. Ilkovski, B. *et al.* Nemaline myopathy caused by mutations in the muscle alpha-skeletal-actin gene. *Am. J. Hum. Genet.* **68**, 1333-1343 (2001).
83. Ryan, M.M. *et al.* Clinical course correlates poorly with muscle pathology in nemaline myopathy. *Neurology* **60**, 665-673 (2003).
84. North, K.N., Laing, N.G. & Wallgren-Pettersson, C. Nemaline myopathy: current concepts. The ENMC International Consortium and Nemaline Myopathy. *J. Med. Genet.* **34**, 705-713 (1997).
85. Domazetovska, A. *et al.* Mechanisms underlying intranuclear rod formation. *Brain* **130**, 3275-3284 (2007).
86. Vandebrouck, A. *et al.* In vitro analysis of rod composition and actin dynamics in inherited myopathies. *J. Neuropathol. Exp. Neurol.* **69**, 429-441 (2010).
87. Hutchinson, D.O., Charlton, A., Laing, N.G., Ilkovski, B. & North, K.N. Autosomal dominant nemaline myopathy with intranuclear rods due to mutation of the skeletal muscle ACTA1 gene: clinical and pathological variability within a kindred. *Neuromuscul. Disord.* **16**, 113-121 (2006).
88. Domazetovska, A. *et al.* Intranuclear rod myopathy: molecular pathogenesis and mechanisms of weakness. *Ann. Neurol.* **62**, 597-608 (2007).
89. Yamaguchi, M., Robson, R.M., Stromer, M.H., Dahl, D.S. & Oda, T. Nemaline myopathy rod bodies. Structure and composition. *J. Neurol. Sci.* **56**, 35-56 (1982).
90. Wallgren-Pettersson, C. *et al.* Alpha-actinin in nemaline bodies in congenital nemaline myopathy: immunological confirmation by light and electron microscopy. *Neuromuscul. Disord.* **5**, 93-104 (1995).
91. Morris, E.P., Nneji, G. & Squire, J.M. The three-dimensional structure of the nemaline rod Z-band. *J. Cell Biol.* **111**, 2961-2978 (1990).
92. Ladha, S. *et al.* Histopathologic progression and a novel mutation in a child with nemaline myopathy. *J. Child Neurol.* **23**, 813-817 (2008).

93. Reimann, J., Irintchev, A. & Wernig, A. Regenerative capacity and the number of satellite cells in soleus muscles of normal and mdx mice. *Neuromuscul. Disord.* **10**, 276-282 (2000).
94. Haslett, J.N. *et al.* Gene expression comparison of biopsies from Duchenne muscular dystrophy (DMD) and normal skeletal muscle. *Proc. Natl. Acad. Sci. U.S.A.* **99**, 15000-15005 (2002).
95. Peña, T.L., Chen, S.H., Konieczny, S.F. & Rane, S.G. Ras/MEK/ERK Up-regulation of the fibroblast KCa channel FIK is a common mechanism for basic fibroblast growth factor and transforming growth factor-beta suppression of myogenesis. *J. Biol. Chem.* **275**, 13677-13682 (2000).
96. Zhang, J.M., Zhao, X., Wei, Q. & Paterson, B.M. Direct inhibition of G(1) cdk kinase activity by MyoD promotes myoblast cell cycle withdrawal and terminal differentiation. *EMBO J.* **18**, 6983-6993 (1999).
97. Chen, S.L., Loffler, K.A., Chen, D., Stallcup, M.R. & Muscat, G.E.O. The coactivator-associated arginine methyltransferase is necessary for muscle differentiation: CARM1 coactivates myocyte enhancer factor-2. *J. Biol. Chem.* **277**, 4324-4333 (2002).
98. Delling, U. *et al.* A calcineurin-NFATc3-dependent pathway regulates skeletal muscle differentiation and slow myosin heavy-chain expression. *Mol. Cell. Biol.* **20**, 6600-6611 (2000).
99. Hesselink, M.K. *et al.* Protein expression of UCP3 differs between human type 1, type 2a, and type 2b fibers. *FASEB J.* **15**, 1071-1073 (2001).
100. Calsbeek, D.J. *et al.* Metabolic and anthropometric factors related to skeletal muscle UCP3 gene expression in healthy human adults. *Am. J. Physiol. Endocrinol. Metab.* **283**, E631-637 (2002).
101. Schrauwen, P. & Hesselink, M. UCP2 and UCP3 in muscle controlling body metabolism. *J. Exp. Biol.* **205**, 2275-2285 (2002).
102. Maloney, J.A. & Wheeler-Clark, E.S. Reduction in sarcoplasmic reticulum Ca2+-ATPase activity contributes to age-related changes in the calcium content and relaxation rate of rabbit aortic smooth muscle. *J. Hypertens.* **14**, 65-74 (1996).
103. Herr, C. *et al.* Loss of annexin A7 leads to alterations in frequency-induced shortening of isolated murine cardiomyocytes. *Mol. Cell. Biol.* **21**, 4119-4128 (2001).
104. Benders, A.A., Groenen, P.J., Oerlemans, F.T., Veerkamp, J.H. & Wieringa, B. Myotonic dystrophy protein kinase is involved in the modulation of the Ca2+ homeostasis in skeletal muscle cells. *J. Clin. Invest.* **100**, 1440-1447 (1997).
105. Striggow, F. & Ehrlich, B.E. Regulation of intracellular calcium release channel function by arachidonic acid and leukotriene B4. *Biochem. Biophys. Res. Commun.* **237**, 413-418 (1997).
106. Zemel, M.B. Nutritional and endocrine modulation of intracellular calcium: implications in obesity, insulin resistance and hypertension. *Mol. Cell. Biochem.* **188**, 129-136 (1998).
107. Petersen, K.F. & Shulman, G.I. Pathogenesis of skeletal muscle insulin resistance in type 2 diabetes mellitus. *Am. J. Cardiol.* **90**, 11G-18G (2002).
108. Bakay, M., Zhao, P., Chen, J. & Hoffman, E.P. A web-accessible complete transcriptome of normal human and DMD muscle. *Neuromuscul. Disord.* **12 Suppl 1**, S125-141 (2002).

109. Chen, Y.W., Zhao, P., Borup, R. & Hoffman, E.P. Expression profiling in the muscular dystrophies: identification of novel aspects of molecular pathophysiology. *J. Cell Biol.* **151**, 1321-1336 (2000).
110. Filipowicz, W., Bhattacharyya, S.N. & Sonenberg, N. Mechanisms of post-transcriptional regulation by microRNAs: are the answers in sight? *Nature Reviews Genetics* **2008**, 102-114 (2008).
111. Ambros, V. The functions of animal microRNAs. *Nature* **431**, 350-355 (2004).
112. Friedman, J.M. & Jones, P.A. MicroRNAs: critical mediators of differentiation, development and disease. *Swiss Med Wkly* **139**, 466-472 (2009).
113. Gomase, V.S. & Parundekar, A.N. microRNA: human disease and development. *Int J Bioinform Res Appl* **5**, 479-500 (2009).
114. Croce, C.M. Causes and consequences of microRNA dysregulation in cancer. *Nat Rev Genet* **10**, 704-714 (2009).
115. Ventura, A. & Jacks, T. MicroRNAs and cancer: short RNAs go a long way. *Cell* **136**, 586-591 (2009).
116. Melo, S.A. & Esteller, M. Dysregulation of microRNAs in cancer: Playing with fire. *FEBS Letters* **585**, 2087-2099 (2011).
117. HÃ©bert, Sã©.S. & De Strooper, B. Alterations of the microRNA network cause neurodegenerative disease. *Trends in Neurosciences* **32**, 199-206 (2009).
118. Lau, P. & de Strooper, B. Dysregulated microRNAs in neurodegenerative disorders. *Seminars in Cell & Developmental Biology* **21**, 768-773 (2010).
119. CAI, X., HAGEDORN, C.H. & CULLEN, B.R. Human microRNAs are processed from capped, polyadenylated transcripts that can also function as mRNAs. *RNA* **10**, 1957 -1966 (2004).
120. Lee, Y. *et al.* MicroRNA genes are transcribed by RNA polymerase II. *EMBO J* **23**, 4051-4060 (2004).
121. Borchert, G.M., Lanier, W. & Davidson, B.L. RNA polymerase III transcribes human microRNAs. *Nat Struct Mol Biol* **13**, 1097-1101 (2006).
122. Zeng, Y. & Cullen, B.R. Efficient Processing of Primary microRNA Hairpins by Drosha Requires Flanking Nonstructured RNA Sequences. *Journal of Biological Chemistry* **280**, 27595 -27603 (2005).
123. Han, J. *et al.* Molecular Basis for the Recognition of Primary microRNAs by the Drosha-DGCR8 Complex. *Cell* **125**, 887-901 (2006).
124. Denli, A.M., Tops, B.B.J., Plasterk, R.H.A., Ketting, R.F. & Hannon, G.J. Processing of primary microRNAs by the Microprocessor complex. *Nature* **432**, 231-235 (2004).
125. Gregory, R.I. *et al.* The Microprocessor complex mediates the genesis of microRNAs. *Nature* **432**, 235-240 (2004).
126. Lee, Y. *et al.* The nuclear RNase III Drosha initiates microRNA processing. *Nature* **425**, 415-419 (2003).
127. Gregory, R.I. *et al.* The Microprocessor complex mediates the genesis of microRNAs. *Nature* **432**, 235-240 (2004).
128. Han, J. *et al.* The Drosha-DGCR8 complex in primary microRNA processing. *Genes Dev.* **18**, 3016-3027 (2004).
129. Morlando, M. *et al.* Primary microRNA transcripts are processed co-transcriptionally. *Nat. Struct. Mol. Biol.* **15**, 902-909 (2008).

130. Kim, Y.-K. & Kim, V.N. Processing of intronic microRNAs. *EMBO J* **26**, 775-783 (2007).
131. Basyuk, E., Suavet, F., Doglio, A., Bordonné, R. & Bertrand, E. Human let-7 stem-loop precursors harbor features of RNase III cleavage products. *Nucleic Acids Res.* **31**, 6593-6597 (2003).
132. Zeng, Y. & Cullen, B.R. Structural requirements for pre-microRNA binding and nuclear export by Exportin 5. *Nucleic Acids Res.* **32**, 4776-4785 (2004).
133. Lund, E., Güttinger, S., Calado, A., Dahlberg, J.E. & Kutay, U. Nuclear Export of MicroRNA Precursors. *Science* **303**, 95 -98 (2004).
134. Yi, R., Qin, Y., Macara, I.G. & Cullen, B.R. Exportin-5 mediates the nuclear export of pre-microRNAs and short hairpin RNAs. *Genes & Development* **17**, 3011 -3016 (2003).
135. Warf, M.B., Johnson, W.E. & Bass, B.L. Improved annotation of C. elegans microRNAs by deep sequencing reveals structures associated with processing by Drosha and Dicer. *RNA* **17**, 563-577 (2011).
136. Bernstein, E., Caudy, A.A., Hammond, S.M. & Hannon, G.J. Role for a bidentate ribonuclease in the initiation step of RNA interference. *Nature* **409**, 363-366 (2001).
137. Hutvágner, G. *et al.* A cellular function for the RNA-interference enzyme Dicer in the maturation of the let-7 small temporal RNA. *Science* **293**, 834-838 (2001).
138. MacRae, I.J. & Doudna, J.A. Ribonuclease revisited: structural insights into ribonuclease III family enzymes. *Current Opinion in Structural Biology* **17**, 138-145 (2007).
139. Zhang, H., Kolb, F.A., Jaskiewicz, L., Westhof, E. & Filipowicz, W. Single Processing Center Models for Human Dicer and Bacterial RNase III. *Cell* **118**, 57-68 (2004).
140. Takeshita, D. *et al.* Homodimeric Structure and Double-stranded RNA Cleavage Activity of the C-terminal RNase III Domain of Human Dicer. *Journal of Molecular Biology* **374**, 106-120 (2007).
141. Gregory, R.I., Chendrimada, T.P., Cooch, N. & Shiekhattar, R. Human RISC couples microRNA biogenesis and posttranscriptional gene silencing. *Cell* **123**, 631-640 (2005).
142. Lee, Y. *et al.* The role of PACT in the RNA silencing pathway. *EMBO J.* **25**, 522-532 (2006).
143. Maniataki, E. & Mourelatos, Z. A human, ATP-independent, RISC assembly machine fueled by pre-miRNA. *Genes & Development* **19**, 2979 -2990 (2005).
144. MacRae, I.J., Ma, E., Zhou, M., Robinson, C.V. & Doudna, J.A. In vitro reconstitution of the human RISC-loading complex. *Proc. Natl. Acad. Sci. U.S.A.* **105**, 512-517 (2008).
145. Chendrimada, T.P. *et al.* TRBP recruits the Dicer complex to Ago2 for microRNA processing and gene silencing. *Nature* **436**, 740-744 (2005).
146. Haase, A.D. *et al.* TRBP, a regulator of cellular PKR and HIV-1 virus expression, interacts with Dicer and functions in RNA silencing. *EMBO Rep* **6**, 961-967 (2005).

147. Mourelatos, Z. *et al.* miRNPs: a novel class of ribonucleoproteins containing numerous microRNAs. *Genes Dev.* **16**, 720-728 (2002).
148. Kawamata, T. & Tomari, Y. Making RISC. *Trends Biochem. Sci.* **35**, 368-376 (2010).
149. Khvorova, A., Reynolds, A. & Jayasena, S.D. Functional siRNAs and miRNAs exhibit strand bias. *Cell* **115**, 209-216 (2003).
150. Krol, J. *et al.* Structural Features of MicroRNA (miRNA) Precursors and Their Relevance to miRNA Biogenesis and Small Interfering RNA/Short Hairpin RNA Design. *Journal of Biological Chemistry* **279**, 42230 -42239 (2004).
151. Okamura, K., Liu, N. & Lai, E.C. Distinct Mechanisms for MicroRNA Strand Selection by Drosophila Argonautes. *Molecular Cell* **36**, 431-444 (2009).
152. Czech, B. *et al.* Hierarchical Rules for Argonaute Loading in Drosophila. *Molecular Cell* **36**, 445-456 (2009).
153. Ghildiyal, M., Xu, J., Seitz, H., Weng, Z. & Zamore, P.D. Sorting of Drosophila small silencing RNAs partitions microRNA* strands into the RNA interference pathway. *RNA* **16**, 43-56 (2010).
154. Warf, M.B., Johnson, W.E. & Bass, B.L. Improved annotation of C. elegans microRNAs by deep sequencing reveals structures associated with processing by Drosha and Dicer. *RNA* **17**, 563-577 (2011).
155. Hu, H.Y. *et al.* Sequence features associated with microRNA strand selection in humans and flies. *BMC Genomics* **10**, 413 (2009).
156. Okamura, K. *et al.* The regulatory activity of microRNA* species has substantial influence on microRNA and 3' UTR evolution. *Nat. Struct. Mol. Biol.* **15**, 354-363 (2008).
157. Miyoshi, K., Miyoshi, T. & Siomi, H. Many ways to generate microRNA-like small RNAs: non-canonical pathways for microRNA production. *Mol. Genet. Genomics* **284**, 95-103 (2010).
158. Berezikov, E., Chung, W.-J., Willis, J., Cuppen, E. & Lai, E.C. Mammalian mirtron genes. *Mol. Cell* **28**, 328-336 (2007).
159. Okamura, K., Hagen, J.W., Duan, H., Tyler, D.M. & Lai, E.C. The Mirtron Pathway Generates microRNA-Class Regulatory RNAs in Drosophila. *Cell* **130**, 89-100 (2007).
160. Ruby, J.G., Jan, C.H. & Bartel, D.P. Intronic microRNA precursors that bypass Drosha processing. *Nature* **448**, 83-86 (2007).
161. Chung, W.-J. *et al.* Computational and experimental identification of mirtrons in Drosophila melanogaster and Caenorhabditis elegans. *Genome Res.* **21**, 286-300 (2011).
162. Yang, J.-S. *et al.* Conserved vertebrate mir-451 provides a platform for Dicer-independent, Ago2-mediated microRNA biogenesis. *Proc. Natl. Acad. Sci. U.S.A.* **107**, 15163-15168 (2010).
163. Cheloufi, S., Dos Santos, C.O., Chong, M.M.W. & Hannon, G.J. A dicer-independent miRNA biogenesis pathway that requires Ago catalysis. *Nature* **465**, 584-589 (2010).
164. Cifuentes, D. *et al.* A novel miRNA processing pathway independent of Dicer requires Argonaute2 catalytic activity. *Science* **328**, 1694-1698 (2010).
165. Lewis, B.P., Shih, I.-hung, Jones-Rhoades, M.W., Bartel, D.P. & Burge, C.B. Prediction of mammalian microRNA targets. *Cell* **115**, 787-798 (2003).

166. Brennecke, J., Stark, A., Russell, R.B. & Cohen, S.M. Principles of microRNA-target recognition. *PLoS Biol.* **3**, e85 (2005).
167. Krek, A. *et al.* Combinatorial microRNA target predictions. *Nat. Genet.* **37**, 495-500 (2005).
168. Lewis, B.P., Burge, C.B. & Bartel, D.P. Conserved seed pairing, often flanked by adenosines, indicates that thousands of human genes are microRNA targets. *Cell* **120**, 15-20 (2005).
169. Farh, K.K.-H. *et al.* The widespread impact of mammalian MicroRNAs on mRNA repression and evolution. *Science* **310**, 1817-1821 (2005).
170. Grimson, A. *et al.* MicroRNA targeting specificity in mammals: determinants beyond seed pairing. *Mol. Cell* **27**, 91-105 (2007).
171. Lee, I. *et al.* New class of microRNA targets containing simultaneous 5'-UTR and 3'-UTR interaction sites. *Genome Res.* **19**, 1175-1183 (2009).
172. Wells, S.E., Hillner, P.E., Vale, R.D. & Sachs, A.B. Circularization of mRNA by eukaryotic translation initiation factors. *Mol. Cell* **2**, 135-140 (1998).
173. Derry, M.C., Yanagiya, A., Martineau, Y. & Sonenberg, N. Regulation of poly(A)-binding protein through PABP-interacting proteins. *Cold Spring Harb. Symp. Quant. Biol.* **71**, 537-543 (2006).
174. Kiriakidou, M. *et al.* An mRNA m7G cap binding-like motif within human Ago2 represses translation. *Cell* **129**, 1141-1151 (2007).
175. Pillai, R.S., Artus, C.G. & Filipowicz, W. Tethering of human Ago proteins to mRNA mimics the miRNA-mediated repression of protein synthesis. *RNA* **10**, 1518-1525 (2004).
176. Doench, J.G. & Sharp, P.A. Specificity of microRNA target selection in translational repression. *Genes Dev.* **18**, 504-511 (2004).
177. Pillai, R.S. *et al.* Inhibition of translational initiation by Let-7 MicroRNA in human cells. *Science* **309**, 1573-1576 (2005).
178. Doench, J.G., Petersen, C.P. & Sharp, P.A. siRNAs can function as miRNAs. *Genes Dev.* **17**, 438-442 (2003).
179. Chendrimada, T.P. *et al.* MicroRNA silencing through RISC recruitment of eIF6. *Nature* **447**, 823-828 (2007).
180. Sanvito, F. *et al.* The beta4 integrin interactor p27(BBP/eIF6) is an essential nuclear matrix protein involved in 60S ribosomal subunit assembly. *J. Cell Biol.* **144**, 823-837 (1999).
181. Si, K. & Maitra, U. The Saccharomyces cerevisiae homologue of mammalian translation initiation factor 6 does not function as a translation initiation factor. *Mol. Cell. Biol.* **19**, 1416-1426 (1999).
182. Basu, U., Si, K., Warner, J.R. & Maitra, U. The Saccharomyces cerevisiae TIF6 gene encoding translation initiation factor 6 is required for 60S ribosomal subunit biogenesis. *Mol. Cell. Biol.* **21**, 1453-1462 (2001).
183. Kim, J. *et al.* Identification of many microRNAs that copurify with polyribosomes in mammalian neurons. *Proc. Natl. Acad. Sci. U.S.A.* **101**, 360-365 (2004).
184. Nelson, P.T., Hatzigeorgiou, A.G. & Mourelatos, Z. miRNP:mRNA association in polyribosomes in a human neuronal cell line. *RNA* **10**, 387-394 (2004).

185. Vasudevan, S. & Steitz, J.A. AU-rich-element-mediated upregulation of translation by FXR1 and Argonaute 2. *Cell* **128**, 1105-1118 (2007).
186. Petersen, C.P., Bordeleau, M.-E., Pelletier, J. & Sharp, P.A. Short RNAs repress translation after initiation in mammalian cells. *Mol. Cell* **21**, 533-542 (2006).
187. Lytle, J.R., Yario, T.A. & Steitz, J.A. Target mRNAs are repressed as efficiently by microRNA-binding sites in the 5' UTR as in the 3' UTR. *Proc. Natl. Acad. Sci. U.S.A.* **104**, 9667-9672 (2007).
188. Wu, L., Fan, J. & Belasco, J.G. MicroRNAs direct rapid deadenylation of mRNA. *Proc. Natl. Acad. Sci. U.S.A.* **103**, 4034-4039 (2006).
189. Chendrimada, T.P. *et al.* MicroRNA silencing through RISC recruitment of eIF6. *Nature* **447**, 823-828 (2007).
190. Wu, L. & Belasco, J.G. Micro-RNA regulation of the mammalian lin-28 gene during neuronal differentiation of embryonal carcinoma cells. *Mol. Cell. Biol.* **25**, 9198-9208 (2005).
191. Parker, R. & Song, H. The enzymes and control of eukaryotic mRNA turnover. *Nat. Struct. Mol. Biol.* **11**, 121-127 (2004).
192. Eulalio, A., Behm-Ansmant, I. & Izaurralde, E. P bodies: at the crossroads of post-transcriptional pathways. *Nat. Rev. Mol. Cell Biol.* **8**, 9-22 (2007).
193. Parker, R. & Sheth, U. P bodies and the control of mRNA translation and degradation. *Mol. Cell* **25**, 635-646 (2007).
194. Bhattacharyya, S.N., Habermacher, R., Martine, U., Closs, E.I. & Filipowicz, W. Relief of microRNA-mediated translational repression in human cells subjected to stress. *Cell* **125**, 1111-1124 (2006).
195. Mishima, Y. *et al.* Differential regulation of germline mRNAs in soma and germ cells by zebrafish miR-430. *Curr. Biol.* **16**, 2135-2142 (2006).
196. Schratt, G.M. *et al.* A brain-specific microRNA regulates dendritic spine development. *Nature* **439**, 283-289 (2006).
197. Ashraf, S.I., McLoon, A.L., Sclarsic, S.M. & Kunes, S. Synaptic protein synthesis associated with memory is regulated by the RISC pathway in Drosophila. *Cell* **124**, 191-205 (2006).
198. Chen, X. *et al.* Characterization of microRNAs in serum: a novel class of biomarkers for diagnosis of cancer and other diseases. *Cell Res.* **18**, 997-1006 (2008).
199. El-Hefnawy, T. *et al.* Characterization of amplifiable, circulating RNA in plasma and its potential as a tool for cancer diagnostics. *Clin. Chem.* **50**, 564-573 (2004).
200. Tsui, N.B.Y., Ng, E.K.O. & Lo, Y.M.D. Stability of endogenous and added RNA in blood specimens, serum, and plasma. *Clin. Chem.* **48**, 1647-1653 (2002).
201. El-Hefnawy, T. *et al.* Characterization of amplifiable, circulating RNA in plasma and its potential as a tool for cancer diagnostics. *Clin. Chem.* **50**, 564-573 (2004).
202. Valadi, H. *et al.* Exosome-mediated transfer of mRNAs and microRNAs is a novel mechanism of genetic exchange between cells. *Nat. Cell Biol.* **9**, 654-659 (2007).
203. Ratajczak, J. *et al.* Embryonic stem cell-derived microvesicles reprogram hematopoietic progenitors: evidence for horizontal transfer of mRNA and protein delivery. *Leukemia* **20**, 847-856 (2006).

204. Cortez, M.A. & Calin, G.A. MicroRNA identification in plasma and serum: a new tool to diagnose and monitor diseases. *Expert Opin Biol Ther* **9**, 703-711 (2009).
205. Ji, X. *et al.* Plasma miR-208 as a biomarker of myocardial injury. *Clin. Chem.* **55**, 1944-1949 (2009).
206. Selth, L.A. *et al.* Discovery of circulating microRNAs associated with human prostate cancer using a mouse model of disease. *International Journal of Cancer. Journal International Du Cancer* (2011).doi:10.1002/ijc.26405
207. Enright, A.J. *et al.* MicroRNA targets in Drosophila. *Genome Biol.* **5**, R1 (2003).
208. John, B. *et al.* Human MicroRNA targets. *PLoS Biol.* **2**, e363 (2004).
209. Lewis, B.P., Burge, C.B. & Bartel, D.P. Conserved seed pairing, often flanked by adenosines, indicates that thousands of human genes are microRNA targets. *Cell* **120**, 15-20 (2005).
210. Rehmsmeier, M., Steffen, P., Hochsmann, M. & Giegerich, R. Fast and effective prediction of microRNA/target duplexes. *RNA* **10**, 1507-1517 (2004).
211. Kertesz, M., Iovino, N., Unnerstall, U., Gaul, U. & Segal, E. The role of site accessibility in microRNA target recognition. *Nat. Genet.* **39**, 1278-1284 (2007).
212. Eisenberg, I. *et al.* Distinctive patterns of microRNA expression in primary muscular disorders. *Proceedings of the National Academy of Sciences* **104**, 17016-17021 (2007).
213. Dennis, G., Jr *et al.* DAVID: Database for Annotation, Visualization, and Integrated Discovery. *Genome Biol.* **4**, P3 (2003).
214 Lee YS, Choi JW, Hwang I, Lee JW, Lee JH, Kim AY, Huh JY, Koh YJ, Koh GY, Son HJ, Masuzaki H, Hotta K, Alfadda AA, Kim JB. Adipocytokine orosomucoid integrates inflammatory and metabolic signals to preserve energy homeostasis by resolving immoderate inflammation J Biol Chem. 2010 Jul 16;285(29):22174-85.
215 Sanoudou D, Corbett MA, Han M, Ghoddusi M, Nguyen MA, Vlahovich N, Hardeman EC, Beggs AH. Skeletal muscle repair in a mouse model of nemaline myopathy. Hum Mol Genet. 2006 Sep 1;15(17):2603-12.
216 Ottenheijm CA, Lawlor MW, Stienen GJ, Granzier H, Beggs AH.
Changes in cross-bridge cycling underlie muscle weakness in patients with tropomyosin 3-based myopathy Hum Mol Genet. 2011 May 15;20(10):2015-25.
217 Sanoudou D, Haslett JN, Kho AT, Guo S, Gazda HT, Greenberg SA, Lidov HG, Kohane IS, Kunkel LM, Beggs AH. Expression profiling reveals altered satellite cell numbers and glycolytic enzyme transcription in nemaline myopathy muscle.
Proc Natl Acad Sci U S A. 2003 Apr 15;100(8):4666-71.
218 Tang H, Liu X, Wang Z, She X, Zeng X, Deng M, Liao Q, Guo X, Wang R, Li X, Zeng F, Wu M, Li G. Interaction of hsa-miR-381 and glioma suppressor LRRC4 is involved in glioma growth. Brain Res. 2011 May 16;1390:21-32.
219 Joya JE, Kee AJ, Nair-Shalliker V, Ghoddusi M, Nguyen MA, Luther P, Hardeman EC.. Muscle weakness in a mouse model of nemaline myopathy can be reversed with exercise and reveals a novel myofiber repair mechanism. Hum Mol Genet. 2004 Nov 1;13(21):2633-45.
220 Brinkmeier H. TRP channels in skeletal muscle: gene expression, function and implications for disease. Adv Exp Med Biol. 2011;704:749-58.

221 Michele DE, Albayya FP, Metzger JM. A nemaline myopathy mutation in alpha-tropomyosin causes defective regulation of striated muscle force production.J Clin Invest. 1999 Dec;104(11):1575-81.
222 Gommans IM, Vlak MH, de Haan A, van Engelen BG. Calcium regulation and muscle disease J Muscle Res Cell Motil. 2002;23(1):59-63.
223 Clarkson E, Costa CF, Machesky LM Congenital myopathies: diseases of the actin cytoskeleton. J Pathol. 2004 Nov;204(4):407-17.
224 Chen, X. et al. Characterization of microRNAs in serum: a novel class of biomarkers for diagnosis of cancer and other diseases. Cell Res. 18, 997-1006 (2008).
225 El-Hefnawy, T. et al. Characterization of amplifiable, circulating RNA in plasma and its potential as a tool for cancer diagnostics. Clin. Chem. 50, 564-573 (2004).
226 Tsui, N.B.Y., Ng, E.K.O. & Lo, Y.M.D. Stability of endogenous and added RNA in blood specimens, serum, and plasma. Clin. Chem. 48, 1647-1653 (2002).
227 El-Hefnawy, T. *et al.* Characterization of amplifiable, circulating RNA in plasma and its potential as a tool for cancer diagnostics. *Clin. Chem.* **50**, 564-573 (2004).
228 Valadi, H. et al. Exosome-mediated transfer of mRNAs and microRNAs is a novel mechanism of genetic exchange between cells. Nat. Cell Biol. 9, 654-659 (2007).
229 Ratajczak, J. *et al.* Embryonic stem cell-derived microvesicles reprogram hematopoietic progenitors: evidence for horizontal transfer of mRNA and protein delivery. *Leukemia* **20**, 847-856 (2006).
230 Cortez, M.A. & Calin, G.A. MicroRNA identification in plasma and serum: a new tool to diagnose and monitor diseases. *Expert Opin Biol Ther* **9**, 703-711 (2009).
231 Ji, X. *et al.* Plasma miR-208 as a biomarker of myocardial injury. *Clin. Chem.* **55**, 1944-1949 (2009).
232 Selth, L.A. et al. Discovery of circulating microRNAs associated with human prostate cancer using a mouse model of disease. International Journal of Cancer. Journal International Du Cancer (2011).doi:10.1002/ijc.26405
233 Enright, A.J. et al. MicroRNA targets in Drosophila. Genome Biol. 5, R1 (2003).
234 John, B. *et al.* Human MicroRNA targets. *PLoS Biol.* **2**, e363 (2004).
235 Lewis, B.P., Burge, C.B. & Bartel, D.P. Conserved seed pairing, often flanked by adenosines, indicates that thousands of human genes are microRNA targets. *Cell* **120**, 15-20 (2005).
236 Rehmsmeier, M., Steffen, P., Hochsmann, M. & Giegerich, R. Fast and effective prediction of microRNA/target duplexes. RNA 10, 1507-1517 (2004).
237 Kertesz, M., Iovino, N., Unnerstall, U., Gaul, U. & Segal, E. The role of site accessibility in microRNA target recognition. *Nat. Genet.* **39**, 1278-1284 (2007).
238 Dennis, G., Jr *et al.* DAVID: Database for Annotation, Visualization, and Integrated Discovery. *Genome Biol.* **4**, P3 (2003).

APPENDIX A

Genes altered in TA and DIA of 3-week-old males and 10-week-old males and females with fold ≥ 1.4 and pvalues < 0.05. Ratio indicate the fold change value.

Table 1. Genes altered in TA of 3-week-old ACTA KI males

No.	Ratio	p-value	Identifier	Gene Name
1	▲ 1.99	0.00458	NM_027093	RIKEN cDNA 2310003L22 gene (2310003L22Rik), mRNA
2	▲ 1.92	0.00969	XM_354684	RIKEN cDNA 1810035L17 gene
3	▲ 1.91	0.03194	NM_007808	Cytochrome c, somatic, mRNA (cDNA clone MGC:6857 IMAGE:2650742)
4	▲ 1.90	0.01813	NM_008466	Karyopherin (importin) alpha 3, mRNA (cDNA clone MGC:30454 IMAGE:3979788)
5	▲ 1.89	0.00124	NM_016956	Hemoglobin, beta adult minor chain, mRNA (cDNA clone MGC:40691 IMAGE:3988455)
6	▲ 1.82	0.04200	NM_017372	Lysozyme 2, mRNA (cDNA clone IMAGE:2655292)
7	▲ 1.76	0.03042	NM_027430	Brain protein 44 (Brp44), mRNA
8	▲ 1.76	0.02180	XM_131914	peptidase (mitochondrial processing) beta
9	▲ 1.74	0.04794	NM_007861	Dihydrolipoamide dehydrogenase, mRNA (cDNA clone MGC:5874 IMAGE:3589344)
10	▲ 1.73	0.02083	NM_133835	Ubiquitin associated domain containing 1 (Ubac1), mRNA
11	▲ 1.73	0.03674	XM_136108	Ureb1
12	▲ 1.70	0.01077	NM_023172	NADH dehydrogenase (ubiquinone) 1 beta subcomplex, 9, mRNA (cDNA clone MGC:18943
13	▲ 1.70	0.01692	NM_019766	Prostaglandin E synthase 3 (cytosolic), mRNA (cDNA clone MGC:5681 IMAGE:3489418)
14	▲ 1.70	0.00105	NM_025468	SEC11 homolog C (S. cerevisiae), mRNA (cDNA clone MGC:47104 IMAGE:3666130)
15	▲ 1.69	0.01889	NM_025894	Proteasome (prosome, macropain) 26S subunit, non-ATPase, 12, mRNA (cDNA clone MG
16	▲ 1.69	0.00252	NM_026844	RIKEN cDNA 2310061C15 gene (2310061C15Rik), mRNA
17	▲ 1.69	0.03728	NM_026434	RNA binding motif protein 18, mRNA (cDNA clone MGC:8172 IMAGE:3590164)
18	▲ 1.69	0.03291	NM_025848	Succinate dehydrogenase complex, subunit D, integral membrane protein, mRNA (cDN
19	▲ 1.68	0.04747	NM_023323	Brix domain containing 1 (Bxdc1), transcript variant 1, mRNA
20	▲ 1.68	0.02502	NM_080556	Transmembrane 9 superfamily member 2 (Tm9sf2), mRNA
21	▲ 1.67	0.00037	NM_026612	NADH dehydrogenase (ubiquinone) 1 beta subcomplex, 2, mRNA (cDNA clone MGC:19178
22	▲ 1.66	0.03976	NM_012019	Apoptosis-inducing factor, mitochondrion-associated 1, mRNA (cDNA clone MGC:5706
23	▲ 1.66	0.04744	NM_026614	NADH dehydrogenase (ubiquinone) 1 alpha subcomplex, 5, mRNA (cDNA clone MGC:4101
24	▲ 1.66	0.04923	NM_026934	Zinc finger CCCH-type containing 15 (Zc3h15), mRNA
25	▲ 1.65	0.04527	NM_174848	Beta-gamma crystallin domain containing 3 (Crybg3), mRNA
26	▲ 1.65	0.01733	NM_011931	Constitutive photomorphogenic protein (Cop1)
27	▲ 1.65	0.02997	NM_198033	Senataxin, mRNA (cDNA clone IMAGE:30355235)
28	▲ 1.64	0.00085	NM_008258	Hematological and neurological expressed sequence 1, mRNA (cDNA clone MGC:5893 I
29	▲ 1.64	0.02794	NM_153567	SLAIN motif family, member 2 (Slain2), transcript variant 1, mRNA
30	▲ 1.64	0.02313	NM_025444	TAF13 RNA polymerase II, TATA box binding protein (TBP)-associated factor (Taf13
31	▲ 1.64	0.00887	NM_019780	Vacuolar protein sorting 29 (S. pombe), mRNA (cDNA clone MGC:11606 IMAGE:2645432
32	▲ 1.63	0.03475	NM_016690	Heterogeneous nuclear ribonucleoprotein D-like, mRNA (cDNA clone MGC:29063 IMAGE
33	▲ 1.63	0.02258	NM_025835	Propionyl Coenzyme A carboxylase, beta polypeptide, mRNA (cDNA clone MGC:46787 I
34	▲ 1.63	0.03066	NM_025846	Related RAS viral (r-ras) oncogene homolog 2, mRNA (cDNA clone MGC:6630 IMAGE:34
35	▲ 1.63	0.01239	NM_177740	RGM domain family, member A, mRNA (cDNA clone MGC:38550 IMAGE:5353958)
36	▲ 1.62	0.02735	NM_028986	CDNA clone IMAGE:4485254
37	▲ 1.62	0.04838	NM_019979	Selenoprotein K, mRNA (cDNA clone MGC:46841 IMAGE:2645414)
38	▲ 1.62	0.02909	NM_022985	Zinc finger, AN1-type domain 6, mRNA (cDNA clone MGC:6494 IMAGE:2647905)
39	▲ 1.61	0.00429	NM_144517	TBC1 domain family, member 19 (Tbc1d19), mRNA
40	▼ 1.60	0.03240	NM_177470	Acetyl-Coenzyme A acyltransferase 2 (mitochondrial 3-oxoacyl-Coenzyme A thiolase
41	▲ 1.60	0.02500	NM_021526	Proteasome (prosome, macropain) 26S subunit, non-ATPase, 14, mRNA (cDNA clone MG
42	▲ 1.60	0.02897	NM_172677	YTH domain family 3, mRNA (cDNA clone IMAGE:3994696)
43	▲ 1.59	0.02953	NM_026425	N-acetyltransferase 5 (ARD1 homolog, S. cerevisiae), mRNA (cDNA clone MGC:6501 I
44	▲ 1.59	0.02935	NM_172695	Phospholipase A2, activating protein, mRNA (cDNA clone MGC:170983 IMAGE:8862378)
45	▲ 1.58	0.02498	NM_025570	Mitochondrial ribosomal protein L20 (Mrpl20), nuclear gene encoding mitochondria
46	▲ 1.58	0.00313	NM_026610	NADH dehydrogenase (ubiquinone) 1 beta subcomplex 4 (Ndufb4), nuclear gene encod

No.	Ratio	p-value	Identifier	Gene Name
47	▲ 1.56	0.04226	NM_007505	CDNA fis, clone TRACH2013369,highly similar to ATP SYNTHASE ALPHA CHAIN, MITOCHO
48	▲ 1.56	0.00250	NM_019794	DnaJ (Hsp40) homolog, subfamily A, member 2, mRNA (cDNA clone MGC:6445 IMAGE:258
49	▲ 1.56	0.00607	NM_010887	NADH dehydrogenase (ubiquinone) Fe-S protein 4, mRNA (cDNA clone MGC:5649 IMAGE:
50	▲ 1.56	0.01835	NM_145984	Prolyl endopeptidase-like (Prepl), mRNA
51	▲ 1.56	0.00377	XM_123431	Usmg5
52	▲ 1.55	0.02669	NM_027326	Myeloid/lymphoid or mixed-lineage leukemia (trithorax homolog, Drosophila); tran
53	▲ 1.55	0.01238	NM_025762	RIKEN cDNA 4933434E20 gene (4933434E20Rik), transcript variant 1, mRNA
54	▲ 1.55	0.02280	XM_134455	Scoc
55	▲ 1.54	0.01441	NM_175489	Oxysterol binding protein-like 8, mRNA (cDNA clone MGC:176345 IMAGE:9055996)
56	▼ 1.54	0.01289	NM_009155	Selenoprotein P, plasma, 1, mRNA (cDNA clone MGC:5722 IMAGE:3486761)
57	▲ 1.53	0.01216	NM_026851	Mitochondrial ribosomal protein L52, mRNA (cDNA clone MGC:57882 IMAGE:5683366)
58	▲ 1.53	0.02756	NM_025690	SAFB-like, transcription modulator (SItm), transcript variant 1, mRNA
59	▲ 1.52	0.01586	NM_008220	Hemoglobin, beta adult minor chain, mRNA (cDNA clone MGC:40691 IMAGE:3988455)
60	▲ 1.52	0.02749	NM_026329	Polymerase (RNA) II (DNA directed) polypeptide G, mRNA (cDNA clone MGC:11735 IMA
61	▲ 1.51	0.01716	NM_145985	Archain 1, mRNA (cDNA clone MGC:36506 IMAGE:5368060)
62	▲ 1.51	0.01451	NM_008379	Karyopherin (importin) beta 1, mRNA (cDNA clone IMAGE:3594201)
63	▲ 1.51	0.01251	NM_133749	RIKEN cDNA 2900064A13 gene (2900064A13Rik), mRNA
64	▲ 1.50	0.03376	NM_011511	ATP-binding cassette, sub-family C (CFTR/MRP), member 9 (Abcc9), transcript vari
65	▲ 1.50	0.00944	NM_175266	EPM2A (laforin) interacting protein 1, mRNA (cDNA clone MGC:27780 IMAGE:3156440)
66	▲ 1.50	0.00613	NM_010368	Glucuronidase, beta, mRNA (cDNA clone IMAGE:3675986)
67	▲ 1.49	0.02031	NM_027352	Golgi reassembly stacking protein 2, mRNA (cDNA clone MGC:25922 IMAGE:4234343)
68	▲ 1.49	0.02669	NM_138599	Translocase of outer mitochondrial membrane 70 homolog A (yeast), mRNA (cDNA clo
69	▲ 1.48	0.02552	NM_181858	CD59b antigen, mRNA (cDNA clone MGC:170830 IMAGE:8862225)
70	▲ 1.48	0.04161	NM_013536	EMG1 nucleolar protein homolog (S. cerevisiae), mRNA (cDNA clone MGC:5775 IMAGE:
71	▲ 1.48	0.00595	XM_194230	mitochondrial ribosomal protein S18C
72	▲ 1.48	0.02636	NM_172699	MKIAA1041 protein
73	▲ 1.48	0.03659	NM_018796	Mus musculus, eukaryotic translation elongation factor 1 beta 2, clone IMAGE:513
74	▲ 1.47	0.03364	NM_010422	Hexosaminidase B (Hexb), mRNA
75	▲ 1.47	0.04527	NM_175413	Leucine rich repeat containing 39, mRNA (cDNA clone MGC:141190 IMAGE:40056121)
76	▲ 1.47	0.00178	NM_026759	Mitochondrial ribosomal protein L13 (Mrpl13), nuclear gene encoding mitochondria
77	▲ 1.47	0.02643	NM_008786	Protein-L-isoaspartate (D-aspartate) O-methyltransferase 1 (Pcmt1), mRNA
78	▲ 1.47	0.01590	NR_002321	taurine upregulated gene 1
79	▲ 1.47	0.02946	NM_013771	YME1-like 1 (S. cerevisiae), mRNA (cDNA clone MGC:5753 IMAGE:3591123)
80	▲ 1.46	0.00954	NM_025895	Mediator of RNA polymerase II transcription, subunit 28 homolog (yeast), mRNA (c
81	▲ 1.46	0.02578	NM_175374	Mitochondrial translational release factor 1-like (Mtrf1l), nuclear gene encodin
82	▲ 1.46	0.02479	NM_021507	Sulfide quinone reductase-like (yeast), mRNA (cDNA clone MGC:18811 IMAGE:4196280
83	▼ 1.46	0.02378	NM_009381	Thyroid hormone responsive SPOT14 homolog (Rattus), mRNA (cDNA clone MGC:6563 IM
84	▲ 1.46	0.02736	NM_181412	Zinc finger, BED domain containing 4, mRNA (cDNA clone IMAGE:4012067)
85	▲ 1.45	0.00713	NM_019673	Actin-like 6A, mRNA (cDNA clone MGC:5731 IMAGE:3491205)
86	▲ 1.45	0.01316	NM_007711	Chloride channel 3 (Clcn3), transcript variant a, mRNA
87	▲ 1.45	0.03685	NM_172381	Expressed sequence AI314180, mRNA (cDNA clone IMAGE:4953720)
88	▲ 1.45	0.01319	NM_198710	Synaptophysin-like protein (Sypl), transcript variant 1, mRNA
89	▲ 1.45	0.01077	NM_011660	Thioredoxin 1, mRNA (cDNA clone MGC:18460 IMAGE:4216106)
90	▲ 1.45	0.00129	NM_016800	Vesicle transport through interaction with t-SNAREs 1B homolog, mRNA (cDNA clone
91	▲ 1.44	0.02543	XM_125157	Atp5l
92	▲ 1.44	0.01843	NM_019650	Golgi SNAP receptor complex member 2, mRNA (cDNA clone IMAGE:1449054)
93	▲ 1.44	0.03858	NM_145374	Missing oocyte, meiosis regulator, homolog (Drosophila) (Mios), mRNA
94	▲ 1.44	0.04699	NM_025544	Mitochondrial ribosomal protein S15, mRNA (cDNA clone MGC:35744 IMAGE:4457237)

No.	Ratio	p-value	Identifier	Gene Name
95	▲ 1.44	0.04422	NM_025316	NADH dehydrogenase (ubiquinone) 1 beta subcomplex, 5, mRNA (cDNA clone MGC:35776
96	▼ 1.44	0.02557	NM_178900	Protein kinase D2, mRNA (cDNA clone MGC:106161 IMAGE:4216827)
97	▲ 1.44	0.00984	NM_025579	TAF12 RNA polymerase II, TATA box binding protein (TBP)-associated factor, mRNA
98	▲ 1.44	0.03030	NM_021522	Ubiquitin specific peptidase 14, mRNA (cDNA clone MGC:7106 IMAGE:3157723)
99	▼ 1.44	0.02063	NM_011909	Ubiquitin specific protease UBP43
100	▲ 1.43	0.00849	NM_026514	CDC42 effector protein (Rho GTPase binding) 3, mRNA (cDNA clone MGC:11796 IMAGE:
101	▲ 1.43	0.03608	NM_025950	Cell division cycle 37 homolog (S. cerevisiae)-like 1, mRNA (cDNA clone MGC:2564
102	▲ 1.43	0.02283	NM_145529	Cleavage stimulation factor, 3' pre-RNA, subunit 3 (Cstf3), transcript variant 1
103	▲ 1.43	0.01322	NM_010880	Nucleolin, mRNA (cDNA clone MGC:6363 IMAGE:3495665)
104	▲ 1.43	0.03646	NM_008774	Poly(A) binding protein, cytoplasmic 1, mRNA (cDNA clone MGC:28185 IMAGE:3988101
105	▲ 1.43	0.03770	NM_025319	RIKEN cDNA 0610009B22 gene, mRNA (cDNA clone MGC:35774 IMAGE:5009365)
106	▲ 1.43	0.02088	NM_027338	Vacuolar protein sorting 36 (yeast), mRNA (cDNA clone MGC:19122 IMAGE:4210911)
107	▲ 1.42	0.04216	NM_145392	BCL2-associated athanogene 2, mRNA (cDNA clone MGC:36682 IMAGE:5371263)
108	▲ 1.42	0.02445	NM_027978	Coenzyme Q2 homolog, prenyltransferase (yeast) (Coq2), mRNA
109	▲ 1.42	0.02008	NM_021876	Embryonic ectoderm development, mRNA (cDNA clone MGC:13909 IMAGE:3991086)
110	▲ 1.42	0.00737	NM_028233	Leucine-rich PPR-motif containing (Lrpprc), mRNA
111	▲ 1.42	0.03927	NM_148937	Phospholipase C, delta 4 (Plcd4), transcript variant 2, mRNA
112	▲ 1.42	0.04664	NM_009273	Signal recognition particle 14, mRNA (cDNA clone MGC:36171 IMAGE:5353575)
113	▼ 1.42	0.00293	NM_001079695	Splicing factor, arginine/serine-rich 5 (SRp40, HRS) (Sfrs5), transcript variant
114	▲ 1.42	0.01220	NM_009536	Strain ILS epsilon 14-3-3
115	▲ 1.41	0.03377	NM_199008	COX11 homolog, cytochrome c oxidase assembly protein (yeast) (Cox11), nuclear ge
116	▲ 1.41	0.01840	NM_053071	Cytochrome c oxidase, subunit VIc, mRNA (cDNA clone MGC:19084 IMAGE:4195595)
117	▲ 1.41	0.00022	NM_007890	Dual-specificity tyrosine-(Y)-phosphorylation regulated kinase 1a (Dyrk1a), tran
118	▲ 1.41	0.04201	NM_019773	RAB9, member RAS oncogene family, mRNA (cDNA clone MGC:11411 IMAGE:3964134)
119	▲ 1.41	0.00481	NM_028355	Transmembrane protein 48, mRNA (cDNA clone MGC:29369 IMAGE:5042118)
120	▲ 1.41	0.00569	NM_019562	Ubiquitin carboxyl-terminal esterase L5, mRNA (cDNA clone MGC:6295 IMAGE:2650799
121	▲ 1.40	0.03209	NM_019727	MSNX1 mRNA for sorting nexin 1
122	▼ 1.40	0.03973	NM_013492	Sulfated glycoprotein-2 isoform 2

Table 2. Genes altered in DIA of 3-week-old ACTA KI males

No.	Ratio	p-value	Identifier	Gene Name
1	▼ 8.08	0.03455	NM_008768	Orosomucoid 1, mRNA (cDNA clone MGC:14080 IMAGE:4162961)
2	▼ 7.60	0.00099	NM_145594	Fibrinogen-like protein 1 (Fgl1), mRNA
3	▼ 7.25	0.00920	NM_007818	Cytochrome P450, family 3, subfamily a, polypeptide 11, mRNA (cDNA clone MGC:186
4	▼ 7.00	0.00021	NM_017371	Hemopexin (Hpx), mRNA
5	▼ 6.89	0.00196	NM_018746	Inter alpha-trypsin inhibitor, heavy chain 4, mRNA (cDNA clone MGC:25281 IMAGE:4
6	▼ 6.54	0.02901	NM_007618	Serine (or cysteine) peptidase inhibitor, clade A, member 6, mRNA (cDNA clone MG
7	▼ 6.47	0.03706	NM_008878	Serine (or cysteine) peptidase inhibitor, clade F, member 2, mRNA (cDNA clone MG
8	▼ 6.43	0.03356	NM_008878	Serine (or cysteine) peptidase inhibitor, clade F, member 2, mRNA (cDNA clone MG
9	▼ 6.19	0.00857	NM_011318	Serum amyloid P-component (Apcs), mRNA
10	▼ 6.10	0.01724	NM_144834	Serine (or cysteine) peptidase inhibitor, clade A (alpha-1 antiproteinase, antit
11	▼ 5.88	0.02383	NM_009714	Asialoglycoprotein receptor 1, mRNA (cDNA clone MGC:36097 IMAGE:5102469)
12	▼ 5.77	0.01604	NM_009654	Serum albumin (alb gene)
13	▼ 5.76	0.01433	NM_019775	Carboxypeptidase B2 (plasma) (Cpb2), mRNA
14	▼ 5.74	2.13e-05	NM_017371	Hemopexin (Hpx), mRNA
15	▼ 5.73	0.01911	NM_016702	Alanine-glyoxylate aminotransferase, mRNA (cDNA clone MGC:35967 IMAGE:5099627)
16	▼ 5.73	0.04532	NM_008878	Serine (or cysteine) peptidase inhibitor, clade F, member 2, mRNA (cDNA clone MG
17	▼ 5.73	0.02500	XM_132178	UDP glucuronosyltransferase 2 family, polypeptide B36
18	▼ 5.67	0.02626	NM_022884	Betaine-homocysteine methyltransferase 2, mRNA (cDNA clone MGC:19186 IMAGE:42354
19	▼ 5.67	0.00135	NM_018746	Inter alpha-trypsin inhibitor, heavy chain 4, mRNA (cDNA clone MGC:25281 IMAGE:4
20	▼ 5.67	0.02616	NM_017473	Retinol dehydrogenase 7, mRNA (cDNA clone MGC:25267 IMAGE:4196075)
21	▼ 5.66	0.01527	NM_013485	Complement component 9, mRNA (cDNA clone MGC:18645 IMAGE:4195787)
22	▼ 5.64	0.02813	NM_133657	Cytochrome P450, family 2, subfamily a, polypeptide 12 (Cyp2a12), mRNA
23	▼ 5.53	0.00620	NM_007385	Apolipoprotein C-IV, mRNA (cDNA clone MGC:18467 IMAGE:4196217)
24	▼ 5.53	0.03075	NM_008645	Mus musculus, clone IMAGE:4195167, mRNA
25	▼ 5.46	0.01146	NM_023125	Kininogen 1, mRNA (cDNA clone MGC:25815 IMAGE:4162960)
26	▼ 5.42	0.01258	NM_080845	Formiminotransferase cyclodeaminase, mRNA (cDNA clone MGC:37815 IMAGE:5098529)
27	▼ 5.40	0.03449	NM_001029867	UDP glucuronosyltransferase 2 family, polypeptide B36, mRNA (cDNA clone MGC:1761
28	▼ 5.39	0.00331	NM_018746	Inter alpha-trypsin inhibitor, heavy chain 4, mRNA (cDNA clone MGC:25281 IMAGE:4
29	▼ 5.38	0.01534	NM_146058	cDNA sequence BC025446
30	▼ 5.38	0.04877	XM_133915	RIKEN cDNA 1190003J15 gene
31	▼ 5.36	0.00372	NM_008223	Serine (or cysteine) peptidase inhibitor, clade D, member 1, mRNA (cDNA clone MG
32	▼ 5.34	0.02973	NM_008406	Inter-alpha trypsin inhibitor, heavy chain 1, mRNA (cDNA clone MGC:36127 IMAGE:5
33	▼ 5.33	0.02274	NM_007768	C-reactive protein, pentraxin-related (Crp), mRNA
34	▼ 5.26	0.02540	NM_008934	Protein C, mRNA (cDNA clone MGC:13870 IMAGE:4211329)
35	▼ 5.25	0.01007	NM_019395	Fructose bisphosphatase 1, mRNA (cDNA clone MGC:18799 IMAGE:4194764)
36	▼ 5.22	0.01363	NM_009512	Solute carrier family 27 (fatty acid transporter), member 5, mRNA (cDNA clone MG
37	▼ 5.07	0.01158	NM_008877	Plasminogen, mRNA (cDNA clone MGC:18525 IMAGE:4193957)
38	▼ 5.05	0.03865	NM_009474	Urate oxidase, mRNA (cDNA clone MGC:30311 IMAGE:5136328)
39	▼ 5.02	0.02393	NM_133997	Apolipoprotein F, mRNA (cDNA clone MGC:37889 IMAGE:5101712)
40	▼ 5.01	0.03611	NM_010005	Cytochrome P450, family 2, subfamily d, polypeptide 22, mRNA (cDNA clone MGC:288
41	▼ 5.00	0.01029	NM_019447	Hepatocyte growth factor activator, mRNA (cDNA clone MGC:30305 IMAGE:5134851)
42	▼ 4.99	0.00100	NM_007824	Cytochrome P450, family 7, subfamily a, polypeptide 1 (Cyp7a1), mRNA
43	▼ 4.95	0.01683	NM_007954	Esterase 1, mRNA (cDNA clone MGC:18575 IMAGE:4196339)
44	▼ 4.92	0.00367	NM_008490	Lecithin cholesterol acyltransferase, mRNA (cDNA clone MGC:25630 IMAGE:4212194)
45	▼ 4.91	0.04930	NM_146101	Hyaluronic acid binding protein 2 (Habp2), mRNA
46	▼ 4.89	0.04610	NM_007954	Esterase 1, mRNA (cDNA clone MGC:18575 IMAGE:4196339)

No.	Ratio	p-value	Identifier	Gene Name
47	▼ 4.89	0.04756	NM_008819	Phosphatidylethanolamine N-methyltransferase, mRNA (cDNA clone MGC:25864 IMAGE:4
48	▼ 4.89	0.01549	NM_144845	UDP glycosyltransferases 3 family, polypeptide A2, mRNA (cDNA clone MGC:37957 IM
49	▼ 4.87	0.02722	NM_022026	Aquaporin 9, mRNA (cDNA clone MGC:35844 IMAGE:5096952)
50	▼ 4.87	7.97e-05	NM_029562	Cytochrome P450, family 2, subfamily d, polypeptide 26, mRNA (cDNA clone MGC:286
51	▼ 4.86	0.04504	NM_001081372	Predicted gene, 382044 (382044), mRNA
52	▼ 4.86	0.01684	NM_007447	Ribonuclease, RNase A family 4, mRNA (cDNA clone MGC:11599 IMAGE:3967265)
53	▼ 4.84	0.00111	NM_138595	Glycine decarboxylase (Gldc), mRNA
54	▼ 4.81	0.02050	NM_017473	Retinol dehydrogenase 7, mRNA (cDNA clone MGC:25267 IMAGE:4196075)
55	▼ 4.79	0.01827	NM_009253	Serine (or cysteine) peptidase inhibitor, clade A, member 3K, mRNA (cDNA clone M
56	▼ 4.75	1.68e-05	NM_001080809	Carbamoyl-phosphate synthetase 1 (Cps1), nuclear gene encoding mitochondrial pro
57	▼ 4.73	0.00208	NM_019546	Proline dehydrogenase (oxidase) 2, mRNA (cDNA clone MGC:25812 IMAGE:4161894)
58	▼ 4.71	0.01517	NM_031164	Coagulation factor XIII, beta subunit, mRNA (cDNA clone MGC:29126 IMAGE:5051604)
59	▼ 4.71	0.02014	NM_029269	Secreted phosphoprotein 2, mRNA (cDNA clone MGC:40991 IMAGE:1433655)
60	▼ 4.70	0.01597	NM_138951	Tetratricopeptide repeat domain 36 (Ttc36), mRNA
61	▼ 4.68	0.02926	NM_183257	Hepcidin antimicrobial peptide 2, mRNA (cDNA clone MGC:107568 IMAGE:6765293)
62	▼ 4.68	4.42e-05	NM_008407	Inter-alpha trypsin inhibitor, heavy chain 3, mRNA (cDNA clone MGC:18839 IMAGE:4
63	▼ 4.67	0.01690	XM_135893	coagulation factor IX
64	▼ 4.66	0.00986	NM_023125	Kininogen 1, mRNA (cDNA clone MGC:25815 IMAGE:4162960)
65	▼ 4.64	0.00066	NM_007494	Argininosuccinate synthetase 1, mRNA (cDNA clone MGC:6218 IMAGE:3491910)
66	▼ 4.63	0.01933	NM_021564	Fetuin beta, mRNA (cDNA clone MGC:25848 IMAGE:4194184)
67	▼ 4.58	0.00104	XM_129769	carbamoyl-phosphate synthetase 1
68	▼ 4.56	0.02175	NM_021489	Coagulation factor XII (Hageman factor), mRNA (cDNA clone IMAGE:5102659)
69	▼ 4.56	0.00569	NM_010196	Fibrinogen, alpha polypeptide, mRNA (cDNA clone MGC:6605 IMAGE:3487861)
70	▼ 4.55	0.02772	NM_010582	Inter-alpha trypsin inhibitor, heavy chain 2, mRNA (cDNA clone MGC:25336 IMAGE:4
71	▼ 4.55	0.01545	NM_133995	Ureidopropionase, beta, mRNA (cDNA clone IMAGE:4974180)
72	▼ 4.54	0.01843	NM_013475	Apolipoprotein H (Apoh), mRNA
73	▼ 4.52	0.00618	NM_134144	Cytochrome P450, family 2, subfamily c, polypeptide 50 (Cyp2c50), mRNA
74	▼ 4.50	0.04968	NM_001042767	Protein C, mRNA (cDNA clone MGC:13870 IMAGE:4211329)
75	▼ 4.48	0.04739	NM_145499	Cytochrome P450, family 2, subfamily c, polypeptide 70, mRNA (cDNA clone MGC:377
76	▼ 4.48	0.02327	NM_010403	Glycolate oxidase
77	▼ 4.46	0.01806	NM_027406	Aldehyde dehydrogenase 1 family, member L1, mRNA (cDNA clone MGC:36387 IMAGE:509
78	▼ 4.45	0.02506	NM_153529	Neuritin 1 (Nrn1), mRNA
79	▼ 4.45	0.02501	NM_011134	Paraoxonase 1, mRNA (cDNA clone MGC:13984 IMAGE:4158951)
80	▼ 4.45	0.01432	NM_019546	Proline dehydrogenase (oxidase) 2, mRNA (cDNA clone MGC:25812 IMAGE:4161894)
81	▼ 4.43	0.00669	NM_001033264	L-type glutaminase 2 pseudogene mRNA, complete sequence
82	▼ 4.41	0.04234	NM_178747	Gulonolactone (L-) oxidase, mRNA (cDNA clone IMAGE:5102719)
83	▼ 4.40	0.01184	NM_021489	Coagulation factor XII (Hageman factor), mRNA (cDNA clone IMAGE:5102659)
84	▼ 4.39	0.00687	NM_053115	Acyl-Coenzyme A oxidase 2, branched chain, mRNA (cDNA clone MGC:29247 IMAGE:5052
85	▼ 4.39	0.00791	NM_010196	Fibrinogen, alpha polypeptide, mRNA (cDNA clone MGC:6605 IMAGE:3487861)
86	▼ 4.37	0.01028	NM_178235	Solute carrier organic anion transporter family, member 1b2 (Slco1b2), transcrip
87	▼ 4.34	0.00308	NM_013478	Alpha-2-glycoprotein 1, zinc (Azgp1), mRNA
88	▼ 4.34	0.01572	NM_031884	ATP-binding cassette, sub-family G (WHITE), member 5 (Abcg5), mRNA
89	▼ 4.33	0.00277	NM_144903	Aldolase 2, B isoform, mRNA (cDNA clone IMAGE:4972777)
90	▼ 4.33	0.00295	NM_010001	Cytochrome P450, family 2, subfamily c, polypeptide 50 (Cyp2c50), mRNA
91	▼ 4.32	0.01818	NM_011707	Vitronectin
92	▼ 4.28	0.01613	NM_027406	Aldehyde dehydrogenase 1 family, member L1, mRNA (cDNA clone MGC:36387 IMAGE:509
93	▼ 4.28	0.01687	NM_144855	Cystathionine beta-synthase (Cbs), transcript variant 1, mRNA
94	▼ 4.28	0.00150	NM_201375	Kininogen 2 (Kng2), transcript variant 3, mRNA

No.	Ratio	p-value	Identifier	Gene Name
95	▼ 4.27	0.03611	NM_027918	RIKEN cDNA 1300017J02 gene (1300017J02Rik), mRNA
96	▼ 4.26	0.00794	NM_008287	Heat-responsive protein 12 (Hrsp12), mRNA
97	▼ 4.25	9.12e-05	NM_010321	Glycine N-methyltransferase, mRNA (cDNA clone MGC:13738 IMAGE:4210236)
98	▼ 4.24	0.00879	NM_010406	Hemolytic complement, mRNA (cDNA clone IMAGE:3488145)
99	▼ 4.23	0.01328	NM_008277	4-hydroxyphenylpyruvic acid dioxygenase, mRNA (cDNA clone MGC:14040 IMAGE:419367
100	▼ 4.22	0.04317	NM_146058	cDNA sequence BC025446
101	▼ 4.21	0.02801	NM_144855	Cystathionine beta-synthase (Cbs), transcript variant 1, mRNA
102	▼ 4.21	0.00015	NM_019792	Cytochrome P450, family 3, subfamily a, polypeptide 25, mRNA (cDNA clone MGC:302
103	▼ 4.20	0.04947	NM_023114	Apolipoprotein C-III, mRNA (cDNA clone MGC:28546 IMAGE:4196708)
104	▼ 4.20	0.00260	NM_010001	Cytochrome P450, family 2, subfamily c, polypeptide 50 (Cyp2c50), mRNA
105	▼ 4.20	0.00576	NM_032541	Prohepcidin (hepc1)
106	▼ 4.19	0.01285	NM_133996	Apolipoprotein N (Apon), mRNA
107	▼ 4.19	0.04693	NM_133995	Ureidopropionase, beta, mRNA (cDNA clone IMAGE:4974180)
108	▼ 4.16	0.00228	NM_008287	Heat-responsive protein 12 (Hrsp12), mRNA
109	▼ 4.15	0.03799	NM_133995	Ureidopropionase, beta, mRNA (cDNA clone IMAGE:4974180)
110	▼ 4.14	0.00997	NM_013478	Alpha-2-glycoprotein 1, zinc (Azgp1), mRNA
111	▼ 4.13	0.00485	NM_010321	Glycine N-methyltransferase, mRNA (cDNA clone MGC:13738 IMAGE:4210236)
112	▼ 4.13	0.01642	NM_008287	Heat-responsive protein 12 (Hrsp12), mRNA
113	▼ 4.07	0.02144	NM_011978	Solute carrier family 27 (fatty acid transporter), member 2, mRNA (cDNA clone MG
114	▼ 4.06	0.00835	NM_019775	Carboxypeptidase B2 (plasma) (Cpb2), mRNA
115	▼ 4.06	0.03356	NM_008030	Flavin containing monooxygenase 3 (Fmo3), mRNA
116	▼ 4.05	0.00266	NM_026085	RIKEN cDNA 3110049J23 gene (3110049J23Rik), mRNA
117	▼ 4.01	0.02048	NM_178713	Aldehyde dehydrogenase 8 family, member A1, mRNA (cDNA clone MGC:46977 IMAGE:422
118	▼ 4.00	0.02426	NM_011979	Vanin 3 (Vnn3), mRNA
119	▼ 3.99	0.01333	NM_027406	Aldehyde dehydrogenase 1 family, member L1, mRNA (cDNA clone MGC:36387 IMAGE:509
120	▼ 3.99	0.01273	NM_007819	Cytochrome P450, family 3, subfamily a, polypeptide 13 (Cyp3a13), mRNA
121	▼ 3.98	0.03235	NM_008767	Solute carrier family 22 (organic cation transporter), member 18, mRNA (cDNA clo
122	▼ 3.98	0.01490	NM_015799	Transferrin receptor 2, mRNA (cDNA clone MGC:18814 IMAGE:4196597)
123	▼ 3.94	0.00564	NM_130452	Butyrobetaine (gamma), 2-oxoglutarate dioxygenase 1 (gamma-butyrobetaine hydroxy
124	▼ 3.93	0.00797	NM_007482	Arginase, liver, mRNA (cDNA clone MGC:13983 IMAGE:4163626)
125	▼ 3.91	0.00822	NM_008125	Gap junction protein, beta 2, mRNA (cDNA clone MGC:18706 IMAGE:4194757)
126	▼ 3.89	0.01642	NM_019546	Proline dehydrogenase (oxidase) 2, mRNA (cDNA clone MGC:25812 IMAGE:4161894)
127	▼ 3.88	0.02550	NM_027853	Methyltransferase like 7B, mRNA (cDNA clone MGC:25885 IMAGE:4215792)
128	▼ 3.87	0.04562	NM_008030	Flavin containing monooxygenase 3 (Fmo3), mRNA
129	▼ 3.85	0.02965	NM_053096	Camello-like 2, mRNA (cDNA clone MGC:49548 IMAGE:4193874)
130	▼ 3.84	0.01999	NM_007819	Cytochrome P450, family 3, subfamily a, polypeptide 13 (Cyp3a13), mRNA
131	▼ 3.84	0.02705	NM_144836	Solute carrier family 17 (sodium phosphate), member 2 (Slc17a2), mRNA
132	▼ 3.82	0.00169	XM_125928	glutaminase 2 (liver, mitochondrial)
133	▼ 3.81	0.04436	NM_011979	Vanin 3 (Vnn3), mRNA
134	▼ 3.80	0.01478	NM_007443	Alpha 1 microglobulin/bikunin, mRNA (cDNA clone MGC:14070 IMAGE:4193922)
135	▼ 3.78	0.04423	NM_028069	Mucin-like protocadherin (Mupcdh), transcript variant 2, mRNA
136	▼ 3.76	0.03590	NM_145565	Serine dehydratase (Sds), mRNA
137	▼ 3.75	0.00731	NM_007469	Apolipoprotein C-I, mRNA (cDNA clone MGC:30241 IMAGE:5124986)
138	▼ 3.74	4.54e-05	NM_008288	Hydroxysteroid 11-beta dehydrogenase 1 (Hsd11b1), transcript variant 1, mRNA
139	▼ 3.74	0.04591	NM_144836	Solute carrier family 17 (sodium phosphate), member 2 (Slc17a2), mRNA
140	▼ 3.73	0.00059	NM_201239	Ribonuclease, RNase A family 4, mRNA (cDNA clone MGC:11599 IMAGE:3967265)
141	▼ 3.72	0.03880	NM_031197	Solute carrier family 2 (facilitated glucose transporter), member 2, mRNA (cDNA
142	▼ 3.70	0.00066	NM_010168	Coagulation factor II, mRNA (cDNA clone MGC:18605 IMAGE:4196988)

No.	Ratio	p-value	Identifier	Gene Name
143	▼ 3.69	0.04114	NM_026180	ATP-binding cassette, sub-family G (WHITE), member 8 (Abcg8), mRNA
144	▼ 3.67	0.03400	NM_139292	Receptor accessory protein 6 (Reep6), mRNA
145	▼ 3.66	5.98e-05	NM_008288	Hydroxysteroid 11-beta dehydrogenase 1 (Hsd11b1), transcript variant 1, mRNA
146	▼ 3.66	0.01158	NM_153133	Retinol dehydrogenase 9 (Rdh9), mRNA
147	▼ 3.65	1.74e-06	NM_008288	Hydroxysteroid 11-beta dehydrogenase 1 (Hsd11b1), transcript variant 1, mRNA
148	▼ 3.63	0.00481	NM_008490	Lecithin cholesterol acyltransferase, mRNA (cDNA clone MGC:25630 IMAGE:4212194)
149	▼ 3.62	0.00440	NM_008555	Masp3 mRNA for MBL-associated serine protease-3
150	▼ 3.61	0.00293	NM_009696	Apolipoprotein E, mRNA (cDNA clone MGC:36251 IMAGE:5136415)
151	▼ 3.57	0.03829	NM_009108	Nuclear receptor subfamily 1, group H, member 4, mRNA (cDNA clone MGC:18424 IMAG
152	▼ 3.56	0.00245	NM_133653	Methionine adenosyltransferase I, alpha (Mat1a), mRNA
153	▼ 3.55	0.00012	NM_029562	Cytochrome P450, family 2, subfamily d, polypeptide 26, mRNA (cDNA clone MGC:286
154	▼ 3.55	0.04612	NM_201641	UDP glucuronosyltransferase 1 family, polypeptide A6B, mRNA (cDNA clone MGC:3624
155	▼ 3.51	0.00583	NM_008364	Interleukin 1 receptor accessory protein (Il1rap), transcript variant 2, mRNA
156	▼ 3.51	0.01299	NM_010398	MHC class Ib antigen Qa-1 (H2-T23)
157	▼ 3.49	0.00019	NM_029562	Cytochrome P450, family 2, subfamily d, polypeptide 26, mRNA (cDNA clone MGC:286
158	▼ 3.46	0.00787	NM_008364	Interleukin 1 receptor accessory protein (Il1rap), transcript variant 2, mRNA
159	▼ 3.45	0.01630	NM_009266	Selenophosphate synthetase 2 (Sephs2), mRNA
160	▼ 3.43	0.04001	NM_021517	Hydrophilic CFTR-binding protein CAP70 (Cap70)
161	▼ 3.42	0.00354	NM_133977	Transferrin (Trf), mRNA
162	▼ 3.39	0.00951	NM_007469	Apolipoprotein C-I, mRNA (cDNA clone MGC:30241 IMAGE:5124986)
163	▼ 3.37	0.00100	NM_138595	Glycine decarboxylase (Gldc), mRNA
164	▼ 3.37	0.02212	NM_144940	Urocanase domain containing 1, mRNA (cDNA clone IMAGE:4162723)
165	▼ 3.35	0.04612	NM_008239	Forkhead box Q1 (Foxq1), mRNA
166	▼ 3.34	0.02887	NM_021022	ATP-binding cassette, sub-family B (MDR/TAP), member 11 (Abcb11), mRNA
167	▼ 3.34	0.00017	NM_011255	Retinol binding protein 4, plasma, mRNA (cDNA clone MGC:19321 IMAGE:4193984)
168	▼ 3.33	0.02402	NM_019775	Carboxypeptidase B2 (plasma) (Cpb2), mRNA
169	▼ 3.33	0.04615	NM_010173	Fatty acid amide hydrolase, mRNA (cDNA clone MGC:11634 IMAGE:3595191)
170	▼ 3.33	0.01888	NM_010356	Glutathione S-transferase, alpha 3 (Gsta3), transcript variant 2, mRNA
171	▼ 3.33	0.04021	NM_133626	Ribosome binding protein 1, mRNA (cDNA clone IMAGE:4238895)
172	▼ 3.28	0.02554	NM_175217	Monocyte to macrophage differentiation-associated 2, mRNA (cDNA clone MGC:36872
173	▼ 3.25	0.00385	NM_007752	Ceruloplasmin (Cp), transcript variant 2, mRNA
174	▼ 3.24	0.04534	NM_016668	Betaine-homocysteine methyltransferase, mRNA (cDNA clone MGC:46866 IMAGE:5100429
175	▼ 3.24	0.03180	NM_201375	Kininogen 2 (Kng2), transcript variant 3, mRNA
176	▼ 3.20	0.00017	NM_008877	Plasminogen, mRNA (cDNA clone MGC:18525 IMAGE:4193957)
177	▼ 3.19	0.01037	NM_008364	Interleukin 1 receptor accessory protein (Il1rap), transcript variant 2, mRNA
178	▼ 3.13	0.00162	NM_013465	Alpha-2-HS-glycoprotein, mRNA (cDNA clone MGC:29969 IMAGE:5123689)
179	▼ 3.13	0.03509	NM_013697	Transthyretin, mRNA (cDNA clone MGC:18651 IMAGE:4192268)
180	▼ 3.12	0.02981	NM_133686	Quinolinate phosphoribosyltransferase (Qprt), mRNA
181	▼ 3.10	0.03208	NM_027552	Kynureninase (L-kynurenine hydrolase), mRNA (cDNA clone MGC:30315 IMAGE:5136970)
182	▼ 3.09	0.02134	NM_009246	Serine (or cysteine) peptidase inhibitor, clade A, member 1D, mRNA (cDNA clone M
183	▼ 3.08	0.03308	NM_001013762	Predicted gene, EG240549 (EG240549), mRNA
184	▼ 3.07	0.00703	NM_009244	Serine (or cysteine) preptidase inhibitor, clade A, member 1B, mRNA (cDNA clone
185	▼ 3.06	0.00198	XM_193784	alanine-glyoxylate aminotransferase 2
186	▼ 3.04	0.00721	NM_013777	Aldo-keto reductase family 1, member C12, mRNA (cDNA clone MGC:13745 IMAGE:42057
187	▼ 3.00	0.01393	NM_008198	CDNA fis, clone TRACH2005017,highly similar to COMPLEMENT FACTOR B PRECURSOR (EC
188	▼ 2.99	0.03070	NM_178936	Transmembrane protein 56 (Tmem56), mRNA
189	▼ 2.97	0.00251	NM_009155	Selenoprotein P, plasma, 1, mRNA (cDNA clone MGC:5722 IMAGE:3486761)
190	▼ 2.95	0.04051	NM_199314	Serine (or cysteine) peptidase inhibitor, clade A (alpha-1 antiproteinase, antit

No.	Ratio	p-value	Identifier	Gene Name
190	▼ 2.95	0.04051	NM_199314	Serine (or cysteine) peptidase inhibitor, clade A (alpha-1 antiproteinase, antit
191	▼ 2.94	0.00347	NM_009780	Complement component 4B (Childo blood group) (C4b), mRNA
192	▼ 2.94	0.00166	NM_008777	Phenylalanine hydroxylase, mRNA (cDNA clone MGC:18609 IMAGE:4223155)
193	▼ 2.94	0.00164	NM_011338	Strain SJL/J small inducible cytokine A10 (ScyA10)
194	▼ 2.91	0.01227	NM_010232	Flavin containing monooxygenase 5, mRNA (cDNA clone MGC:29923 IMAGE:5123876)
195	▼ 2.90	0.02950	NM_007409	Alcohol dehydrogenase 1 (class I), mRNA (cDNA clone MGC:18885 IMAGE:4238555)
196	▼ 2.87	0.03750	NM_146148	Complement component 8, alpha polypeptide (C8a), mRNA
197	▼ 2.85	0.00319	NM_017370	Haptoglobin (Hp), mRNA
198	▼ 2.85	0.00778	NM_008281	Hepsin (Hpn), transcript variant 2, mRNA
199	▼ 2.80	0.00365	NM_027711	IQ motif containing GTPase activating protein 2, mRNA (cDNA clone MGC:183869 IMA
200	▼ 2.79	0.03666	NM_133661	Solute carrier family 6 (neurotransmitter transporter, betaine/GABA), member 12
201	▼ 2.77	0.00636	NM_181849	Fibrinogen, B beta polypeptide, mRNA (cDNA clone MGC:25856 IMAGE:4195310)
202	▼ 2.77	0.00988	NM_017370	Haptoglobin (Hp), mRNA
203	▼ 2.75	0.02573	NM_011976	Semaphorin subclass 4 member G (sema4g)
204	▼ 2.75	0.00306	NM_016771	Sulfotransferase family 1D, member 1 (Sult1d1), mRNA
205	▼ 2.74	0.00271	NM_009692	Apolipoprotein A-I, mRNA (cDNA clone MGC:29972 IMAGE:5123746)
206	▼ 2.74	0.03592	NM_007519	Bile acid-Coenzyme A: amino acid N-acyltransferase (Baat), mRNA
207	▼ 2.71	0.00555	NM_017370	Haptoglobin (Hp), mRNA
208	▼ 2.70	0.01003	NM_008261	Hepatic nuclear factor 4, alpha, mRNA (cDNA clone MGC:31368 IMAGE:4238842)
209	▼ 2.70	0.00259	NM_010401	Histidine ammonia lyase (Hal), mRNA
210	▼ 2.70	0.03974	NM_019909	MHC (A.CA/J(H-2K-f) class I antigen (LOC56628), mRNA.
211	▼ 2.69	0.03482	NM_007493	Asialoglycoprotein receptor 2, mRNA (cDNA clone MGC:18613 IMAGE:4194949)
212	▼ 2.69	0.00051	NM_008342	Insulin-like growth factor binding protein 2, mRNA (cDNA clone MGC:14074 IMAGE:2
213	▼ 2.68	0.01242	NM_009929	Collagen, type XVIII, alpha 1 (Col18a1), transcript variant 2, mRNA
214	▼ 2.68	0.00690	NM_008439	Ketohexokinase, mRNA (cDNA clone MGC:18722 IMAGE:4235560)
215	▼ 2.67	0.04186	NM_001081015	predicted gene, EG630499 (EG630499), mRNA.
216	▼ 2.65	0.02804	NM_010172	Coagulation factor VII (F7), mRNA
217	▼ 2.65	0.01904	NM_178053	N-acetylglutamate synthase (Nags), transcript variant 1, mRNA
218	▼ 2.64	0.01355	NM_144903	Aldolase 2, B isoform, mRNA (cDNA clone IMAGE:4972777)
219	▼ 2.64	0.01947	NM_144909	Glucokinase regulatory protein (Gckr), mRNA
220	▼ 2.64	0.00244	NM_023124	Histocompatibility 2, Q region locus 8 (H2-Q8), mRNA
221	▼ 2.61	0.04218	XM_203596	asparaginase homolog (S. cerevisiae)
222	▼ 2.60	0.01334	NM_007409	Alcohol dehydrogenase 1 (class I), mRNA (cDNA clone MGC:18885 IMAGE:4238555)
223	▼ 2.58	0.01321	NM_010394	Histocompatibility 2, Q region locus 7 (H2-Q7), mRNA
224	▼ 2.57	0.00048	NM_181325	Ornithine transporter mRNA, complete cds; nuclear gene for mitochondrial product
225	▼ 2.57	0.00251	NM_016785	Thiopurine methyltransferase, mRNA (cDNA clone MGC:35956 IMAGE:5098857)
226	▼ 2.56	0.00223	NM_080434	Apolipoprotein A-V (Apoa5), mRNA
227	▼ 2.56	0.04006	NM_022316	SPARC related modular calcium binding 1, mRNA (cDNA clone MGC:30627 IMAGE:367373
228	▼ 2.55	0.01908	NM_009244	Serine (or cysteine) preptidase inhibitor, clade A, member 1B, mRNA (cDNA clone
229	▼ 2.52	0.03071	NM_007428	Angiotensinogen (serpin peptidase inhibitor, clade A, member 8), mRNA (cDNA clon
230	▼ 2.51	0.01160	NM_021282	Cytochrome P450, family 2, subfamily e, polypeptide 1, mRNA (cDNA clone MGC:1852
231	▼ 2.51	0.02303	NM_007870	Deoxyribonuclease 1-like 3, mRNA (cDNA clone MGC:13854 IMAGE:4160709)
232	▼ 2.50	0.00611	NM_133862	Fibrinogen, gamma polypeptide, mRNA (cDNA clone MGC:29970 IMAGE:5123696)
233	▼ 2.50	0.00320	XM_132170	group specific component
234	▼ 2.48	0.00300	NM_008342	Insulin-like growth factor binding protein 2, mRNA (cDNA clone MGC:14074 IMAGE:2
235	▼ 2.46	0.00377	NM_033037	Cysteine dioxygenase 1, cytosolic, mRNA (cDNA clone MGC:18800 IMAGE:4194939)
236	▼ 2.44	0.01009	NM_008061	Glucose-6-phosphatase, catalytic, mRNA (cDNA clone MGC:18472 IMAGE:4237115)
237	▼ 2.44	0.04463	NM_178577	Transmembrane protein 205, mRNA (cDNA clone MGC:18837 IMAGE:4211629)

No.	Ratio	p-value	Identifier	Gene Name
238	▼ 2.43	0.00549	NM_172961	4-aminobutyrate aminotransferase, mRNA (cDNA clone IMAGE:30532686)
239	▼ 2.43	0.01277	NM_008439	Ketohexokinase, mRNA (cDNA clone MGC:18722 IMAGE:4235560)
240	▼ 2.42	0.02142	NM_027391	Iodotyrosine deiodinase (Iyd), mRNA
241	▼ 2.42	0.01549	NM_016917	Solute carrier family 40 (iron-regulated transporter), member 1, mRNA (cDNA clon
242	▼ 2.41	0.00081	NM_009735	Beta-2 microglobulin mRNA, segment 1, clones pBRcB-(1-3).
243	▼ 2.37	0.01660	NM_010517	Insulin-like growth factor binding protein 4, mRNA (cDNA clone MGC:29917 IMAGE:5
244	▼ 2.34	0.02682	NM_008156	Glycosylphosphatidylinositol phospholipase D
245	▼ 2.34	0.00528	NM_177789	V-set and immunoglobulin domain containing 4, mRNA (cDNA clone MGC:36211 IMAGE:4
246	▼ 2.33	0.00174	NM_009735	Beta-2 microglobulin mRNA, segment 1, clones pBRcB-(1-3).
247	▼ 2.30	0.01684	NM_181344	Complement component 1, r subcomponent-like, mRNA (cDNA clone MGC:92956 IMAGE:30
248	▲ 2.25	0.04907	NM_011308	RIP-13 (RIP13)
249	▼ 2.24	0.04718	NM_029631	Abhydrolase domain containing 14b (Abhd14b), mRNA
250	▼ 2.24	0.04617	NM_008278	Hydroxyprostaglandin dehydrogenase 15 (NAD), mRNA (cDNA clone MGC:14001 IMAGE:42
251	▼ 2.22	0.00567	NM_001031851	Alanine-glyoxylate aminotransferase 2, mRNA (cDNA clone MGC:176209 IMAGE:9055860
252	▼ 2.22	0.04982	NM_145933	Beta galactoside alpha 2,6 sialyltransferase 1 (St6gal1), mRNA
253	▼ 2.22	0.02410	NM_007639	CD1d1 antigen (Cd1d1), mRNA
254	▼ 2.21	0.00777	NM_008877	Plasminogen, mRNA (cDNA clone MGC:18525 IMAGE:4193957)
255	▼ 2.19	4.40e-05	NM_013474	Apolipoprotein A-II, mRNA (cDNA clone MGC:18589 IMAGE:4195958)
256	▼ 2.19	0.03927	NM_019823	Cytochrome P450, family 2, subfamily d, polypeptide 22, mRNA (cDNA clone MGC:288
257	▼ 2.18	0.04233	NM_144559	Fc receptor, IgG, low affinity IV (Fcgr4), mRNA
258	▼ 2.18	0.02604	NM_194268	One cut domain, family member 2, mRNA (cDNA clone IMAGE:40046649)
259	▼ 2.18	0.04933	NM_008961	Phosphotriesterase related, mRNA (cDNA clone MGC:6034 IMAGE:3601675)
260	▼ 2.17	0.02022	NM_026405	RAB32 (Rab32)
261	▼ 2.15	0.01386	NM_023268	Quiescin Q6 sulfhydryl oxidase 1, mRNA (cDNA clone IMAGE:4920854)
262	▼ 2.15	0.03504	NM_146013	SEC14-like 4 (S. cerevisiae), mRNA (cDNA clone IMAGE:5097361)
263	▼ 2.14	0.00231	NM_009778	Complement component 3 (C3), mRNA
264	▼ 2.12	0.02442	NM_027827	Arylformamidase (Afmid), mRNA
265	▼ 2.12	0.04930	NM_178082	INSIG-2 membrane protein
266	▼ 2.11	0.02456	NM_008952	Pipecolic acid oxidase, mRNA (cDNA clone MGC:19202 IMAGE:4237443)
267	▼ 2.09	0.00748	NM_133768	Argininosuccinate lyase (Asl), mRNA
268	▼ 2.09	0.00425	NM_026152	RIKEN cDNA 0610010D20 gene, mRNA (cDNA clone MGC:25926 IMAGE:4235003)
269	▼ 2.09	0.03218	NM_178600	Vitamin K epoxide reductase complex, subunit 1, mRNA (cDNA clone MGC:25747 IMAGE
270	▼ 2.08	0.03187	NM_013465	Alpha-2-HS-glycoprotein, mRNA (cDNA clone MGC:29969 IMAGE:5123689)
271	▼ 2.08	0.00153	NM_177322	Angiotensin II receptor, type 1a, mRNA (cDNA clone MGC:37610 IMAGE:4989471)
272	▼ 2.08	0.04133	NM_009171	Serine hydroxymethyltransferase 1 (soluble), mRNA (cDNA clone MGC:14007 IMAGE:41
273	▼ 2.07	0.01011	NM_053176	Histidine-rich glycoprotein (Hrg), mRNA
274	▼ 2.06	0.00919	NM_009804	Mutant catalase (Cas1)
275	▲ 2.06	0.02664	NM_025282	Myocyte enhancer factor 2C, mRNA (cDNA clone MGC:46981 IMAGE:4500786)
276	▼ 2.06	0.02375	NM_009252	Serine (or cysteine) peptidase inhibitor, clade A, member 3K, mRNA (cDNA clone M
277	▼ 2.05	0.04350	NM_080844	Serine (or cysteine) peptidase inhibitor, clade C (antithrombin), member 1, mRNA
278	▼ 2.05	0.04419	NM_027917	Shroom family member 1, mRNA (cDNA clone MGC:36261 IMAGE:3497170)
279	▼ 2.05	0.03283	NM_012030	Solute carrier family 9 (sodium/hydrogen exchanger), member 3 regulator 1 (Slc9a
280	▼ 2.04	0.00806	NM_016751	C-type lectin domain family 4, member f, mRNA (cDNA clone MGC:18808 IMAGE:419556
281	▼ 2.04	0.00556	NM_009803	Nuclear receptor subfamily 1, group I, member 3, mRNA (cDNA clone IMAGE:5052215)
282	▼ 2.02	0.00086	NM_019911	Tryptophan 2,3-dioxygenase, mRNA (cDNA clone MGC:25811 IMAGE:4159877)
283	▼ 2.01	0.04905	NM_178053	N-acetylglutamate synthase (Nags), transcript variant 1, mRNA
284	▼ 2.00	0.01172	NM_010396	H2-T17
285	▼ 1.98	0.02676	NM_010356	Glutathione S-transferase, alpha 3 (Gsta3), transcript variant 2, mRNA

No.	Ratio	p-value	Identifier	Gene Name
286	▼ 1.97	0.00400	NM_011082	Polymeric immunoglobulin receptor, mRNA (cDNA clone MGC:5797 IMAGE:3601095)
287	▼ 1.96	0.02936	NM_010517	Insulin-like growth factor binding protein 4, mRNA (cDNA clone MGC:29917 IMAGE:5
288	▼ 1.96	0.02712	NM_029796	Leucine-rich alpha-2-glycoprotein 1, mRNA (cDNA clone MGC:37928 IMAGE:5123909)
289	▼ 1.96	0.03592	NM_001017959	Lysosomal-associated membrane protein 2 (Lamp2), transcript variant 2, mRNA
290	▼ 1.96	0.04564	NM_016783	Progesterone receptor membrane component 1, mRNA (cDNA clone MGC:5817 IMAGE:3591
291	▼ 1.96	0.00416	NM_023377	START domain-containing 5 protein (Stard5)
292	▼ 1.94	0.00777	NM_172961	4-aminobutyrate aminotransferase, mRNA (cDNA clone IMAGE:30532686)
293	▼ 1.93	0.00133	NM_173763	Cysteine conjugate-beta lyase 2, mRNA (cDNA clone IMAGE:4954508)
294	▼ 1.93	0.02450	NM_172607	Nicotinate phosphoribosyltransferase-like protein
295	▼ 1.92	0.02923	NM_134102	Phospholipase A1 member A, mRNA (cDNA clone MGC:41255 IMAGE:1247206)
296	▼ 1.91	0.02473	XM_358306	ATP-binding cassette, sub-family C (CFTR/MRP), member 3
297	▲ 1.91	0.00777	NM_207663	CDNA clone IMAGE:40099060
298	▼ 1.91	0.02273	NM_008101	Glucagon receptor, mRNA (cDNA clone MGC:30235 IMAGE:5137340)
299	▼ 1.91	0.04107	NM_181540	Transmembrane 6 superfamily member 2, mRNA (cDNA clone MGC:37441 IMAGE:4982620)
300	▼ 1.90	0.02709	NM_007514	Solute carrier family 7 (cationic amino acid transporter, y+ system), member 2 (
301	▼ 1.89	9.13e-05	NM_028270	Aldehyde dehydrogenase 1 family, member B1 (Aldh1b1), nuclear gene encoding mito
302	▼ 1.89	0.04948	NM_029357	Protocadherin 1, mRNA (cDNA clone IMAGE:5097808)
303	▼ 1.89	0.01338	NM_146126	Sorbitol dehydrogenase (Sord), mRNA
304	▼ 1.87	0.01918	NM_011327	Sterol carrier protein 2, liver, mRNA (cDNA clone MGC:29961 IMAGE:5123611)
305	▼ 1.86	0.02228	NM_145152	Leucine rich repeat containing 3 (Lrrc3), mRNA
306	▼ 1.86	0.00014	NM_183249	RIKEN cDNA 1100001G20 gene, mRNA (cDNA clone IMAGE:1364952)
307	▲ 1.85	0.03722	NM_019809	PDZ and LIM domain 5, mRNA (cDNA clone MGC:46824 IMAGE:4457868)
308	▼ 1.85	0.01309	NM_145079	UDP glucuronosyltransferase 1 family, polypeptide A6B, mRNA (cDNA clone MGC:3624
309	▼ 1.84	0.04425	NM_172607	Nicotinate phosphoribosyltransferase-like protein
310	▼ 1.82	0.00249	NM_009929	Collagen, type XVIII, alpha 1 (Col18a1), transcript variant 2, mRNA
311	▼ 1.82	0.04787	NM_010074	Dipeptidylpeptidase 4, mRNA (cDNA clone MGC:14076 IMAGE:3982742)
312	▼ 1.82	0.01455	NM_026152	RIKEN cDNA 0610010D20 gene, mRNA (cDNA clone MGC:25926 IMAGE:4235003)
313	▼ 1.81	0.02668	NM_080844	Serine (or cysteine) peptidase inhibitor, clade C (antithrombin), member 1, mRNA
314	▼ 1.80	0.00085	NM_011519	Syndecan 1, mRNA (cDNA clone MGC:5879 IMAGE:3501359)
315	▼ 1.79	0.04332	NM_024264	Cytochrome P450, family 27, subfamily a, polypeptide 1 (Cyp27a1), nuclear gene e
316	▲ 1.79	0.04880	NM_144859	Praja 2, RING-H2 motif containing (Pja2), transcript variant 2, mRNA
317	▲ 1.79	0.02723	NM_026313	RIKEN cDNA 3300001P08 gene (3300001P08Rik), mRNA
318	▼ 1.78	0.00448	NM_177836	AW046396
319	▼ 1.78	0.04167	NM_025797	Cytochrome b-5, mRNA (cDNA clone MGC:35713 IMAGE:4973059)
320	▼ 1.78	0.04497	NM_001044744	Glutaryl-Coenzyme A dehydrogenase (Gcdh), nuclear gene encoding mitochondrial pr
321	▼ 1.78	0.04332	NM_178701	Leucine rich repeat containing 8D, mRNA (cDNA clone MGC:47330 IMAGE:4239389)
322	▼ 1.78	0.00591	NM_009344	Pleckstrin homology-like domain, family A, member 1, mRNA (cDNA clone MGC:11486
323	▲ 1.78	0.00081	NM_001003930	reticulon 3
324	▼ 1.78	0.02576	NM_021472	Ribonuclease, RNase A family 4, mRNA (cDNA clone MGC:11599 IMAGE:3967265)
325	▼ 1.77	0.00505	NM_011327	Sterol carrier protein 2, liver, mRNA (cDNA clone MGC:29961 IMAGE:5123611)
326	▼ 1.76	0.02780	NM_010959	EF-9 polyadenylation variant II mRNA, complete cds, alternatively spliced
327	▼ 1.76	0.04357	NM_146020	Glycolipid transfer protein domain containing 2 (Gltpd2), mRNA
328	▼ 1.76	0.00199	NM_033354	SEC16 homolog B (S. cerevisiae) (Sec16b), mRNA
329	▼ 1.75	0.02297	NM_019775	Carboxypeptidase B2 (plasma) (Cpb2), mRNA
330	▼ 1.75	0.03194	NM_026428	DCXR mRNA for Dicarbonyl/L-Xylulose Reductase
331	▼ 1.75	0.01726	NM_008156	Glycosylphosphatidylinositol phospholipase D
332	▼ 1.75	0.00655	NM_001017959	Lysosomal-associated membrane protein 2 (Lamp2), transcript variant 2, mRNA
333	▼ 1.75	0.04805	NM_008952	Pipecolic acid oxidase, mRNA (cDNA clone MGC:19202 IMAGE:4237443)

No.	Ratio	p-value	Identifier	Gene Name
334	▼ 1.74	0.00330	NM_016661	S-adenosylhomocysteine hydrolase (Ahcy), mRNA
335	▼ 1.73	0.03198	NM_007976	Coagulation factor V (F5), mRNA
336	▼ 1.72	0.00283	NM_001025575	CDNA sequence BC026782, mRNA (cDNA clone IMAGE:5132971)
337	▼ 1.72	0.02048	NM_021345	Protein tyrosine phosphatase-like A domain containing 1, mRNA (cDNA clone MGC:25
338	▼ 1.71	0.00501	NM_133768	Argininosuccinate lyase (Asl), mRNA
339	▲ 1.71	0.03210	NM_009784	Calcium channel, voltage-dependent, alpha2/delta subunit 1 (Cacna2d1), transcrip
340	▼ 1.70	0.04236	NM_008039	Formyl peptide receptor 2 (Fpr2), mRNA
341	▼ 1.70	0.00326	NM_009401	Tumor necrosis factor receptor superfamily, member 8 (Tnfrsf8), mRNA
342	▼ 1.69	0.00042	NM_023125	Kininogen 1, mRNA (cDNA clone MGC:25815 IMAGE:4162960)
343	▼ 1.69	0.04487	NM_008642	Microsomal triglyceride transfer protein, mRNA (cDNA clone MGC:13921 IMAGE:41639
344	▼ 1.69	0.01643	NM_020042	Molybdenum cofactor synthesis 1, mRNA (cDNA clone IMAGE:4163356)
345	▼ 1.69	0.03410	NM_172778	Monoamine oxidase B, mRNA (cDNA clone MGC:132955 IMAGE:40061991)
346	▼ 1.69	0.00913	NM_015799	Transferrin receptor 2, mRNA (cDNA clone MGC:18814 IMAGE:4196597)
347	▼ 1.68	0.04602	NM_170599	Immunoglobulin superfamily, member 11 (Igsf11), mRNA
348	▼ 1.67	0.00152	NM_008881	Plexin A1 (Plxna1), mRNA
349	▼ 1.67	0.04270	NM_175090	Solute carrier family 31, member 1, mRNA (cDNA clone MGC:28108 IMAGE:3968084)
350	▼ 1.67	0.01444	NM_025326	Transmembrane protein 176A (Tmem176a), transcript variant 1, mRNA
351	▼ 1.66	0.00843	NM_145953	Cystathionase (cystathionine gamma-lyase) (Cth), mRNA
352	▲ 1.66	0.03801	NM_010017	Dystroglycan 1, mRNA (cDNA clone MGC:6651 IMAGE:3496914)
353	▲ 1.66	0.01963	NM_001039511	Influenza virus NS1A binding protein (Ivns1abp), transcript variant 2, mRNA
354	▲ 1.65	0.01880	NM_010017	Dystroglycan 1, mRNA (cDNA clone MGC:6651 IMAGE:3496914)
355	▼ 1.64	0.02131	NM_009777	Complement component 1, q subcomponent, beta polypeptide (C1qb), mRNA
356	▼ 1.64	0.02086	XM_129912	RIKEN cDNA 5033414K04 gene
357	▲ 1.63	0.02860	NM_153534	Adenylate cyclase 2 (Adcy2), mRNA
358	▼ 1.63	0.03585	NM_144848	Epiplakin 1 (Eppk1), mRNA
359	▼ 1.63	0.03655	NM_139295	Multiple coagulation factor deficiency 2 (Mcfd2), transcript variant 2, mRNA
360	▼ 1.62	0.04526	NM_010187	Fc receptor, IgG, low affinity IIb, mRNA (cDNA clone MGC:46888 IMAGE:3993915)
361	▼ 1.62	0.00465	NM_053176	Histidine-rich glycoprotein (Hrg), mRNA
362	▼ 1.62	0.01241	NM_023670	Insulin-like growth factor 2 mRNA binding protein 3 (Igf2bp3), mRNA
363	▼ 1.62	0.02658	NM_138745	Methylenetetrahydrofolate dehydrogenase (NADP+ dependent), methenyltetrahydrofol
364	▼ 1.62	0.03941	NM_025623	NIPSNAP-related protein
365	▼ 1.61	0.02801	NM_177614	Amplified in osteosarcoma, mRNA (cDNA clone MGC:25481 IMAGE:4487829)
366	▼ 1.61	0.00532	NM_144821	Expressed sequence AI317395 (AI317395), mRNA
367	▼ 1.61	0.00282	NM_008199	Histocompatibility 2, blastocyst (H2-Bl), mRNA
368	▼ 1.61	0.00997	NM_017405	Lipolysis stimulated lipoprotein receptor, mRNA (cDNA clone MGC:7815 IMAGE:35000
369	▼ 1.61	0.01412	NM_134102	Phospholipase A1 member A, mRNA (cDNA clone MGC:41255 IMAGE:1247206)
370	▼ 1.60	0.03241	NM_198095	Bone marrow stromal cell antigen 2, mRNA (cDNA clone MGC:28276 IMAGE:4009434)
371	▼ 1.60	0.02775	NM_145570	Family with sequence similarity 176, member A (Fam176a), mRNA
372	▼ 1.60	0.02805	NM_134021	Pyridoxine 5'-phosphate oxidase, mRNA (cDNA clone MGC:36350 IMAGE:4971745)
373	▼ 1.60	0.00816	NM_011893	SH3-domain binding protein 2, mRNA (cDNA clone MGC:11535 IMAGE:3967543)
374	▲ 1.60	0.00147	NM_026071	Solute carrier family 25 (mitochondrial thiamine pyrophosphate carrier), member
375	▲ 1.59	0.03279	NM_009769	Kruppel-like factor 5, mRNA (cDNA clone MGC:13705 IMAGE:4208633)
376	▼ 1.59	0.03881	NM_177920	Serine (or cysteine) peptidase inhibitor, clade A (alpha-1 antiproteinase, antit
377	▼ 1.58	0.01806	NM_007899	Extracellular matrix protein 1 (Ecm1), mRNA
378	▼ 1.58	0.02049	NM_007952	Protein disulfide isomerase associated 3, mRNA (cDNA clone MGC:28333 IMAGE:40163
379	▼ 1.58	0.03950	NM_001013607	Vitelline membrane outer layer 1 homolog (chicken) (Vmo1), mRNA
380	▼ 1.57	0.00614	NM_173763	Cysteine conjugate-beta lyase 2, mRNA (cDNA clone IMAGE:4954508)
381	▲ 1.57	0.04490	NM_025802	Patatin-like phospholipase domain containing 2, mRNA (cDNA clone IMAGE:4982482)

No.	Ratio	p-value	Identifier	Gene Name
382	▲ 1.57	0.01444	NM_024221	Pyruvate dehydrogenase (lipoamide) beta (Pdhb), mRNA
383	▼ 1.57	0.03799	NM_027852	Retinoic acid receptor responder (tazarotene induced) 2, mRNA (cDNA clone MGC:49
384	▼ 1.57	0.00679	NM_009776	Serine (or cysteine) peptidase inhibitor, clade G, member 1, mRNA (cDNA clone MG
385	▼ 1.57	0.00751	NM_145079	UDP glucuronosyltransferase 1 family, polypeptide A6B, mRNA (cDNA clone MGC:3624
386	▼ 1.56	0.03452	NM_153151	Acetyl-Coenzyme A acetyltransferase 3 (Acat3), mRNA
387	▼ 1.56	0.01236	NM_031159	Apolipoprotein B mRNA editing enzyme, catalytic polypeptide 1 (Apobec1), transcr
388	▼ 1.56	0.01788	NM_030687	Solute carrier organic anion transporter family, member 1a4 (Slco1a4), mRNA
389	▲ 1.56	0.03511	NM_019879	Succinate-CoA ligase, GDP-forming, alpha subunit, mRNA (cDNA clone MGC:18990 IMA
390	▲ 1.56	0.02803	NM_022314	Tropomyosin 3, gamma, mRNA (cDNA clone MGC:36031 IMAGE:4502880)
391	▼ 1.55	0.00258	NM_019975	2-hydroxyacyl-CoA lyase 1, mRNA (cDNA clone MGC:29195 IMAGE:5011451)
392	▲ 1.55	0.00311	NM_010423	Brain cDNA, clone MNCb-2686, similar to Mus musculus hairy/enhancer-of-split rel
393	▼ 1.55	2.59e-05	NM_007977	Coagulation factor VIII (F8), mRNA
394	▼ 1.55	0.03627	NM_008929	DnaJ (Hsp40) homolog, subfamily C, member 3, mRNA (cDNA clone MGC:6474 IMAGE:264
395	▲ 1.55	0.02530	NM_133852	Golgi autoantigen, golgin subfamily a, 2 (Golga2), transcript variant 1, mRNA
396	▼ 1.55	0.03596	NM_029789	LAG1 homolog, ceramide synthase 2 (Lass2), mRNA
397	▼ 1.55	0.00302	NM_011017	Ornithine transporter mRNA, complete cds; nuclear gene for mitochondrial product
398	▲ 1.55	0.01515	NM_026872	Ubiquitin-associated protein 2, mRNA (cDNA clone MGC:7679 IMAGE:3496608)
399	▼ 1.54	0.00347	NM_134079	Adenosine kinase (Adk), mRNA
400	▼ 1.54	0.02554	NM_175438	Aldehyde dehydrogenase 4 family, member A1, mRNA (cDNA clone MGC:37323 IMAGE:497
401	▼ 1.54	0.00468	NM_015780	Complement factor H-related 1 (Cfhr1), mRNA
402	▲ 1.54	0.03774	NM_175656	Histone cluster 1, H4i, mRNA (cDNA clone MGC:159301 IMAGE:40130113)
403	▼ 1.54	0.04146	NM_133732	RIKEN cDNA 4931406C07 gene (4931406C07Rik), mRNA
404	▼ 1.53	0.04264	NM_007574	Complement component 1, q subcomponent, C chain (C1qc), mRNA
405	▼ 1.53	0.00572	NM_010874	N-acetyltransferase 2 (arylamine N-acetyltransferase), mRNA (cDNA clone MGC:1402
406	▲ 1.53	0.02131	NM_133220	Serum/glucocorticoid regulated kinase 3 (Sgk3), transcript variant 1, mRNA
407	▲ 1.52	0.02787	NM_207663	CDNA clone IMAGE:40099060
408	▼ 1.52	0.03934	NM_182805	Glutamic pyruvic transaminase, soluble, mRNA (cDNA clone MGC:18798 IMAGE:4194336
409	▼ 1.52	0.02116	NM_011327	Sterol carrier protein 2, liver, mRNA (cDNA clone MGC:29961 IMAGE:5123611)
410	▲ 1.51	0.02835	NM_010087	Alpha-dystrobrevin 2b
411	▼ 1.51	0.00213	NM_001001892	Histocompatibility 2, K1, K region, mRNA (cDNA clone MGC:7052 IMAGE:3156482)
412	▼ 1.51	0.01225	NM_134102	Phospholipase A1 member A, mRNA (cDNA clone MGC:41255 IMAGE:1247206)
413	▼ 1.51	0.02107	NM_026183	Solute carrier family 47, member 1 (Slc47a1), mRNA
414	▲ 1.49	0.01989	NM_019832	G kinase anchoring protein 1 (Gkap1), mRNA
415	▼ 1.49	0.01290	NM_133970	heparan-alpha-glucosaminide N-acetyltransferase
416	▼ 1.49	0.03208	NM_053262	Hydroxysteroid (17-beta) dehydrogenase 11, mRNA (cDNA clone MGC:28723 IMAGE:4458
417	▲ 1.49	0.04519	NM_145503	Leucine zipper, putative tumor suppressor 2 (Lzts2), transcript variant 1, mRNA
418	▲ 1.49	0.00372	NM_008633	Microtubule-associated protein 4 (Mtap4), mRNA
419	▼ 1.49	0.02858	NM_026669	Transmembrane BAX inhibitor motif containing 6 (Tmbim6), mRNA
420	▼ 1.48	0.02755	NM_022325	Cathepsin Z, mRNA (cDNA clone MGC:5694 IMAGE:3588457)
421	▼ 1.48	0.02961	NM_008813	Ectonucleotide pyrophosphatase/phosphodiesterase 1 allotype b (Enpp1) mRNA, Enpp
422	▲ 1.48	0.00348	NM_021527	McKusick-Kaufman syndrome protein, mRNA (cDNA clone IMAGE:5039074)
423	▲ 1.48	0.01250	NM_019411	Protein phosphatase 2 (formerly 2A), catalytic subunit, alpha isoform, mRNA (cDN
424	▼ 1.48	0.02671	NM_030685	Stress-associated endoplasmic reticulum protein 1 (Serp1), mRNA
425	▲ 1.48	0.02654	NM_009366	TSC22-related inducible leucine zipper 1b (Tilz1b)
426	▼ 1.48	0.01927	NM_146214	Tyrosine aminotransferase, mRNA (cDNA clone MGC:38102 IMAGE:5310059)
427	▲ 1.47	0.00175	NM_019735	APAF1 interacting protein, mRNA (cDNA clone MGC:41093 IMAGE:1245515)
428	▼ 1.47	0.01231	NM_025295	Biotinidase, mRNA (cDNA clone MGC:35781 IMAGE:5099802)
429	▼ 1.47	0.01803	NM_008176	Chemokine (C-X-C motif) ligand 1 (Cxcl1), mRNA

No.	Ratio	p-value	Identifier	Gene Name
430	▼ 1.47	0.03022	NM_008133	Glutamate dehydrogenase 1 (Glud1), mRNA
431	▲ 1.47	0.04178	NM_026425	N-acetyltransferase 5 (ARD1 homolog, S. cerevisiae), mRNA (cDNA clone MGC:6501 I
432	▲ 1.47	0.04378	NM_023196	Phospholipase A2, group XIIA, mRNA (cDNA clone MGC:25458 IMAGE:4456431)
433	▼ 1.47	0.01224	NM_020495	Solute carrier organic anion transporter family, member 1b2 (Slco1b2), transcrip
434	▼ 1.46	0.04609	NM_013930	CDNA fis, clone TRACH2010974,highly similar to Mus musculus mRNA encoding lysine
435	▲ 1.46	0.04396	NM_028906	Dipeptidylpeptidase 8, mRNA (cDNA clone MGC:66620 IMAGE:6410075)
436	▼ 1.46	0.02344	NM_011046	Furin (paired basic amino acid cleaving enzyme) (Furin), mRNA
437	▲ 1.46	0.03474	XM_125586	glutaminyl-tRNA synthase (glutamine-hydrolyzing)-like 1
438	▲ 1.46	0.02142	NM_028733	Protein kinase C and casein kinase II substrate 3 (Pacsin3)
439	▲ 1.46	0.02775	NM_029601	RIKEN cDNA 1700019E19 gene, mRNA (cDNA clone MGC:49305 IMAGE:5148723)
440	▼ 1.46	0.04989	NM_138665	Sarcosine dehydrogenase (Sardh), nuclear gene encoding mitochondrial protein, mR
441	▼ 1.46	0.02659	NM_013709	Sh3 domain YSC-like 1, mRNA (cDNA clone MGC:11615 IMAGE:3154966)
442	▼ 1.46	0.04165	NM_153598	UDP glucuronosyltransferase 2 family, polypeptide B34 (Ugt2b34), mRNA
443	▼ 1.45	0.03507	NM_175270	Ankyrin repeat domain 56 (Ankrd56), mRNA
444	▼ 1.45	0.04432	NM_181344	Complement component 1, r subcomponent-like, mRNA (cDNA clone MGC:92956 IMAGE:30
445	▲ 1.45	0.01345	NM_009824	Core-binding factor, runt domain, alpha subunit 2, translocated to, 3 (human) (C
446	▲ 1.45	0.01558	NM_007928	MAP/microtubule affinity-regulating kinase 2 (Mark2), transcript variant 1, mRNA
447	▲ 1.45	0.03834	NM_011127	Paired related homeobox 1 (Prrx1), transcript variant 1, mRNA
448	▲ 1.45	0.00906	NM_001005767	Presenilin associated, rhomboid-like (Parl), nuclear gene encoding mitochondrial
449	▼ 1.45	0.03092	NM_025572	RIKEN cDNA 2610528J11 gene, mRNA (cDNA clone MGC:32151 IMAGE:4925508)
450	▼ 1.45	0.00776	NM_013761	Serine racemase, mRNA (cDNA clone MGC:18670 IMAGE:4195695)
451	▼ 1.44	0.00322	NM_134247	Acyl-CoA thioesterase 4 (Acot4), mRNA
452	▲ 1.44	0.03836	XM_147222	Cldn5
453	▲ 1.44	0.00221	XM_133510	methylmalonyl CoA epimerase
454	▲ 1.44	0.00295	NM_025357	SMPX protein (Smpx)
455	▲ 1.44	0.00352	NM_026254	TBC1 domain family, member 23, mRNA (cDNA clone MGC:25849 IMAGE:4194266)
456	▲ 1.44	0.04414	NM_022314	Tropomyosin 3, gamma, mRNA (cDNA clone MGC:36031 IMAGE:4502880)
457	▲ 1.43	0.00458	NM_178928	Actin filament associated protein 1-like 1, mRNA (cDNA clone MGC:170550 IMAGE:88
458	▼ 1.43	0.04167	NM_146034	CTAGE family, member 5, mRNA (cDNA clone IMAGE:5097489)
459	▼ 1.43	0.01611	NM_170599	Immunoglobulin superfamily, member 11 (Igsf11), mRNA
460	▲ 1.43	0.00293	NM_023514	Mitochondrial ribosomal protein S9, mRNA (cDNA clone IMAGE:4036755)
461	▼ 1.43	0.00763	NM_013545	Protein tyrosine phosphatase, non-receptor type 6, mRNA (cDNA clone MGC:13821 IM
462	▼ 1.43	0.03855	NM_011344	Sel-1 suppressor of lin-12-like (C. elegans), mRNA (cDNA clone MGC:25250 IMAGE:4
463	▼ 1.43	0.04057	NM_054055	Solute carrier family 13 (sodium-dependent dicarboxylate transporter), member 3,
464	▼ 1.43	0.00299	NM_031197	Solute carrier family 2 (facilitated glucose transporter), member 2, mRNA (cDNA
465	▲ 1.43	0.01357	NM_028841	Tetraspanin 17 (Tspan17), mRNA
466	▼ 1.42	0.02394	NM_007410	Alcohol dehydrogenase 5 (class III), chi polypeptide (Adh5), mRNA
467	▼ 1.42	0.00834	NM_027827	Arylformamidase (Afmid), mRNA
468	▲ 1.42	0.03445	NM_013853	ATP-binding cassette, sub-family F (GCN20), member 2 (Abcf2), nuclear gene encod
469	▲ 1.42	0.01944	NM_028057	Cytochrome b5 reductase 1 (Cyb5r1), mRNA
470	▲ 1.42	0.01448	NM_001026212	Endosulfine alpha (Ensa), transcript variant 1, mRNA
471	▲ 1.42	0.00236	NM_010827	Musculin (Msc), mRNA
472	▲ 1.42	0.02024	NM_011202	Protein tyrosine phosphatase, non-receptor type 11, mRNA (cDNA clone IMAGE:34901
473	▲ 1.42	0.04568	NM_009161	Sarcoglycan, alpha (dystrophin-associated glycoprotein) (Sgca), transcript varia
474	▲ 1.42	0.02399	NM_172310	Threonyl-tRNA synthetase-like 2, mRNA (cDNA clone MGC:31414 IMAGE:4458085)
475	▲ 1.42	0.01251	NM_033042	Tumor necrosis factor receptor superfamily, member 25, mRNA (cDNA clone MGC:2768
476	▲ 1.41	0.00440	NM_028105	AarF domain containing kinase 1 (Adck1), mRNA
477	▲ 1.41	0.02723	NM_019686	Calcium and integrin binding family member 2, mRNA (cDNA clone MGC:11420 IMAGE:3

No.	Ratio	p-value	Identifier	Gene Name
477	▲ 1.41	0.02723	NM_019686	Calcium and integrin binding family member 2, mRNA (cDNA clone MGC:11420 IMAGE:3
478	▲ 1.41	0.04308	NM_013767	Casein kinase 1, epsilon, mRNA (cDNA clone MGC:13740 IMAGE:4010696)
479	▼ 1.41	0.00713	NM_013484	Complement component 2 (within H-2S), mRNA (cDNA clone MGC:18582 IMAGE:3992881)
480	▲ 1.41	0.04526	NM_011991	COP9 (constitutive photomorphogenic) homolog, subunit 3 (Arabidopsis thaliana) (
481	▼ 1.41	0.03748	NM_010236	Folylpolyglutamyl synthetase, mRNA (cDNA clone MGC:7296 IMAGE:3485401)
482	▲ 1.41	0.04535	NM_011906	G protein-coupled receptor 175, mRNA (cDNA clone MGC:36786 IMAGE:5363085)
483	▼ 1.41	0.02396	NM_134103	Interleukin 1 receptor accessory protein (Il1rap), transcript variant 2, mRNA
484	▼ 1.41	0.04152	NM_025828	Lectin, mannose-binding 2 (Lman2), mRNA
485	▲ 1.41	0.03658	NM_026025	MADP-1 protein
486	▲ 1.41	0.00308	NM_009087	Polymerase (RNA) I polypeptide D, mRNA (cDNA clone MGC:36184 IMAGE:4987975)
487	▲ 1.41	0.03304	NM_023374	Succinate dehydrogenase complex, subunit B, iron sulfur (Ip), mRNA (cDNA clone M
488	▲ 1.40	0.03612	NM_027867	breast cancer metastasis-suppressor 1-like
489	▲ 1.40	0.01660	NM_009842	CD151 antigen, mRNA (cDNA clone MGC:5773 IMAGE:3500850)
490	▲ 1.40	0.00097	NM_025304	Leucine carboxyl methyltransferase 1, mRNA (cDNA clone IMAGE:3595687)
491	▲ 1.40	0.03824	NM_026145	Potassium channel tetramerisation domain containing 10 (Kctd10), mRNA
492	▲ 1.40	0.00144	NM_011231	RAB geranylgeranyl transferase, b subunit, mRNA (cDNA clone IMAGE:3487367)
493	▲ 1.40	0.01063	NM_024432	UBX domain protein 6, mRNA (cDNA clone MGC:25886 IMAGE:4215883)

Table 3. Genes altered in TA of 10-week-old ACTA KI males

No.	Ratio	p-value	Identifier	Gene Name
1	▼ 2.58	0.01483	NM_009349	Indolethylamine N-methyltransferase, mRNA (cDNA clone MGC:19191 IMAGE:4236077)
2	▼ 2.29	0.02280	NM_008493	Leptin, mRNA (cDNA clone IMAGE:1513077)
3	▼ 2.13	0.00810	NM_013459	Complement factor D (adipsin) (Cfd), mRNA
4	▼ 2.05	0.01091	NM_031176	Tenascin XB (Tnxb), mRNA
5	▼ 2.03	0.01842	NM_009605	Adiponectin, C1Q and collagen domain containing, mRNA (cDNA clone MGC:41360 IMAG
6	▼ 1.96	0.01487	NM_031176	Tenascin XB (Tnxb), mRNA
7	▼ 1.83	0.03003	NM_031176	Tenascin XB (Tnxb), mRNA
8	▲ 1.81	0.04362	NM_001009548	Testase-8, mRNA (cDNA clone MGC:183704 IMAGE:9087704)
9	▲ 1.77	0.04756	NM_009932	Collagen alpha-2(IV) chain
10	▼ 1.73	0.01122	NM_178373	Adipocyte-specific
11	▼ 1.72	0.03333	NM_020027	HLA-B associated transcript 2, mRNA (cDNA clone IMAGE:3499233)
12	▼ 1.61	0.00045	NM_009465	AXL receptor tyrosine kinase (Axl), mRNA
13	▼ 1.61	0.03590	NM_010865	Myocilin (Myoc), mRNA
14	▼ 1.61	0.02421	NM_029620	Procollagen C-endopeptidase enhancer 2 (Pcolce2), mRNA
15	▼ 1.60	0.00180	NM_053094	CD163 antigen (Cd163), mRNA
16	▼ 1.60	0.04960	NM_176920	CDNA clone IMAGE:9053747
17	▼ 1.60	0.00749	NM_144936	Transmembrane protein 45b (Tmem45b), mRNA
18	▼ 1.59	0.00556	NM_029803	Interferon stimulated gene 12 (Isg12)
19	▼ 1.59	0.01246	NM_013750	Pleckstrin homology-like domain, family A, member 3, mRNA (cDNA clone MGC:30999
20	▲ 1.53	0.01689	NM_019686	Calcium and integrin binding family member 2, mRNA (cDNA clone MGC:11420 IMAGE:3
21	▼ 1.52	0.04614	NM_023734	Peptidase inhibitor 16, mRNA (cDNA clone IMAGE:3586291)
22	▼ 1.51	0.03795	NM_016693	Mitogen-activated protein kinase kinase kinase 6 (Map3k6), mRNA
23	▲ 1.50	0.02456	NM_207265	RIKEN cDNA C230071H18 gene (C230071H18Rik), mRNA.
24	▼ 1.48	0.02975	XM_129987	coiled-coil domain containing 3
25	▲ 1.46	0.04389	NM_026865	RIKEN cDNA 1700113I22 gene (1700113i22rik), mRNA
26	▼ 1.45	0.04481	NM_133888	Sphingomyelin phosphodiesterase, acid-like 3B (Smpdl3b), mRNA
27	▼ 1.45	0.04399	NM_175480	Zinc finger protein 612, mRNA (cDNA clone IMAGE:3586510)
28	▼ 1.44	0.00473	NM_019739	Forkhead box O1 (Foxo1), mRNA
29	▼ 1.43	0.03213	NM_029976	CDKN2A interacting protein N-terminal like (Cdkn2aipnl), mRNA
30	▲ 1.43	0.03784	NM_019395	Fructose bisphosphatase 1, mRNA (cDNA clone MGC:18799 IMAGE:4194764)
31	▼ 1.42	0.04773	NM_175177	3-hydroxybutyrate dehydrogenase, type 1, mRNA (cDNA clone IMAGE:5051325)
32	▼ 1.42	0.02847	NM_007554	Bone morphogenetic protein 4, mRNA (cDNA clone MGC:31017 IMAGE:4192158)
33	▼ 1.42	0.03935	NM_010516	Cysteine rich protein 61 (Cyr61), mRNA
34	▼ 1.42	0.00237	NM_001042487	Discs, large homolog-associated protein 4 (Drosophila) (Dlgap4), transcript vari
35	▼ 1.42	0.00344	NM_023196	Phospholipase A2, group XIIA, mRNA (cDNA clone MGC:25458 IMAGE:4456431)
36	▲ 1.42	0.00186	NM_009223	Stannin, mRNA (cDNA clone MGC:12052 IMAGE:3707801)
37	▼ 1.42	0.01069	NM_030100	Within bgcn homolog (Drosophila) (Wibg), mRNA
38	▼ 1.41	0.00868	NM_008344	Insulin-like growth factor binding protein 6, mRNA (cDNA clone MGC:14073 IMAGE:4
39	▲ 1.41	0.04336	NM_011212	Protein tyrosine phosphatase, receptor type, E (Ptpre), mRNA
40	▼ 1.41	0.01865	NM_029035	SPRY domain-containing SOCS box protein SSB-1
41	▼ 1.41	0.02418	NM_001077364	TSC22 domain family, member 3, mRNA (cDNA clone MGC:36071 IMAGE:5136440)
42	▼ 1.41	0.01928	NM_019742	Tumor suppressor candidate 2 (Tusc2), mRNA
43	▲ 1.40	0.03176	NM_177613	Cell division cycle 34 homolog (S. cerevisiae), mRNA (cDNA clone MGC:25601 IMAGE
44	▲ 1.40	0.03897	NM_007925	Elastin (Eln), mRNA
45	▼ 1.40	0.03152	NM_010897	NF1GRP mRNA for neurofibromatosis type-1-GTPase activating-protein type IV
46	▼ 1.40	0.01251	NM_008873	Plasminogen activator, urokinase (Plau), mRNA

Table 4. Genes altered in DIA of 10-week-old ACTA KI males

No.	Ratio	p-value	Identifier	Gene Name
1	▼ 2.27	0.00099	NM_008059	G0/G1 switch gene 2 (G0s2), mRNA
2	▲ 2.16	0.04819	NM_007993	Fibrillin 1, mRNA (cDNA clone IMAGE:3483994)
3	▲ 2.14	0.04702	NM_152817	Tetratricopeptide repeat domain 27 (Ttc27), mRNA
4	▼ 1.89	0.04712	NM_001025382	Predicted gene, EG574403 (EG574403), mRNA
5	▼ 1.89	0.03448	NM_080639	Tissue inhibitor of metalloproteinase 4 (Timp4), mRNA
6	▲ 1.87	0.02034	NM_013743	Pyruvate dehydrogenase kinase, isoenzyme 4, mRNA (cDNA clone MGC:13840 IMAGE:418
7	▼ 1.87	0.02408	NM_033314	Solute carrier organic anion transporter family, member 2a1, mRNA (cDNA clone MG
8	▼ 1.86	0.03290	NM_175641	Latent transforming growth factor beta binding protein 4 long splice variant (Lt
9	▼ 1.85	0.01954	NM_010129	Epithelial membrane protein 3, mRNA (cDNA clone MGC:5759 IMAGE:3485948)
10	▲ 1.82	0.00676	NM_145434	Nuclear receptor subfamily 1, group D, member 1 (Nr1d1), mRNA
11	▼ 1.76	0.00992	NM_008230	Histidine decarboxylase (Hdc), mRNA
12	▲ 1.69	0.04174	NM_010838	Strain ILS microtubule binding protein tau
13	▼ 1.68	0.01687	NM_013484	Complement component 2 (within H-2S), mRNA (cDNA clone MGC:18582 IMAGE:3992881)
14	▲ 1.68	0.03532	NM_178791	RIKEN cDNA E130203B14 gene, mRNA (cDNA clone IMAGE:40052401)
15	▲ 1.64	0.03503	NM_019684	Serine/arginine-rich protein specific kinase 3 (Srpk3), mRNA
16	▲ 1.63	0.01356	NM_019662	Ras-related associated with diabetes (Rrad), mRNA
17	▼ 1.62	0.02711	XM_134227	arrestin domain containing 2
18	▼ 1.59	0.02800	NM_008557	FXYD domain-containing ion transport regulator 3, mRNA (cDNA clone MGC:6001 IMAG
19	▲ 1.57	0.02182	XM_126635	dysferlin interacting protein 1
20	▲ 1.57	0.01691	NM_008596	Synaptophysin-like 2, mRNA (cDNA clone MGC:41202 IMAGE:1068035)
21	▼ 1.56	0.01772	NM_013705	Zinc finger protein 30 (Zfp30), mRNA
22	▲ 1.53	0.03095	NM_175429	Potassium channel tetramerisation domain containing 12b, mRNA (cDNA clone MGC:69
23	▲ 1.51	0.04491	NM_080563	Ring finger protein 144A (Rnf144a), transcript variant 2, mRNA
24	▲ 1.50	0.01733	NM_010194	Feline sarcoma oncogene, mRNA (cDNA clone MGC:150316 IMAGE:40111855)
25	▼ 1.50	0.04851	NM_028527	RIKEN cDNA 1700047I17 gene 2 (1700047I17Rik2), mRNA
26	▲ 1.48	0.00194	NM_013712	Integrin beta 1 binding protein 2, mRNA (cDNA clone MGC:41122 IMAGE:1346742)
27	▲ 1.48	0.00839	NM_021359	Integrin beta 6 (Itgb6), mRNA
28	▼ 1.48	0.00930	NM_021459	ISL1 transcription factor, LIM/homeodomain (Isl1), mRNA
29	▼ 1.47	0.02678	NM_032003	Ectonucleotide pyrophosphatase/phosphodiesterase 5 (Enpp5), mRNA
30	▲ 1.47	0.03542	NM_011406	Solute carrier family 8 (sodium/calcium exchanger), member 1 (Slc8a1), transcrip
31	▲ 1.47	0.02167	NM_025985	Ubiquitin-conjugating enzyme E2G 1 (UBC7 homolog, C. elegans) (Ube2g1), mRNA
32	▼ 1.46	0.02058	NM_145489	Expressed sequence AI661453, mRNA (cDNA clone IMAGE:5051947)
33	▼ 1.45	0.02513	NM_199057	RUN and SH3 domain containing 2, mRNA (cDNA clone IMAGE:5357662)
34	▼ 1.45	0.00809	NM_027324	Sideroflexin 1 (Sfxn1), mRNA
35	▼ 1.44	0.00380	NM_001025192	Coxsackie virus and adenovirus receptor, mRNA (cDNA clone MGC:25298 IMAGE:421672
36	▲ 1.44	0.01408	NM_011892	Gamma sarcoglycan
37	▼ 1.44	0.00610	NM_178708	PCI domain containing 2, mRNA (cDNA clone MGC:143948 IMAGE:40095328)
38	▲ 1.43	0.00777	NM_009360	Transcription factor A, mitochondrial, mRNA (cDNA clone MGC:5667 IMAGE:3487433)
39	▲ 1.41	0.01986	NM_015735	Damaged-DNA recognition protein 1 (Ddb1 gene)
40	▼ 1.41	0.03899	NM_153150	Solute carrier family 25 (mitochondrial carrier, citrate transporter), member 1
41	▼ 1.41	0.03910	NM_139307	Vasorin (Vasn), mRNA

Table 5. Genes altered in TA of 10-week-old ACTA KI females

No.	Ratio	p-value	Identifier	Gene Name
1	▼ 5.11	0.02416	NM_008220	Hemoglobin, beta adult minor chain, mRNA (cDNA clone MGC:40691 IMAGE:3988455)
2	▲ 3.43	0.00949	NM_183336	CDNA clone IMAGE:9053310
3	▲ 2.49	0.02814	NM_183336	CDNA clone IMAGE:9053310
4	▼ 2.30	0.03502	NM_176920	CDNA clone IMAGE:9053747
5	▲ 2.27	0.01669	NM_010368	Glucuronidase, beta, mRNA (cDNA clone IMAGE:3675986)
6	▼ 2.14	0.04745	NM_019806	Vesicle-associated membrane protein, associated protein B and C (Vapb), mRNA
7	▼ 2.09	0.01708	NM_007421	Adenylosuccinate synthetase like 1 (Adssl1), mRNA
8	▼ 2.09	0.04409	NM_172707	Protein phosphatase 1 (dis2m2)
9	▼ 2.04	0.00070	NM_008218	Hemoglobin alpha, adult chain 1 (Hba-a1), mRNA
10	▲ 2.03	0.04161	NM_178577	Transmembrane protein 205, mRNA (cDNA clone MGC:18837 IMAGE:4211629)
11	▼ 2.00	0.01727	NM_010477	Heat shock protein 1 (chaperonin) (Hspd1), nuclear gene encoding mitochondrial p
12	▼ 1.92	0.00565	NM_009762	SET and MYND domain containing 1 (Smyd1), mRNA
13	▲ 1.91	0.02383	NM_183335	CDNA clone IMAGE:9053310
14	▲ 1.88	0.00299	NM_007427	Agouti related protein (Agrp), mRNA
15	▲ 1.86	0.01923	NM_010838	Strain ILS microtubule binding protein tau
16	▲ 1.82	0.03841	NM_008610	Matrix metallopeptidase 2 (Mmp2), mRNA
17	▲ 1.82	0.01561	NM_011185	Proteasome (prosome, macropain) subunit, beta type 1, mRNA (cDNA clone MGC:5916
18	▼ 1.80	0.01358	NM_008195	Gys3
19	▲ 1.76	0.01508	NM_019440	Immunity-related GTPase family M member 2 (Irgm2), mRNA
20	▲ 1.72	0.02531	NM_007440	Arachidonate 12-lipoxygenase (Alox12), mRNA
21	▼ 1.72	0.00496	NM_011797	Carbonic anhydrase 14 (Car14), mRNA
22	▲ 1.72	0.02453	NM_152808	Solute carrier family 44, member 2 (Slc44a2), mRNA
23	▼ 1.71	0.02783	NM_008866	Lysophospholipase 1, mRNA (cDNA clone MGC:19218 IMAGE:4240573)
24	▼ 1.70	0.03715	NM_010028	DEAD/H (Asp-Glu-Ala-Asp/His) box polypeptide 3, X-linked (Ddx3x), mRNA
25	▲ 1.69	0.01452	NM_008486	Alanyl (membrane) aminopeptidase, mRNA (cDNA clone MGC:8171 IMAGE:3590117)
26	▲ 1.69	0.03817	NM_139198	C15 protein
27	▲ 1.67	0.01557	NM_176842	Tp53rk binding protein, mRNA (cDNA clone MGC:38694 IMAGE:5357332)
28	▲ 1.66	0.00538	NM_026677	RAB13, member RAS oncogene family (Rab13), mRNA
29	▼ 1.65	0.03545	NM_007981	Acyl-CoA synthetase long-chain family member 1, mRNA (cDNA clone IMAGE:3582717)
30	▼ 1.63	0.04300	NM_016875	Y box protein 2 (Ybx2), mRNA
31	▼ 1.62	0.00967	NM_008733	Nebulin-related anchoring protein (Nrap), transcript variant 2, mRNA
32	▼ 1.61	0.01575	NM_170689	Ankyrin 3, epithelial (Ank3), transcript variant 2, mRNA
33	▲ 1.61	0.01483	NM_026677	RAB13, member RAS oncogene family (Rab13), mRNA
34	▼ 1.60	0.00188	NM_010160	CUG triplet repeat, RNA binding protein 2, mRNA (cDNA clone MGC:25225 IMAGE:4503
35	▲ 1.60	0.04292	NM_022432	Sirtuin 2 (silent mating type information regulation 2, homolog) 2 (S. cerevisia
36	▼ 1.59	0.00800	NM_145507	Aspartyl-tRNA synthetase (Dars), transcript variant 2, mRNA
37	▼ 1.58	0.02007	NM_028398	Alanine-glyoxylate aminotransferase 2-like 2, mRNA (cDNA clone MGC:37320 IMAGE:4
38	▲ 1.58	0.04717	NM_011877	Protein tyrosine phosphatase, non-receptor type 21 (Ptpn21), mRNA
39	▼ 1.58	0.04676	NM_011622	Target of myb1 homolog (chicken), mRNA (cDNA clone MGC:13816 IMAGE:4208226)
40	▼ 1.58	0.04134	NM_145441	UBX domain protein 2A (Ubxn2a), mRNA
41	▲ 1.57	0.01959	NM_019972	Sortilin 1, mRNA (cDNA clone IMAGE:4920258)
42	▲ 1.56	0.03722	NM_031173	L-type calcium channel beta 1C subunit
43	▲ 1.56	0.01703	XM_109794	NAC alpha domain containing
44	▲ 1.55	0.04893	NM_009599	Acetylcholinesterase (Ache), mRNA
45	▼ 1.55	0.01403	NM_198609	CDNA sequence BC003885, mRNA (cDNA clone MGC:6735 IMAGE:3590401)
46	▼ 1.55	0.00914	NM_183250	Coiled-coil domain containing 72, mRNA (cDNA clone IMAGE:5363354)
47	▼ 1.55	0.00673	NM_133485	Protein phosphatase 1, regulatory (inhibitor) subunit 14c (Ppp1r14c), mRNA

No.	Ratio	p-value	Identifier	Gene Name
48	▼ 1.53	0.03437	NM_175266	EPM2A (laforin) interacting protein 1, mRNA (cDNA clone MGC:27780 IMAGE:3156440)
49	▼ 1.53	0.03069	NM_029409	Mitochondrial fission factor (Mff), nuclear gene encoding mitochondrial protein,
50	▲ 1.53	0.04612	NM_008113	Rho GDP dissociation inhibitor (GDI) gamma, mRNA (cDNA clone MGC:5923 IMAGE:3490
51	▼ 1.53	0.02234	NM_194054	RTN4 (Rtn4) mRNA, complete cds, alternatively spliced
52	▲ 1.52	0.01291	NM_139272	UDP-N-acetyl-alpha-D-galactosamine:polypeptide N-acetylgalactosaminyltransferase
53	▲ 1.51	0.00846	NM_009046	Avian reticuloendotheliosis viral (v-rel) oncogene related B, mRNA (cDNA clone M
54	▼ 1.50	0.04183	NM_020575	Membrane-associated ring finger (C3HC4) 7, mRNA (cDNA clone MGC:35882 IMAGE:4935
55	▼ 1.50	0.04572	NM_207515	MKIAA4072 protein
56	▲ 1.50	0.00310	NM_053123	SWI/SNF related, matrix associated, actin dependent regulator of chromatin, subf
57	▼ 1.50	0.01372	NM_144801	Transmembrane protein 143 (Tmem143), mRNA
58	▲ 1.50	0.00915	NM_009413	Tumor protein D52-like 1 (Tpd52l1), mRNA
59	▼ 1.49	0.04486	NM_027430	Brain protein 44 (Brp44), mRNA
60	▲ 1.49	0.03209	NM_008815	Ets variant gene 4 (E1A enhancer binding protein, E1AF) (Etv4), mRNA
61	▲ 1.49	0.01546	NM_023794	Ets variant gene 5, mRNA (cDNA clone MGC:28414 IMAGE:4036564)
62	▼ 1.48	0.04466	NM_175357	Cereblon (Crbn), transcript variant 1, mRNA
63	▲ 1.48	0.00561	NM_010189	Fc receptor, IgG, alpha chain transporter, mRNA (cDNA clone MGC:6014 IMAGE:34856
64	▲ 1.48	0.00712	NM_010255	Guanidinoacetate methyltransferase (Gamt), mRNA
65	▲ 1.48	0.01259	NM_001025074	Neurotrophic tyrosine kinase, receptor, type 2 (Ntrk2), transcript variant 2, mR
66	▼ 1.48	0.01199	NR_002883	predicted gene, EG434858 (EG434858) on chromosome X.
67	▼ 1.47	0.02580	NM_010309	GNAS (guanine nucleotide binding protein, alpha stimulating) complex locus, mRNA
68	▼ 1.47	0.02088	NM_025980	Notch-regulated ankyrin repeat protein (Nrarp), mRNA
69	▲ 1.47	0.02736	NM_153786	Vestigial like 2 homolog (Drosophila) (Vgll2), mRNA
70	▼ 1.46	0.01065	NM_018832	MAGI family member, X-linked (Magix), mRNA
71	▼ 1.46	0.02631	NM_011943	MAP Kinase Kinase
72	▼ 1.46	0.01527	NM_145457	Polyadenylate binding protein-interacting protein 1 (Paip1), transcript variant
73	▼ 1.46	0.03491	NM_080556	Transmembrane 9 superfamily member 2 (Tm9sf2), mRNA
74	▲ 1.46	0.04954	NM_178577	Transmembrane protein 205, mRNA (cDNA clone MGC:18837 IMAGE:4211629)
75	▼ 1.45	0.04258	NM_001039710	Coenzyme Q10 homolog B (S. cerevisiae) (Coq10b), transcript variant 2, mRNA
76	▼ 1.45	0.01912	NM_145569	Methionine adenosyltransferase II, alpha (Mat2a), mRNA
77	▼ 1.44	0.03490	NM_016877	CCR4-NOT transcription complex, subunit 4 (Cnot4), mRNA
78	▲ 1.44	0.01884	NM_010421	Hexosaminidase A, mRNA (cDNA clone MGC:18443 IMAGE:4225233)
79	▼ 1.44	0.01064	NM_021500	Macrophage erythroblast attacher (Maea), mRNA
80	▲ 1.44	0.04009	NM_001039530	Poly (ADP-ribose) polymerase family, member 14, mRNA (cDNA clone IMAGE:5065398)
81	▲ 1.43	0.04479	NM_031397	Bicaudal C homolog 1 (Drosophila) (Bicc1), mRNA
82	▼ 1.43	0.00839	NM_020046	Dihydroorotate dehydrogenase, mRNA (cDNA clone MGC:35899 IMAGE:5253723)
83	▲ 1.43	0.04212	NM_010260	Guanylate binding protein 2, mRNA (cDNA clone MGC:41173 IMAGE:1230883)
84	▼ 1.43	0.04661	NM_138756	Solute carrier family 25, member 36 (Slc25a36), mRNA
85	▲ 1.43	0.00924	NM_138721	U7 snRNP-specific Sm-like protein LSM10 (Lsm10), mRNA
86	▼ 1.42	0.02398	NM_001033279	DNA segment, Chr 17, Wayne State University 92, expressed, mRNA (cDNA clone MGC:
87	▲ 1.42	0.02015	NM_011375	GM3 synthase
88	▼ 1.42	0.03667	NM_023844	Junction adhesion molecule 2, mRNA (cDNA clone MGC:41518 IMAGE:1195543)
89	▲ 1.42	0.01678	NM_008502	Lethal giant larvae homolog 1 (Drosophila) (Llgl1), mRNA
90	▼ 1.42	0.02025	NM_026950	OCIA domain containing 2 (Ociad2), mRNA
91	▲ 1.42	0.03330	NM_028841	Tetraspanin 17 (Tspan17), mRNA
92	▲ 1.42	0.01128	NM_009369	Transforming growth factor, beta induced (Tgfbi), mRNA
93	▲ 1.41	0.02209	NM_010299	GM2 ganglioside activator protein, mRNA (cDNA clone MGC:5949 IMAGE:3482848)
94	▲ 1.41	0.02213	NM_011941	Mitogen activated protein kinase binding protein 1, mRNA (cDNA clone IMAGE:14464
95	▲ 1.41	0.01920	NM_021880	Protein kinase, cAMP dependent regulatory, type I, alpha, mRNA (cDNA clone MGC:1

No.	Ratio	p-value	Identifier	Gene Name
96	▲ 1.41	0.03404	NM_009130	Secretogranin III, mRNA (cDNA clone MGC:36181 IMAGE:5362975)
97	▲ 1.40	0.02469	NM_153502	Ankyrin repeat domain 23 (Ankrd23), mRNA
98	▼ 1.40	0.04710	NM_026394	Late cornified envelope 1F (Lce1f), mRNA
99	▼ 1.40	0.04115	NM_011844	Monoglyceride lipase (Mgll gene), transcript 2
100	▼ 1.40	0.01944	NM_025898	N-ethylmaleimide sensitive fusion protein attachment protein alpha, mRNA (cDNA c
101	▲ 1.40	0.03318	NM_011909	Ubiquitin specific protease UBP43
102	▲ 1.40	0.03413	NM_153786	Vestigial like 2 homolog (Drosophila) (Vgll2), mRNA

Table 6. Genes altered in DIA of 10-week-old ACTA KI females

No.	Ratio	p-value	Identifier	Gene Name
1	▼ 3.41	0.02839	NM_033037	Cysteine dioxygenase 1, cytosolic, mRNA (cDNA clone MGC:18800 IMAGE:4194939)
2	▲ 2.13	0.04991	NM_175259	Shisa homolog 4 (Xenopus laevis) (Shisa4), mRNA
3	▼ 2.06	0.04861	NM_133198	Liver glycogen phosphorylase (Pygl), mRNA
4	▼ 2.01	0.02995	NM_016785	Thiopurine methyltransferase, mRNA (cDNA clone MGC:35956 IMAGE:5098857)
5	▲ 1.91	0.03145	NM_009149	Golgi apparatus protein 1, mRNA (cDNA clone MGC:29292 IMAGE:4239405)
6	▼ 1.86	0.01869	NM_153088	CTD (carboxy-terminal domain, RNA polymerase II, polypeptide A) small phosphatas
7	▼ 1.84	0.00345	NM_009895	Cytokine inducible SH2-containing protein, mRNA (cDNA clone MGC:14022 IMAGE:4193
8	▼ 1.82	0.03005	NM_007639	CD1d1 antigen (Cd1d1), mRNA
9	▲ 1.77	0.04644	NM_009974	Casein kinase 2, alpha prime polypeptide (Csnk2a2), mRNA
10	▲ 1.71	0.03067	NM_010148	Epsin 2, mRNA (cDNA clone MGC:19376 IMAGE:2647379)
11	▲ 1.69	0.02493	NM_010516	Cysteine rich protein 61 (Cyr61), mRNA
12	▲ 1.69	0.01769	NM_178055	DnaJ (Hsp40) homolog, subfamily B, member 2, mRNA (cDNA clone MGC:19256 IMAGE:39
13	▲ 1.69	0.00329	XM_125970	GATS protein-like 3
14	▲ 1.66	0.00137	NM_001045489	Milk fat globule-EGF factor 8 protein, mRNA (cDNA clone MGC:6771 IMAGE:3601565)
15	▲ 1.65	0.02947	NM_010817	Proteasome (prosome, macropain) 26S subunit, non-ATPase, 7 (Psmd7), mRNA
16	▼ 1.65	0.03442	NM_178446	RNA binding motif protein 47, mRNA (cDNA clone MGC:37504 IMAGE:4984936)
17	▲ 1.65	0.02017	NM_028283	Uveal autoantigen with coiled-coil domains and ankyrin repeats, mRNA (cDNA clone
18	▲ 1.59	0.04645	NM_009974	Casein kinase 2, alpha prime polypeptide (Csnk2a2), mRNA
19	▲ 1.59	0.03711	NM_021355	Fibromodulin (Fmod), mRNA
20	▲ 1.59	0.04671	NM_025709	Gapex-5
21	▼ 1.59	0.04733	NM_144916	Transmembrane protein 150 (Tmem150), mRNA
22	▲ 1.55	0.03239	NM_027707	Nipped-B homolog (Drosophila), mRNA (cDNA clone IMAGE:5354629)
23	▼ 1.55	0.00723	NM_011327	Sterol carrier protein 2, liver, mRNA (cDNA clone MGC:29961 IMAGE:5123611)
24	▲ 1.55	0.03422	NM_011708	Von Willebrand factor
25	▲ 1.54	0.00222	NM_026436	Transmembrane protein 86A (Tmem86a), mRNA
26	▼ 1.53	0.03754	NM_010497	Isocitrate dehydrogenase 1 (NADP+), soluble (Idh1), transcript variant 2, mRNA
27	▼ 1.53	0.03309	NM_013625	Platelet-activating factor acetylhydrolase, isoform 1b, beta1 subunit, mRNA (cDN
28	▲ 1.52	0.03827	NM_013642	Dual specificity phosphatase 1, mRNA (cDNA clone MGC:6265 IMAGE:3589849)
29	▲ 1.50	0.02813	NM_028774	Ring finger protein (C3H2C3 type) 6 (Rnf6), mRNA
30	▲ 1.50	0.04288	NM_009357	Testis expressed gene 261, mRNA (cDNA clone MGC:6079 IMAGE:3486968)
31	▲ 1.49	0.01617	NM_016679	Kelch-like ECH-associated protein 1 (Keap1), transcript variant 1, mRNA
32	▲ 1.49	0.02926	NM_175836	Mus musculus, clone IMAGE:4951562, mRNA
33	▲ 1.49	0.01662	NM_011535	T-box 3, mRNA (cDNA clone MGC:106457 IMAGE:30547736)
34	▼ 1.48	0.01336	NM_139295	Multiple coagulation factor deficiency 2 (Mcfd2), transcript variant 2, mRNA
35	▲ 1.48	0.03421	NM_025321	Succinate dehydrogenase complex, subunit C, integral membrane protein, mRNA (cDN
36	▲ 1.47	0.02021	NM_013468	Ankyrin repeat domain 1 (cardiac muscle), mRNA (cDNA clone MGC:46879 IMAGE:49531
37	▲ 1.47	0.02025	NM_010148	Epsin 2, mRNA (cDNA clone MGC:19376 IMAGE:2647379)
38	▲ 1.47	0.04129	NM_016696	Glypican 1 (Gpc1), mRNA
39	▲ 1.47	0.03624	NM_133839	Methylmalonic aciduria (cobalamin deficiency) cblD type, with homocystinuria (Mm
40	▲ 1.47	0.01087	NM_009176	ST3 beta-galactoside alpha-2,3-sialyltransferase 3, mRNA (cDNA clone MGC:5896 IM
41	▲ 1.47	0.01958	NM_138579	TRIO and F-actin binding protein, mRNA (cDNA clone IMAGE:3491252)
42	▲ 1.47	0.03226	NM_001039198	Zinc finger homeobox 2 (Zfhx2), mRNA
43	▲ 1.46	0.04031	NM_030251	BPOZ mRNA for BPOZ
44	▲ 1.46	0.03004	NM_001039160	GTPase, very large interferon inducible 1 (Gvin1), transcript variant B, mRNA
45	▲ 1.46	0.01775	NM_144529	Rho GTPase activating protein 17 (Arhgap17), transcript variant 1, mRNA
46	▲ 1.45	0.00342	NM_178116	Calmodulin binding transcription activator 2, mRNA (cDNA clone IMAGE:5324169)
47	▼ 1.45	0.01141	NM_026821	DNA segment, Chr 4, Brigham & Women's Genetics 0951 expressed, mRNA (cDNA clone

No.	Ratio	p-value	Identifier	Gene Name
48	▼ 1.45	0.01198	NM_026728	Enoyl Coenzyme A hydratase domain containing 2 (Echdc2), mRNA
49	▲ 1.45	0.04625	NM_010145	Epoxide hydrolase 1, microsomal, mRNA (cDNA clone MGC:30577 IMAGE:3491966)
50	▼ 1.45	0.02984	NM_146006	Lanosterol synthase (Lss), mRNA
51	▲ 1.45	0.04781	NM_007928	MAP/microtubule affinity-regulating kinase 2 (Mark2), transcript variant 1, mRNA
52	▲ 1.45	0.03578	NM_009031	Retinoblastoma binding protein 7, mRNA (cDNA clone MGC:6013 IMAGE:3600013)
53	▲ 1.45	0.02730	NM_019684	Serine/arginine-rich protein specific kinase 3 (Srpk3), mRNA
54	▼ 1.45	0.03809	NM_146126	Sorbitol dehydrogenase (Sord), mRNA
55	▲ 1.45	0.04221	NM_009367	Transforming growth factor, beta 2, mRNA (cDNA clone MGC:7998 IMAGE:3585774)
56	▲ 1.44	0.00460	NM_013863	Bcl-2-binding protein BIS (Bis)
57	▲ 1.44	0.02012	NM_007595	Calcium/calmodulin-dependent protein kinase II, beta (Camk2b), mRNA
58	▲ 1.44	0.03683	NM_172410	Nucleoporin 93, mRNA (cDNA clone MGC:28230 IMAGE:3991335)
59	▲ 1.44	0.00034	NM_145404	Protein arginine N-methyltransferase 7 (Prmt7), mRNA
60	▲ 1.43	0.04797	NM_023878	Claudin 10 (Cldn10), transcript variant 1, mRNA
61	▼ 1.43	0.00836	NM_024208	Enoyl Coenzyme A hydratase domain containing 3 (Echdc3), mRNA
62	▼ 1.43	0.03380	NM_023505	Glutaredoxin 2
63	▲ 1.43	0.04877	NM_023514	Mitochondrial ribosomal protein S9, mRNA (cDNA clone IMAGE:4036755)
64	▲ 1.43	0.00262	NM_029811	Suppression of tumorigenicity 5, mRNA (cDNA clone IMAGE:4984792)
65	▲ 1.42	0.00583	NM_001017426	Jumonji domain containing 3, mRNA (cDNA clone IMAGE:1378940)
66	▲ 1.42	0.04070	NM_026859	MAF1 homolog (S. cerevisiae) (Maf1), mRNA
67	▲ 1.42	0.04492	NM_027422	Mesoderm induction early response 1, family member 2 (Mier2), mRNA
68	▲ 1.42	0.03786	NM_016798	PDZ and LIM domain 3 (Pdlim3), mRNA
69	▲ 1.42	0.00782	NM_134129	PRP19/PSO4 pre-mRNA processing factor 19 homolog (S. cerevisiae) (Prpf19), mRNA
70	▲ 1.42	0.02773	NM_009503	Valosin containing protein (Vcp), mRNA
71	▼ 1.42	0.04836	NM_030100	Within bgcn homolog (Drosophila) (Wibg), mRNA
72	▲ 1.42	0.04465	NM_011768	Zinc finger protein X-linked, mRNA (cDNA clone IMAGE:1448640)
73	▲ 1.41	0.02542	NM_008913	Calcineurin catalytic subunit
74	▼ 1.41	0.02880	NM_026598	Emopamil binding protein-like, mRNA (cDNA clone MGC:35635 IMAGE:4035224)
75	▲ 1.41	0.01410	NM_024471	MLIP1 mRNA for lipoic acid synthase
76	▲ 1.41	0.00942	NM_134058	Pelota homolog (Drosophila) (Pelo), mRNA
77	▲ 1.41	0.04435	NM_011070	Prefoldin 2, mRNA (cDNA clone MGC:25898 IMAGE:4219635)
78	▲ 1.41	0.00463	NM_173735	RIKEN cDNA 2310044G17 gene, mRNA (cDNA clone MGC:31149 IMAGE:4168224)
79	▲ 1.41	0.01428	XM_148568	Ube2l3
80	▼ 1.40	0.04268	NM_172778	Monoamine oxidase B, mRNA (cDNA clone MGC:132955 IMAGE:40061991)
81	▼ 1.40	0.01091	NM_010874	N-acetyltransferase 2 (arylamine N-acetyltransferase), mRNA (cDNA clone MGC:1402
82	▲ 1.40	0.04902	NM_011420	Survival motor neuron 1 (Smn1), mRNA
83	▲ 1.40	0.02211	NM_018804	Synaptotagmin XI, mRNA (cDNA clone MGC:32353 IMAGE:5030173)